(2)

TECHNICAL REPORT SL-92-27

US Army Corps of Engineers

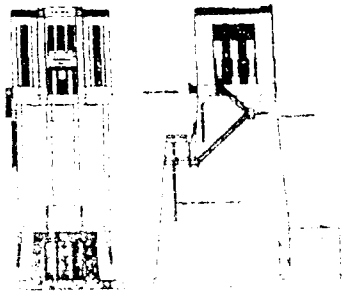

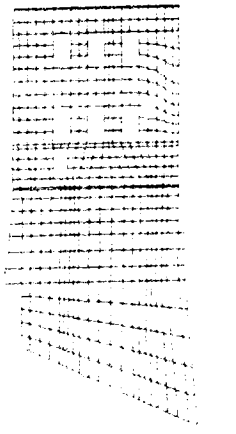

SEISMIC ANALYSIS OF ARKABUTLA INTAKE-OUTLET STRUCTURES

by

Wayne G. Johnson, Vincent P. Chiarito, Randy L. Holmes

Structures Laboratory

DEPARTMENT OF THE ARMY
Waterways Experiment Station, Corps of Engineers
3909 Halls Ferry Road, Vicksburg, Mississippi 39180-6199

November 1992
Final Report

STRUCTURES LABORATORY

Prepared for DEPARTMENT OF THE ARMY
US Army Engineer District, Vicksburg
Vicksburg, Mississippi 39180-0060

When this report is no longer needed return it to the originator.

The findings in this report are not to be construed as an official Department of the Army position unless so designated by other authorized documents.

The contents of this report are not to be used for advertising, publication, or promotional purposes. Citation of trade names does not constitute an official endorsement or approval of the use of such commercial products.

REPORT DOCUMENTATION PAGE

Form Approved
OMB No. 0704-0188

1. AGENCY USE ONLY (Leave blank)	2. REPORT DATE	3. REPORT TYPE AND DATES COVERED
	November 1992	Final report

4. TITLE AND SUBTITLE
Seismic Analysis of Arkabutla Intake-Outlet Structures

5. FUNDING NUMBERS

6. AUTHOR(S)
Wayne G. Johnson
Vincent P. Chiarito
Randy L. Holmes

7. PERFORMING ORGANIZATION NAME(S) AND ADDRESS(ES)
USAE Waterways Experiment Station
Structures Laboratory
3909 Halls Ferry Road
Vicksburg, MS 39180-6199

8. PERFORMING ORGANIZATION REPORT NUMBER
Technical Report
SL-92-27

9. SPONSORING/MONITORING AGENCY NAME(S) AND ADDRESS(ES)
US Army Engineer District, Vicksburg
PO Box 60
Vicksburg, MS 39180-0060

10. SPONSORING/MONITORING AGENCY REPORT NUMBER

11. SUPPLEMENTARY NOTES
Available from National Technical Information Service, 5285 Port Royal Road, Springfield, VA 22161

12a. DISTRIBUTION/AVAILABILITY STATEMENT
Approved for public release; distribution is unlimited.

12b. DISTRIBUTION CODE

13. ABSTRACT *(Maximum 200 words)*

This report summarizes the dynamic finite element studies for the seismic evaluation of intake-outlet structures (intake towers and stilling basin walls). The seismic evaluation involves linear elastic finite element calculations for one- and two-dimensional models of an intake tower and two-dimensional models for the stilling basin. A response spectrum technique is utilized in the analyses.

The work was conducted as a part of the Safety Assurance Program for the Corps of Engineers' inventory of flood control structures. The analyses were conducted to determine the adequacy of the Arkabutla Dam intake/outlet structures when subjected to a previously specified seismic event for the Arkabutla area.

The analyses showed no major points of concern for safety of the structures. Some superficial damage would occur, but results show that the structure

(Continued)

14. SUBJECT TERMS		15. NUMBER OF PAGES
Earthquakes	Response spectrum analysis	92
Hydrodynamic interaction	Seismic analysis	16. PRICE CODE

17. SECURITY CLASSIFICATION OF REPORT	18. SECURITY CLASSIFICATION OF THIS PAGE	19. SECURITY CLASSIFICATION OF ABSTRACT	20. LIMITATION OF ABSTRACT
UNCLASSIFIED	UNCLASSIFIED		

13. (Concluded).

would be intact and operational following the specified event. The analysis assumes no foundation failures occur which would interact with the tower or stilling basin.

PREFACE

This study was conducted during the period August through December 1989 by the Structures Laboratory (SL), US Army Engineer Waterways Experiment Station (WES), under the sponsorship of the US Army Engineer District, Vicksburg. Technical Monitor for the Vicksburg District was Mr. Ken Klaus.

The analyses were conducted and the report prepared by Messrs. Wayne G. Johnson, Vincent P. Chiarito, and Randy Holmes, Structural Mechanics Division (SMD), under the supervision of Messrs. Bryant Mather, Director, SL; J.T. Ballard, Assistant Director, SL; Dr. J. P. Balsara, Chief, SMD; and Dr. Robert L. Hall, Chief, Structural Analysis Group, SMD. Mr. Chiarito, Dr. Hall, and Dr. Sammy A. Kiger (formerly SMD) provided technical guidance.

At the time of publication of this report, Director of WES was Dr. Robert W. Whalin. Commander was COL Leonard G. Hassell, EN.

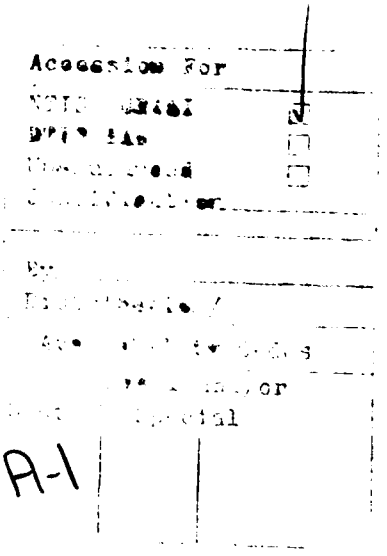

CONTENTS

CONVERSION FACTORS, NON-SI TO METRIC (SI) UNITS OF MEASUREMENT

Non-SI units of measurement used in this report can be converted to SI (metric) units as follows:

Multiply	By	To Obtain
cubic feet	0.02832	cubic metres
degrees (angle)	0.01745329	radian
feet	0.3048	metres
inches	25.4	millimetres
kips (force)	4.448222	kilonewtons
kips (force) per square inch	6.894757	megapascals
miles	1.609	kilometres
pounds (force)	4.448	newtons
pounds (force) per square inch	0.006895	megapascals
pounds (mass)	0.4536	kilograms
pounds (mass) per cubic foot	16.02	kilograms per cubic metre
square feet	0.0929	square metres

PART I: INTRODUCTION

Objective

1. This report documents the results of stress and stability analyses of the seismic response for critical structures of the Arkabutla intake-outlet works.

Scope

2. The scope of work covers the stress, overturning stability, and sliding stability analyses of the intake tower and stress analysis of selected sections of the stilling basin. The latest seismic analysis techniques have been applied to provide the best understanding of the dynamic structural response of the intake-outlet structures during the specified earthquake.

Problem Background

3. In support of the Safety Assurance Program for Arkabutla Dam, the Waterways Experiment Station (WES) was asked to propose calculations to determine the dynamic stability and maximum stress levels under seismic loading for the intake tower and stilling basin for this Corps facility. Arkabutla Dam is located in an area of high seismic risk (Zone 3 as set forth in ER-1110-2-1806 (Headquarters, Department of the Army, 1983)). Thus, structural damage is of concern in the event of a severe seismic occurrence affecting this area. ER-1110-2-1806 states that "major" damage would be expected in Zone 3 given occurrence of the Maximum Credible Earthquake (MCE).

4. The seismic analysis of the structures and foundations is a very complex, three-dimensional (3-D), soil-structure interaction problem. Complex 3-D analyses are not generally cost effective (nor necessary) tools due to the length of time in model development and lack of definition for many of the parameters involved (especially in the foundation). Thus, in most cases, simplified analyses are sufficient. Such appropriate techniques are available for analysis of the Arkabutla structures of concern. The intake tower analyses used many techniques outlined in ETL 1110-8-8(FR) (Headquarters, Department of the Army, 1992).

Project Description

5. The project description is best given by the brochure on Arkabutla Lake, US Army Engineer District, Vicksburg, June 1988:

a. "Arkabutla Lake and Dam is located on the Coldwater River 4 miles north of the Community of Arkabutla and east of the town of Coldwater."

b. "Arkabutla Lake was placed in operation in June of 1943 by the US Army Corps of Engineers, Vicksburg District. One of the most important highlights of the construction of this project was the relocation of the town of Coldwater, which now lies approximately 1 mile south of its original location."

c. The intake tower maintains the reservoir elevation for flood control and recreation. A vicinity map is shown in Figure 1.

Procedures and Methods of Analysis

6. Intake towers are quite susceptible to earthquake damage due to their geometric shape and support conditions. The initial calculations were conducted on a detailed beam model. Steps in the analysis procedure included (a) definition of the structural properties of the tower-reservoir system; (b) computation of the periods and mode shapes of the lower natural vibration modes; (c) determination of the maximum response for the structure subjected to the given earthquake; (d) computation of the internal moments and shears at a given cross section; and (e) estimation of the maximum moment and shear at any cross section. Each of these items involves a number of computations pertinent to that particular step in the analysis.

7. Final calculations for the intake tower were performed using a two-dimensional (2-D) finite element (FE) model. This model served as a check on the results of the beam model and also produced very useful information on deflections of the structure during the earthquake. This information was useful in assessing the degree of damage (nonstructural as well as structural) that would occur during the specified event.

8. Stability analyses were also conducted for the intake tower. Sliding stability analyses were conducted using the Corps-developed program CSLIDE (Pace and Noddin 1987). This program uses the principles set forth in ETL 1110-2-256 (Headquarters, Department of the Army, 1981) entitled "Sliding Stability for Concrete Structures." The approach is essentially an automated seismic coefficient method which is quite conservative by nature. Overturning

stability analysis was conducted using the latest procedures. The method used is described in a paper by Dr. S.A. Kiger (1989), Appendix A.

9. Stress analyses of the stilling basin were conducted on selected 2-D sections using FE methods. This process involved (a) definition of the structural properties of the stilling basin sections; (b) computation of the periods and mode shapes of the lower natural vibration modes; (c) determination of the maximum response of the sections subjected to the given earthquake; (d) computation of the maximum stresses (maximum moments at a given crossection); and (e) verification of ability of existing reinforced structural members to carry the calculated moments.

PART II: ANALYSES OF INTAKE TOWER

Stress Analyses

10. Seismic stress analyses for the Arkabutla Intake Tower were accomplished using FE models in the Automatic Dynamic Incremental Nonlinear Analysis (ADINA) code (ADINA R&D 1987). A beam model was used and the results were compared to results of a 2-D model of the tower to better localize problem areas. The beam model revealed that no severe structural damage would occur in the tower, given the specified earthquake for the Arkabutla area. The 2-D model (developed for the E-W response direction) showed similar results with small relative deflections and associated stresses.

Beam model

11. Arkabutla Lake is located within a Zone 3 seismic area as defined by ER-1110-2-1806 (Headquarters, Department of the Army, 1983). Thus, the earthquake specification for this area is relatively severe with a peak ground acceleration of 0.28g and a maximum velocity of 1.31 ft/sec. These values were extrapolated from the test earthquake developed for Sardis Dam. The general extrapolation process is defined in Miscellaneous Paper S-73-1 (Nuttli 1979). The Reconnaissance Report of June 1982 gives specific information concerning extrapolation of the Arkabotla design earthquake from the Sardis test earthquake, (US Army Engineer District, Vicksburg, 1982). Seed's normalized response spectrum for a stiff soil geology scaled to 0.28g was used as the seismic input and is shown in Figure 2 (Seed, Ugas, and Lysmer 1974). Table 1 gives a listing of values for the scaled response spectrum.

12. The approach used consisted of a number of steps, the first of which was to discretize the length of the structure into a series of cross-sections and calculate the structural properties of these sections. For this model, el 211.83 (Figure 3) was used as the base, and the beam model was assumed fixed at this point. Figure 4 shows the beam model and gives section properties for the segments. Figures 5 and 6 show plan views of two of the sections used. Material properties are given in Table 2.

13. Upon assembly of the structural portion of the beam model, it was necessary to attach added masses at various node points throughout the structure. These masses included equipment, floors, roofs, and bridge masses. A summary of the attached masses is contained in Table 3.

14. It was also necessary to attach masses due to surrounding and inside water. To accomplish this, the procedure developed by Goyal and Chopra (1989) was utilized. To calculate the masses to be attached, it was necessary to define the pool elevation to be used. The procedure for selecting this value was to utilize available hydrographs and statistically determine a pool elevation.

15. The process for selection of the pool elevation for Arkabutla Dam involved taking the highest and lowest pool elevation for each month in the study period (January 1975 through March 1984; US Army Engineer District, Vicksburg, 1984) and averaging these values. These numbers were combined into a data base, then statistically analyzed to arrive at a pool elevation. Figure 7 contains two histograms for the data thus obtained. It was decided to choose the lake elevation at which there is only a 10-percent probability of exceedence (Figure 8). The choice was el 230.0, and this elevation was used for all Arkabutla Tower calculations.

16. Upon completion of the beam model with attached masses, the calculations were initiated. It was decided to combine the dynamic contributions for the first 10 mode shapes. Studies have indicated that a combination of the contributions from the first two mode shapes is sufficient for this type of analysis. Due to automation of analysis for the Arkabutla Tower, it was convenient to include additional modes into the calculations. Shear deformation effects were also included in the final beam model calculations.

17. The first step in the analysis process consists of an eigenvalue extraction for the specified modes. The first 20 natural frequencies are given in Table 4 for the model without attached masses. Table 5 contains the first 20 frequencies for the model with all masses included. The Arkabutla Tower is a relatively short tower. The fundamental frequency ,f_1, is 11.49 Hz. The fundamental frequency was 14.00 Hz when shear effects were ignored; thus, these effects are significant and should be considered in the solution.

18. After extraction of the eigenvalues, the earthquake loading is applied to the model in the form of the scaled response spectrum. The structural response results for a beam element model using ADINA are given in terms of local moments for the tower section. The analyses were conducted for the specified earthquake along both major structural axes. For a N-S earthquake, the resulting moments are given in Table 6. The axial and shear forces are also shown in this table. The bending moment diagram is shown in Figure 9.

Maximum combined stresses are given in Table 7. These numbers represent an upper bound to the actual stresses due to the method of combination, i.e., modal contributions were combined based on an absolute sum method.

19. The largest stress value is 37.57 psi at el 230. This stress level is not sufficient to cause any severe structural damage and the worst damage to be expected would be hairline cracks in the exterior concrete surface. Note that this excludes other possibilities of damage mentioned in Part V, Recommendations.

20. For an earthquake along the E-W axis, the calculated moments are given in Table 8. Axial forces are identical to those shown previously for the N-S direction. The bending moment diagram is shown in Figure 10. Maximum combined stresses are given in Table 9. Here also, the highest stresses occur at el 130 (77.62 psi tension) but are not significant enough to cause structural damage.

21. These analyses show that Arkabutla Intake Tower would receive relatively minor structural damage, if any, from the specified earthquake. With the exception of the possibilities for damage mentioned in Part V, there is no reason to believe that the structure would not be operational following an earthquake of the specified intensity. It should be noted that this statement assumes there are no foundation failures or soil failures that would interact with the tower or bridge.

Two-dimensional model

22. The 2-D model for the Arkabutla Tower in the E-W direction is shown in Figure 11. The model consists of 594 2-D plane stress elements (673 nodes) with varied element thicknesses to account for the 3-D geometry of the structure. Eleven element groups (each with a different thickness) were required to adequately model the structure.

23. The process of analysis for the 2-D model was similar to that for the beam model. It should be noted, however, that the 2-D model includes a shorter section of the structure than was modeled in the beam model. Further, dynamic properties (mode shapes and frequencies) for the 2-D model are limited to in-plane response only, i.e., the model cannot capture the out-of-plane dynamic properties which were reflected in the beam model. The 2-D analysis does provide better estimates of deflections of the tower for the direction studied and also aids in determination of areas where stress concentrations are likely. The 2-D results are thus helpful in determining response of nonstructural components such as the tile windows and internal hardware.

24. The first five mode shapes for the 2-D model are given in Figures 12 through 16. The associated frequencies are shown in Table 10. For this analysis, the dynamic response was approximated by combining the contributions for the lowest five modes. The resulting displacements along the west wall of the operation room are given in Table 11. The deflected shape is shown in Figure 17. The maximum displacement (relative to the supports) was 0.129 in. at the top of the tower. The deflection of the top of the tower relative to the operating room floor was 0.09 in. This amount of movement does not imply a significant threat to structural integrity. However, concern for damage to the glass block windows is warranted. There is a possibility of damage to and subsequent dislodging of the blocks, thus a threat to internal personnel and equipment.

25. Figure 18 gives a stress vector plot for the principal stresses given the specified Arkabutla event. This plot reflects some areas of tensile principal stress, especially around openings. For the most part, these stresses are the result of a numerical singularity which would be expected for this type of analysis, especially at edges and reentrant corners. Also, the results are based on an absolute sum combination of the dynamic effects. These stresses are upperbound values due to this method of combination. Given these considerations, the results show areas of low tensile stresses especially in the north and south walls. The stresses shown are smaller than the tensile strength of the concrete, thus no debilitating structural damage will result. However, some small cracks would probably develop in the walls (especially at corners of openings). The reinforced sections will, however, retain full structural integrity. As shown by the plot, the most likely area for cracking is at the base of the lowest window group (el 273.0) and above the door located in the north wall.

Stability Analyses

Sliding

26. The Arkabutla Intake Tower is a complex structure for sliding stability analysis. This sliding situation for this structure is shown in Figure 19. This figure gives a cross-sectional view of the most critical sliding situation for the Arkabutla tower, West to East sliding. The Corps-developed sliding stability program CSLIDE was used for this analysis (Pace and Noddin

1987). This program uses the principles set forth in ETL-1110-2-256 (Headquarters, Department of the Army, 1981) entitled "Sliding Stability for Concrete Structures."

27. The model used in the calculations is shown in Figure 20. A number of possible scenarios were investigated, the most conservative of which yielded a factor of safety of 1.33 against sliding under the specified earthquake for the Arkabutla area. Note that the model ignores the approach channel slab. This slab would add to the stability of the tower, thus excluding this slab in the analysis is conservative. Further, the west side of the tower is attached to the discharge culvert which would also inhibit sliding of the tower. For the most conservative sliding analysis, the restraining properties of the culvert/tower connection are ignored and the culvert section west of the tower is smeared with the soil in that region and essentially modeled as a soil material. This procedure will later be described in greater detail.

28. Properties of the passive soil wedge (Soil A in Figure 20) were taken to be 125 lb/ft^3 unit weight with an internal angle of friction of 25.33°. Cohesive properties of this material (specified to be a compacted, impervious soil) although applicable, were ignored. The passive wedge was specified to have a failure angle of $45° - \phi/2 = 32.33°$ from the horizontal plane.

29. The structure was modeled by "smearing" the concrete across the entire volume of the tower and taking a 1-ft strip as required by CSLIDE. This procedure ignores water inside the tower which fills many of the voids assumed in the "smearing" process. However, the net uplift force due to the presence of water is greater than the downward hydraulic forces. For this reason, an uplift force of 28,000 lb was applied to the base of the structure. This value was obtained from the difference in pressure between the top and bottom of the base slab of the tower. Other hydraulic pressures are assumed to cancel out. This nonconservative approximation is easily countered by other very conservative assumptions described previously for the passive wedge and as described below for the active wedge.

30. The active soil wedge (located on the west side of the tower) was modeled using two soil layers. Layer 1 (soil B in Figure 20) consists primarily of the concrete culvert section (Figure 21). Conservatively, the soil properties assigned for this layer consist of a unit weight obtained by smearing the concrete and soil together (based on the area of each in the

cross section) and an impervious soil angle of friction (25.33°). No cohesion was specified for this layer; however, the concrete culvert section would provide a significant stabilizing force for E-W sliding. The effect of assigning cohesive properties to this layer is investigated, and the results follow.

31. Layer 2 of the active wedge (soil C in Figure 20) was given the properties of the impervious compacted fill (identical to soil A). Effects of the sloped embankment were included.

32. The initial (and most conservative) CSLIDE calculation consisted of the geometry shown in Figure 20 and the soil properties discussed in the previous paragraphs. Hand calculations were required to check the percentage of the base in compression. These calculations revealed that the reaction force falls within the kern; thus, the entire base is in compression. A total uplift force of 28,000 lb was applied to the structure base and a single-failure plane analysis was initiated. The results of the final iteration for the safety factor are given in Table 12. The results show a safety factor of at least 1.33 against sliding for this very conservative situation.

33. Due to the uncertainty in the actual failure angles of the wedges, a calculation was also conducted with all soil wedges specified to have a failure angle of $45° - \phi/2 = 32.3°$. It was expected that the safety factor would be higher for this situation due to the reduced active loading. The safety factor for this situation was 1.71. Results for this situation are given in Table 13.

34. The final stability calculation included the effects of a relatively small cohesive capacity for the bottom layer of the active wedge. This cohesive capacity was assigned a value of 1 psf (a value much smaller than the cohesive capacity of concrete or most clay soils). The calculations for this situation resulted in a factor of safety of 2.28 (Table 14). Thus, a small cohesive force on the active side significantly contributes to the stability of the structure against sliding. The actual cohesive force available is considerably larger than that specified.

35. These calculations show that there is very little danger of sliding of the Arkabutla Intake Tower under the specified earthquake. The minimum factor of safety against sliding is 1.33.

Overturning

36. The Arkabutla Intake Tower is a comparatively short, broad-based tower with a large portion of its mass located in the lower one-third of the

structure. This low center of gravity combined with a relatively wide base provides reasonable stability against overturning. The most critical direction for overturning for this tower (assuming structural integrity is maintained) is North to South, thus, only this direction was analyzed. The structure is shown in Figure 22.

37. Calculations have shown that the center of mass for the tower is located between H/4 and H/3 from the base where H is the overall tower height. A summary of these calculations is given in Table 15. The cumulative mass distribution from the base to the top of the tower is given in Figure 23. This figure reflects the nonuniform mass distribution of the structure. To assume a uniform mass distribution (mass center at structure midheight) is obviously a conservative assumption for this tower for overturning calculations. It should be noted that a significant amount of the mass is concentrated near the top of the tower where mass effects are most noticeable for seismic conditions.

38. For the overturning calculations, a tower height (H) of 134 ft is used along with a base width (B) of 59 ft. As a preliminary calculation, West's formula (Meek 1978 and Ishiyama 1980) was used. This procedure shows that overturning is not possible when the first mode spectral acceleration (S_a) is less than the fraction *(B/H) of gravity* (g)(Kiger (1989) in Appendix A. At incipient tipping,

$$M \times S_a \times H/2 = M \times g \times B/2$$

or for the above assumptions,

$$S_a = B \times g/H$$

39. For the Arkabutla Tower (assumed to be on a stiff soil foundation), the frequency associated with the primary mode is 11.49 Hz (Table 4). The spectral acceleration associated with this frequency (period of 0.087 sec) is 0.529 g for a stiff soil site (from Figure 2). Since B x g/H = 0.44 g is less than 0.529 g, tipping may be of concern. Note that if the actual distance to the mass center is used (38.2 ft):

$$(59/2)/38.2 \times g = 0.77\ g$$

Since

$$S_a = 0.529\ g < 0.77\ g$$

tipping would not occur using the actual mass center. However, due to uncertainties in the exact location of the mass center, an additional calculation is required.

40. Housner (1963) has shown that for rigid, block-type structures (Figure 24) with uniform mass, height H, and base B, the earthquake energy input can be computed from the velocity response spectrum, S_v, yielding a critical angle, α, as follows:

$$\alpha = S_v \times \sqrt{\frac{M \times R}{g \times I_o}}$$

where

M = total structure mass

R = distance from the center of gravity to the corner about which tipping is expected

I_o = mass moment of inertia about that corner

α = angle between the vertical and R (Kiger (1989) in Appendix A).

Since α is a known value for an existing tower (under the uniform mass distribution assumption, i.e., the mass center is at H/2), it is convenient to calculate a critical spectral velocity and compare this number to the specified velocity for the Arkabutla earthquake (maximum of 1.31 ft/sec). If the calculated S_v matches the specified S_v, the probability of overturning would be one-half. Of course, a larger calculated S_v means a corresponding lower probability of overturning.

41. For the Arkabutla tower,

$$H = 135 \text{ ft}$$

$$B = 59 \text{ ft}$$

$$M = 717{,}187 \text{ lb X sec}^2/\text{ft}$$

$$R = \sqrt{(29.5)^2 + (67)^2} = 73.2 \text{ ft}$$

$$g = 32.2 \text{ ft/sec}^2$$

$$I_o \text{ (Table 16)} = M \times (B^2 + H^2)/12 = 1{,}281{,}195{,}168.0$$

$$\tan^{-1} \alpha = (59/2)/(134/2) = \alpha\ 23.76^\circ = 0.415 \text{ rad}$$

$$S_v = (0.415) \sqrt{\frac{(32.2)(1{,}281{,}195{,}1680.0)}{(717{,}187.2)(73.2)}}$$

$$S_v = 11.627 \text{ ft/sec} > 1.31 \text{ ft/sec}$$

Thus, overturning is very unlikely. Further, S_v increases to greater than 20 ft/sec when the apparent value of R of 48.4 ft is used. The calculations are quite conservative. As reflected in the specified spectral velocity for the Arkabutla area, a spectral velocity of 2.0 ft/sec represents strong ground motion in the United States (Housner 1963). Therefore, the overturning of Arkabutla Intake Tower is, for all practical purposes, not an event of major concern.

PART III: STRESS ANALYSIS OF STILLING BASIN

42. Stress analysis for the Arkabutla Stilling Basin was conducted on two 2-D cross sections. The analysis included a section at Station 104+80.0 and a section at Station 105+8.50. Figure 25 gives a plan view of the outlet works and stilling basin. It can be seen from this figure that both of the Stations investigated are in the upstream portion of the outlet channel. The remaining portion of the stilling basin was not analyzed as it consists primarily of T-wall-type construction.

43. The grid developed for Station 105+8.50 is shown in Figure 26. Due to symmetry of the cross section, only one-half of this structure was modeled. Thus, it was possible to use a fine mesh efficiently. Initially, three approaches were taken to modeling this structure. The goal was to obtain the most conservative analysis. The three approaches are shown in Figure 32. The loading for models I and III was obtained using the Mononobe-Okabe procedure (Leeman and Hynes 1988). Model I consisted of a fixed base structure with the lateral load applied to the vertical wall. Model III utilized identical loading, but with an elastic foundation. Model II utilized at-rest soil pressure in conjunction with lateral soil springs.

44. Static results for Model I (including only lateral earth loads and structural weight) are shown in Figure 28. The vectors shown in this plot represent principal stress values for the integration points of the elements. Tensile stresses are represented by lines with arrows while compressive stresses are depicted by line segments alone. The maximum static principal stress is 512.5 psi. Figure 29 gives a close-up of the area of greatest stress.

45. The Corps-developed program entitled Calculate Shear Moment and Thrust (CSMT) (Tracy et al. 1988) was used to extract a maximum moment from the finite element results. The section taken is shown in Figure 30 and the resulting stress distributions and forces are given in Figure 31. This figure shows a maximum moment of 123,400 in.-lb for this situation.

46. Application of the specified earthquake for the Arkabutla area leads to the stress vector plot shown in Figure 32. The contributions of the first five modes were combined using an absolute sum method for the dynamic analysis. Figures 33 through 35 show the first 3 mode shapes for this structure. As is evident in Figure 32, the maximum principal stress is 629.6 psi

for these conditions. Figure 36 gives a close-up of the high stress area for this cross section.

47. A CSMT section was also taken for the dynamic model as shown in Figure 30. The stress distribution and forces at the section are shown in Figure 37. The maximum moment for this situation is 210,600 in.-lb per inch of thickness (210.6 ft-k/ft).

48. Figure 38 contains the grid for Model II. The static results for this model are given in Figures 39 and 40, and the dynamic results are presented in Figures 41 and 42. Obviously, this is not as conservative as Model I, thus, this procedure was not used beyond this point.

49. Figure 43 contains the finite element grid for Model III. The static stress results for the structure are shown in Figures 44 and 45. It is apparent from these figures that the maximum structural stresses are slightly less than those for Model I. Thus, Model I was used throughout the stilling basin calculations.

50. Thus, for Station 105+8.50, the maximum observed principal stress is 829.6 psi and the maximum moment is approximately 210,600 in.-lb per inch (210.6 ft-k/ft). Obviously, at this high stress value, problems would occur in an unreinforced section. However, since the wall is reinforced, little damage should occur. A moment capacity check was made, and the wall has adequate capacity to resist the calculated moment without significant damage (Table 17). The ultimate moment capacity of the section was 400.11 ft-k/ft. This represents a factor of safety of 1.90 against collapse of the stilling basin wall. The "high" stress is not of great concern if the section has sufficient moment capacity. However, the calculated stress does indicate that some cracking of the exterior concrete is likely.

51. The model at Station 104+80.0 is shown in Figure 46. The static stress pattern for this model is given in Figures 47 and 48. As expected, this section is not as highly stressed as the comparatively slender section taken at Station 105+8.50. The maximum static stress observed is 194.4 psi.

52. The dynamic vector plot for section 104+80.0 is shown in Figures 49 and 50. The maximum dynamic stress is 374.2 psi. Thus, there is little danger of failure of this wall during an earthquake. Some cracking of the exterior concrete might occur, but structural integrity would be maintained.

53. The analysis for the upstream portion of the Arkabutla stilling basin shows it would survive the specified earthquake. Some cracking would probably occur, however, no significant structural damage would take place.

PART IV: CONCLUSIONS AND RECOMMENDATIONS

Conclusions

54. The results show that the tower will adequately resist the ground motion from the specified earthquake event and remain operational. The stilling basin sections chosen as the most critical will also adequately respond and remain intact. During the specified ground motions, the 8-ft* glass block windows (above elevations (el) 286.5 and 290.5**) could be susceptible to cracking and falling into the operating house onto personnel and equipment. It is recommended that a shield of some type (screen, plexiglass, etc.) be installed to protect the interior of the operating house from potential falling debris from the glass block windows during an earthquake. Also, other potential hazards should be inspected periodically. This would include adequacy of machinery connections.

55. Calculated tower deflections due to seismic loadings are small compared to expansion/contraction movements of the system. The calculated maximum relative displacement of the tower is 0.04 in. with respect to the base. This amount of seismicly induced deflection is very small compared to seasonal expansion/contraction of the bridge. Expansion pads on the bridge pier can easily accommodate the amount of deflection expected in the specified earthquake; therefore, loss of the bridge during the specified seismic event is not considered a threat.

56. Loss of electrical power to the tower is also a concern for this type of structure due to the use of electrical devices for gate operation. However, loss of electrical lines to the tower is not likely because they are supported by the bridge. In the event of outside power loss, an emergency generator is available as an emergency power source. This generator is maintained in a fully operational capacity at all times.

57. Some cracking of the stilling basin walls would be expected, given occurrence of the specified event. However, the reinforced cross section of the stilling basin is adequate to prevent significant damage. Any cracking

---

* A table of factors for converting non-SI units of measurement to SI (metric) units is presented on page 3.

** All elevations (el) cited herein are in feet referred to the National Geodetic Vertical Datum (NGVD) of 1929.

which occurs would be superficial and would not impair the structural integrity of the outlet works.

58. The stress analyses contained in this report were conducted assuming a fixed base condition for the tower and the stilling basin. This is generally a conservative approach but does not constitute a detailed investigation of the foundation properties or geotechnical considerations. All of the conclusions stated in the previous paragraphs assume that no foundation failures occur.

59. The outlet tunnels leading from the tower to the stilling basin are also of concern. The primary concern would be relative movement between the tower and the stilling basin which could result in collapse of the exit tunnels. However, this is not deemed likely due to the adequate safety factor for sliding of the intake tower. No relative movement of the tower and stilling basin would be expected provided the embankment is stable during the specified event.

Recommendations

60. Since the main tower structure will adequately resist the specified ground motion, no structural changes are necessary. However, during the specified ground motions the 8-ft glass block windows (above el 286.5 and 290.5) could be susceptible to cracking and falling into the operating house on personnel and equipment. Therefore, it is recommended that a shield of some type (screen, plexiglass, etc.) protect the interior of the operating house from potential falling debris from the glass block windows during an earthquake. Also, other potential hazards should be investigated. A check should be made on all base connections or attachments of essential equipment.

REFERENCES

ADINA R&D, INC. 1987. "ADINA-IN for ADINA Users Manual; A Program for Pre-Processing and Display of ADINA, ADINA-T, and ADINA-F Input Data," Report ARD 87-4, ADINA R&D, INC., Watertown, MA.

Goyal, Alok, and Chopra, Anil K. 1989. "Simplified Evaluation of Added Hydrodynamic Mass for Intake Towers," Journal of Engineering Mechanics, American Society of Civil Engineers, Vol 115, No. 7, pp 1688-1708.

Housner, George W. 1963 (Feb). "The Behavior of Inverted Pendulum Structures During Earthquakes," Bulletin of the Seismological Society of America, Vol 53, No. 2, pp 403-417.

Headquarters, Department of the Army. 1981. "Sliding Stability for Concrete Structures," Engineer Technical Letter 1110-2-256, Washington, DC.

_____. 1983. "Earthquake Design and Analysis for Corps of Engineers Dams," Engineer Regulation 1110-2-1806, Washington, DC.

_____. 1992. "Seismic Design and Evaluation of Intake Towers," Engineer Technical Letter 1110-8-8(FR), Washington, D.C.

Ishiyama, Yuji. 1980 (Jun). "Review and Discussion on Overturning of Bodies by Earthquake Motions," BRI Research Paper No. 85, Building Research Institute, Ministry of Construction.

Leeman, Harold J., Hynes, Mary E., Vanadit-Ellis, Wipawi, and Tsuchida, Takashi. 1988. "Seismic Stability Evaluation of Folsom Dam and Reservoir Project; Report 7: Upstream Retaining Wall," Technical Report GL-87-14, US Army Engineer Waterways Experiment Station, Vicksburg, MS.

Meek, J. W. 1978 (Sep-Oct). "Dynamic Response of Tipping Core Building," Earthquake Engineering and Structural Dynamics, Vol 6, No. 5, pp 437-454.

Nuttli, Otto W. 1979 (Nov). "State-of-the-Art for Assessing Earthquake Hazards in the United States, The Relation of Sustained Ground Acceleration and Velocity to Earthquake Intensity and Magnitude," Miscellaneous Paper S-73-1, Report 16, US Army Engineer Waterways Experiment Station, Vicksburg, MS.

Pace, Michael E., and Noddin, Virginia R. 1987. "Sliding Stability of Concrete Structures (CSLIDE)," Instruction Report ITL-87-5, US Army Engineer Waterways Experiment Station, Vicksburg, MS.

Seed, H. Bolton, Ugas, Celso, and Lysmer, John. 1974 (Nov). "Site-Dependent Spectra for Earthquake-Resistant Design," Report No. EERC 74-12, Earthquake Engineering Research Center, University of California, Berkeley, CA.

Tracy, Fred T., Hall, Robert L., Trahan, Kenneth W., Abraham, Jones, H. Wayne, and Huff, Dick. 1988. "User's Guide for Revised Computer Program to Calculate Shear, Moment, and Thrust (CSMT)," Instruction Report ITL-87-5, US Army Engineer Waterways Experiment Station, Vicksburg, MS.

US Army Engineer District, Vicksburg. 1982 (Jun). "Reconnaissance Report for a Special Engineering Investigation, Arkabutla Dam," Vicksburg, MS.

_____. 1984 (Aug). "Yazoo Headwater Project, Coldwater River and Tributaries, Mississippi, Arkabutla Dam, Outlet Works, and Spillway," Periodic Inspection Report No. 4, Vicksburg, MS.

Table 1

Scaled Response Spectrum Values for the Arkabutla Area

Period sec	Spectral Acceleration g's
0.006	0.280
0.052	0.349
0.072	0.420
0.088	0.498
0.106	0.559
0.125	0.620
0.142	0.673
0.161	0.720
0.187	0.763
0.215	0.789
0.231	0.794
0.239	0.795
0.247	0.796
0.268	0.792
0.289	0.779
0.328	0.749
0.366	0.661
0.425	0.618
0.455	0.574
0.505	0.515
0.548	0.468
0.6.0	0.422
0.663	0.380
0.736	0.346
0.796	0.321
0.884	0.294
0.992	0.268
1.075	0.245
1.175	0.222
1.310	0.196
1.437	0.170
1.610	0.146
1.753	0.137
2.055	0.129
2.289	0.127
2.476	0.121
2.660	0.114
2.784	0.109
2.886	0.104
2.990	0.099

Table 2

Material Properties for Arkabutla Tower Analyses

Description	Value
Young's modulus	3.12×10^6 psi
Poisson's ratio	0.20
Mass density	0.2246×10^{-3} lbf sec^2/in.^{4}
Compressive strength	3,000 psi

Table 3

Added Masses for the Arkabutla Tower

Elevation, ft	Description	Mass, lb sec^2/in.
215.0	Water	897.4 hor.
220.0	Water	984.5 hor.
225.0	Water	663.4 hor
230.0	Water, exit channel slabs, platforms	415.8 hor., 292.1 ver.
241.0	Exit channel slab, platforms	151.5 ver.
252.0	Bridge, platforms	219.3 ver.
265.0	Floor slab, platforms, machinery, columns	1,829.6 ver.
273.0	Windows, columns	21.5 ver.
281.5	Windows, columns	22.0 ver.
290.0	Windows, crane and rails, columns	87.1 ver.
298.0	Windows, columns	15.7 ver.
304.0	Roof, beams	333.8 ver.

Table 4

Dynamic Properties Without Added Masses

Frequency Number	Frequency rad/sec	Frequency cycles/sec	Period sec
1	83.37	13.27	0.07537
2	83.64	13.31	0.07512
3	192.20	30.59	0.03269
4	211.00	33.58	0.02978
5	250.50	39.87	0.02508
6	391.40	62.29	0.01605
7	426.80	67.93	0.01472
8	450.50	71.70	0.01395
9	462.10	73.54	0.01360
10	505.10	80.39	0.01244
11	630.00	100.30	0.00997
12	701.70	111.70	0.00895
13	714.70	113.80	0.00879
14	822.30	130.90	0.00764
15	843.70	134.30	0.00745
16	866.00	137.80	0.00726
17	905.50	144.10	0.00694
18	948.90	151.00	0.00662
19	1,090.00	173.50	0.00576
20	1,180.00	187.70	0.00533

Table 5

Dynamic Properties With Added Masses

Frequency Number	Frequency rad/sec	Frequency cycles/sec	Period sec
1	72.18	11.49	0.08705
2	72.38	11.52	0.08681
3	166.10	26.43	0.03783
4	182.30	29.02	0.03446
5	219.40	34.92	0.02864
6	349.00	55.54	0.01800
7	374.00	59.53	0.01680
8	396.70	63.14	0.01584
9	408.20	64.96	0.01539
10	446.20	71.02	0.01408
11	554.20	88.21	0.01134
12	612.20	97.43	0.01026
13	650.50	103.50	0.00966
14	738.20	117.50	0.00851
15	791.30	125.90	0.00794
16	793.00	126.90	0.00792
17	859.20	136.70	0.00731
18	889.50	141.60	0.00706
19	1,026.00	163.30	0.00612
20	1,067.00	169.90	0.00589

Table 6

Resulting Loads for a N-S Event

Element	Point	Moment in.-lb	Shear lb	Axial lb
1	1	1.57480E+09	2.40892E+06	8.81670E+06
	2	1.48317E+09	2.40892E+06	-8.81670E+06
2	1	1.48317E+09	2.41659E+06	8.07911E+06
	2	1.34687E+09	2.41659E+06	-8.07911E+06
3	1	1.34687E+09	2.43158E+06	7.17632E+06
	2	1.16356E+09	2.43158E+06	-7.17632E+06
4	1	1.16356E+09	2.43581E+06	6.27352E+06
	2	9.94532E+08	2.43581E+06	-6.27352E+06
5	1	9.94532E+08	2.44803E+06	5.13392E+06
	2	7.24814E+08	2.44804E+06	-5.13392E+06
6	1	7.24814E+08	1.96304E+06	3.94058E+06
	2	5.71723E+08	1.96304E+06	-3.94058E+06
7	1	5.71723E+08	1.28802E+06	2.64486E+06
	2	3.66017E+08	1.28802E+06	-2.64486E+06
8	1	3.66017E+08	1.16873E+06	1.15833E+06
	2	2.59771E+08	1.16873E+06	-1.15833E+06
9	1	2.59771E+08	1.02502E+06	9.15639E+05
	2	1.60335E+08	1.02502E+06	-9.15639E+05
10	1	1.60335E+08	8.09768E+05	6.94505E+05
	2	7.77385E+07	8.09768E+05	-6.94505E+05
11	1	7.77385E+07	5.73694E+05	4.52219E+05
	2	2.26639E+07	5.73694E+05	-4.52219E+05
12	1	2.26639E+07	3.14776E+05	2.36409E+05
	2	0.00000E+00	3.14776E+05	-2.36409E+05

Table 7

Resulting Stress Levels for a N-S Event

Node	El ft	Maximum Tensile Stress Due to Bending, psi	Maximum Compressive Stress Due to Axial Load, psi	Total psi
1	211.83	82.58	-50.88	31.70
12	215.00	77.78	-46.62	31.16
13	220.00	70.63	-41.41	29.22
14	225.00	61.02	-36.20	24.82
2	230.00	88.70	-51.13	37.57
3	241.00	66.67	-40.25	26.42
4	251.97	53.86	-27.56	26.30
5	265.00	64.88	-37.69	27.19
6	273.00	58.37	-38.14	20.23
7	281.50	36.03	-28.93	7.10
8	290.00	17.45	-18.42	-0.97
9	298.00	5.09	-6.88	-1.79

Table 8

Resulting Loads for an E-W Event

Element	Point	Moment in.-lb	Shear lb	Axial lb
1	1	1.52810E+09	2.09088E+06	8.81670E+06
	2	1.44856E+09	2.09088E+06	-8.81670E+06
2	1	1.44856E+09	2.12400E+06	8.07911E+06
	2	1.31435E+09	2.12400E+06	-8.07911E+06
3	1	1.31435E+09	2.21354E+06	7.17632E+06
	2	1.13478E+09	2.21354E+06	-7.17632E+06
4	1	1.13478E+09	2.31410E+06	6.27352E+06
	2	9.62910E+08	2.31410E+06	-6.27352E+06
5	1	9.62910E+08	2.36790E+06	5.13392E+06
	2	6.88676E+08	2.36790E+06	-5.13392E+06
6	1	6.88676E+08	1.85637E+06	3.94058E+06
	2	5.58174E+08	1.85637E+06	-3.94058E+06
7	1	5.58174E+08	1.24214E+06	2.64486E+06
	2	3.55907E+08	1.24214E+06	-2.64486E+06
8	1	3.55907E+08	1.02554E+06	1.15833E+06
	2	2.41808E+08	1.02554E+06	-1.15833E+06
9	1	2.41808E+08	9.43622E+06	9.15639E+05
	2	1.40454E+08	9.43622E+06	-9.15639E+05
10	1	1.40454E+08	7.54810E+05	6.94505E+05
	2	6.34638E+07	7.54810E+05	-6.94505E+05
11	1	6.34638E+07	4.76022E+05	4.52219E+05
	2	1.77657E+07	4.76022E+05	-4.52219E+05
12	1	1.77657E+07	2.46746E+05	2.36409E+05
	2	0.00000E+00	2.46746E+05	-2.36409E+05

Table 9

Resulting Stress Levels for an E-W Event

Node	El ft	Maximum Tensile Stress Due to Bending, psi	Maximum Compressive Stress Due to Axial Load, psi	Total psi
1	211.83	86.29	-50.88	35.41
12	215.00	81.80	-46.62	35.18
13	220.00	74.22	-41.41	32.81
14	225.00	64.08	-36.20	27.88
2	230.00	128.75	-51.13	77.62
3	241.00	96.80	-40.25	56.55
4	251.97	79.83	-27.56	52.27
5	265.00	82.83	-37.69	45.14
6	273.00	65.44	-38.14	27.30
7	281.50	38.01	-28.93	9.08
8	290.00	17.05	-18.42	-1.37
9	298.00	3.42	-6.88	-3.46

Table 10

Dynamic Properties of the 2-D E-W Model

Frequency Number	Frequency rad/sec	Frequency cycles/sec	Period seconds
1	56.95	9.06	0.11030
2	143.20	22.80	0.04387
3	207.50	33.03	0.03028
4	255.80	40.72	0.02456
5	296.30	47.16	0.02120
6	338.80	53.92	0.01855
7	404.10	64.31	0.01555
8	411.70	65.53	0.01526

Table 11

Dynamic Horizontal Deflections Along West Wall

Node Number	Elevation ft	Horizontal Displacement in.
1	304.0	0.1291
30	303.6	0.1282
245	300.8	0.1227
31	298.0	0.1167
666	294.2	0.0107
667	290.3	0.0981
60	286.5	0.0884
251	284.0	0.0819
253	281.5	0.0751
61	279.0	0.0694
595	277.0	0.0645
596	275.0	0.0597
90	273.0	0.0551
92	272.0	0.0530
597	269.7	0.0483
598	267.3	0.0439
120	265.0	0.0399

Table 12

Single Failure Plane Analysis Hydrostatic Water

For: Computed for Wedges

Wedge Number	Horizontal Loads Left Side kips	Horizontal Loads Right Side kips	Vertical Load kips
1	1524.977	0.000	-1894.562
2	0.000	1267.924	2460.785
3	141.852	45.125	65.643
4	13.398	0.000	82.651

Water Pressures on Wedges

Leftside Wedges

Wedge No.	Top Pressure ksf	Bottom Pressure ksf
1	1.969	0.000
2	0.000	3.750

Uplift Force on Structural Wedge kips

28.000

Rightside Wedges

Wedge No.	Top Pressure ksf	Bottom Pressure ksf
4	2.375	3.750

Wedge Number	Failure Angle deg	Total Length ft	Weight of Wedge kips	Submerged Length ft	Uplift Force kips
1	-5.659	967.030	5446.345	-319.436	-314.445
2	-5.659	1256.044	-4528.301	608.450	1140.844
3	0.000	92.750	390.879	92.750	28.000
4	32.300	41.171	47.851	41.171	126.087

Wedge Number	Net Force on Wedge kips
1	-533.545
2	359.490
3	89.549
4	84.507

Sum of forces on system ---- 0.000

Factor of safety ---- 1.328

Table 13

Single Failure Plane Analysis Hydrostatic Water

Force Computed for Wedges

Wedge Number	Horizontal Loads Left Side kips	Horizontal Loads Right Side kips	Vertical Load kips
1	119.083	0.000	-209.608
2	0.000	90.698	298.365
3	141.426	45.125	65.643
4	13.398	0.000	82.651

Water Pressures on Wedges

Leftside Wedges

Wedge No.	Top Pressure ksf	Bottom Pressure ksf
1	1.969	0.000
2	0.000	3.750

Uplift Force on Structural Wedge
kips

28.000

Rightside Wedges

Wedge No.	Top Pressure ksf	Bottom Pressure ksf
4	2.375	3.750

Wedge Number	Failure Angle deg	Total Length ft	Weight of Wedge kips	Submerged Length ft	Uplift Force kips
1	-32.300	125.958	425.295	-58.950	-58.029
2	-32.300	179.294	-323.921	112.286	210.535
3	0.000	92.750	389.358	92.750	28.000
4	32.300	41.171	47.851	41.171	126.087

Wedge Number	Net Force on Wedge kips
1	-168.063
2	39.688
3	48.022
4	80.352

Sum of forces on system ---- 0.000

Factor of safety ---- 1.708

Table 14

Single Failure Plane Analysis Hydrostatic Water

Force Computed for Wedges

Wedge Number	Horizontal Loads: Left Side kips	Horizontal Loads: Right Side kips	Vertical Load kips
1	23.586	0.000	-68.314
2	0.000	9.399	115.918
3	141.426	45.125	65.643
4	13.398	0.000	82.651

Water Pressures on Wedges

Wedge No.	Leftside Wedges: Top Pressure ksf	Leftside Wedges: Bottom Pressure ksf
1	1.969	0.000
2	0.000	3.750

Uplift Force on Structural Wedge kips
28.000

Wedge No.	Rightside Wedges: Top Pressure ksf	Rightside Wedges: Bottom Pressure ksf
4	2.375	3.750

Wedge Number	Failure Angle deg	Total Length ft	Weight of Wedge kips	Submerged Length ft	Uplift Force kips
1	-49.688	53.635	84.234	-41.310	-40.664
2	-49.688	91.010	-33.567	78.685	147.534
3	0.000	92.750	389.358	92.750	28.000
4	32.300	41.171	47.851	41.171	126.087

Wedge Number	Net Force on Wedge kips
1	3.756
2	-92.892
3	12.015
4	77.120

Sum of forces on system ---- 0.000

Factor of safety ---- 2.276

Table 15

Mass Distribution and Location of Mass Center

Approximate Elevation, ft	Mass, lb $sec^2/in.$
304.0	333.8
301.0	555.9
298.0	15.7
294.0	529.5
290.0	87.1
285.75	550.2
281.5	22.0
277.25	550.2
273.0	21.5
269.0	662.7
265.0	1,829.6
258.5	3,371.5
251.97	219.3
246.48	2,895.2
241.0	151.5
235.5	2,977.3
230.0	292.1
220.9	8,488.8
202.5	8,680.3
184.1	12,886.9
184.0	2,359.3
179.2	1,663.6
172.5	10,621.6

Note: Using the base as a reference point, the distance to the mass center is given by:

$$D = [333.8(134.0) + 555.9(131.0) + 15.7(128.0) + 529.5(124.0) + 87.1(120.0) + 550.2(115.75) + 22.0(111.5) + 550.3(107.25) + 21.5(103.0) + 662.7(99.0) + 1829.6(95.0) + 3371.5(88.5) + 219.3(81.97) + 2895.2(76.48) + 151.5(71.0) + 2977.3(65.5) + 292.1(60.0) + 8488.8(50.9) + 8680.3(32.5) + 2359.3(14.0) + 12886.9(14.1) + 1663.6(9.2) + 10621.6(2.5)]/59765.6$$

$$= 38.4 \text{ ft}$$

Table 16

Equations for Mass Moment of Inertia

Body	Moment of inertia	Product of inertia
Cylinder 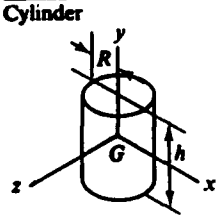	$I_x = I_z = \frac{m}{12}(3R^2 + h^2)$ $I_y = mR^2/2$	$I_{xy} = I_{yz} = I_{zx} = 0$
Sphere 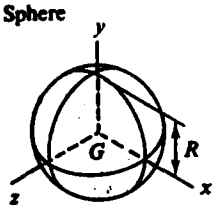	$I_x = I_y = I_z = 2mR^2/5$	$I_{xy} = I_{yz} = I_{zx} = 0$
Rectangular prism 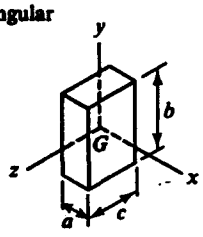	$I_x = m(b^2 + c^2)/12$ $I_y = m(c^2 + a^2)/12$ $I_z = m(a^2 + b^2)/12$	$I_{xy} = I_{yz} = I_{zx} = 0$
Triangular wedge 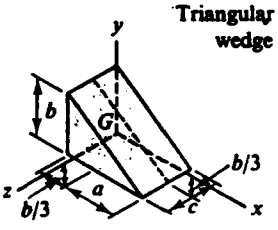	$I_x = m(2b^2 + 3c^2)/36$ $I_y = m(2a^2 + 3c^2)/36$ $I_z = m(a^2 + b^2)/18$	$I_{xy} = -mab/36$ $I_{yz} = 0$ $I_{zx} = 0$
Cone 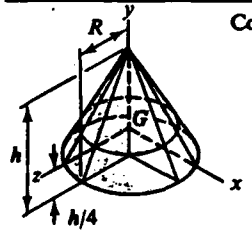	$I_x = I_z = 3m(h^2 + 4R^2)/80$ $I_y = 3mR^2/10$	$I_{xy} = I_{yz} = I_{zx} = 0$

Table 17

Moment Capacity Check for Arkabutla Stilling Basin Wall

Input Data	
Concrete Strength, ksi	3.000
Concrete Modulus, ksi	3120.000
Modulus of Rupture, ksi	0.300
Ordinary Reinf. Concrete - No Prestressing	
Ordinary Tensile Steel Yield, ksi	40.000
Ordinary Compression Steel Yield, ksi	0.000
Total Section Depth, in.	48.000
Depth Top to Neutral Axis-Uncracked Section, in.	24.808
Uncracked Section Moment of Inertia, $in.^4$	120369.9
Area of Total Section, $in.^2$	599.06
Beta Value	0.850

Concrete Compression Area Data

Segment No.	Top Width, in.	Bottom Width, in.	Height, in.
1	12.00	12.00	48.00

Ordinary Tensile Steel Data

Level No.	Depth from Top of Member, in.	Area, in^2
1	45.00	2.780

Design Values

Concrete Strength, ksi	3.000
Ordinary Reinf. Concrete - No Prestressing	
Ordinary Tensile Steel Yield, ksi	40.000
Ordinary Compression Steel Yield, ksi	0.000
Total Section Depth, in.	48.000
Depth to Neutral Axis at Failure, in.	4.282
Beta Value	0.850

Ordinary Tensile Steel Data

Level No.	Depth from Top of Member, in.	Stress, ksi
1	45.00	40.00

Ultimate Moment Capacity, ft-k	400.11
Factored Ultimate Moment, ft-k	360.099
Cracking Moment, ft-k	129.756
Ratio : Ultimate Moment/ Cracking Moment	3.08

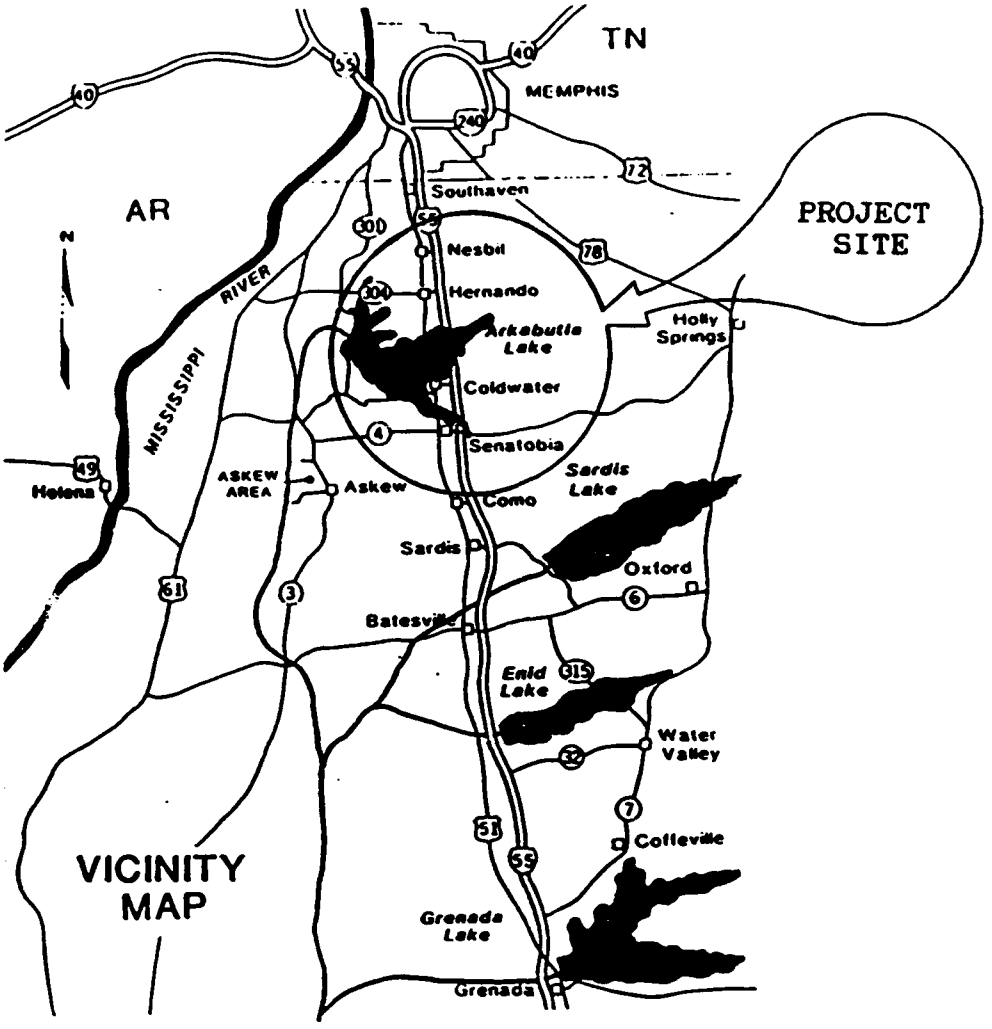

Highway Mileage to Arkabutla Dam

Memphis, TN	30
Grenada, MS	79
Vicksburg, MS	202
Tupelo, MS	111
St. Louis, MO	327
New Orleans, LA	363
Little Rock, AR	165

Figure 1. Vicinity map

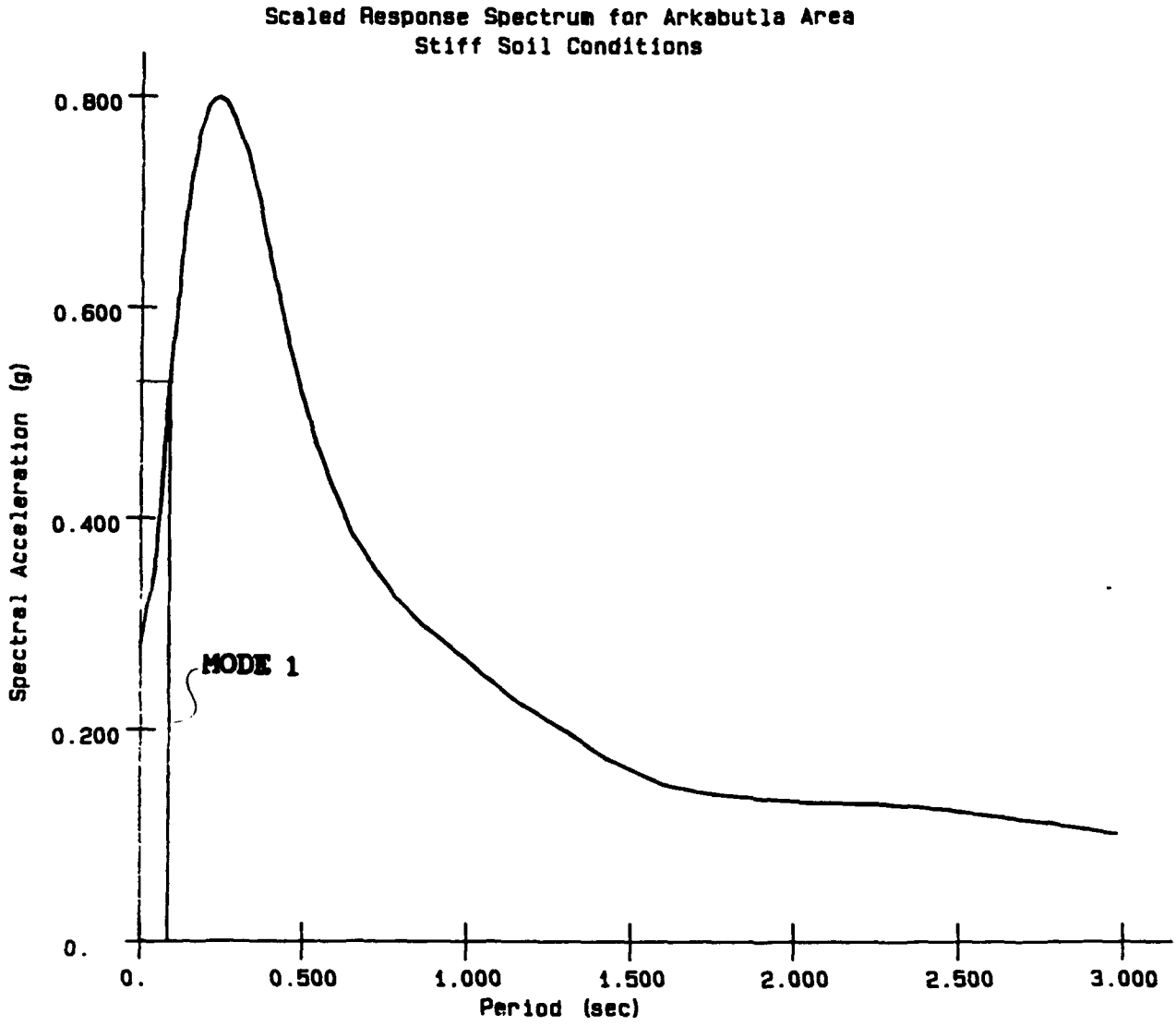

Figure 2. Response spectrum for the Arkabutla area

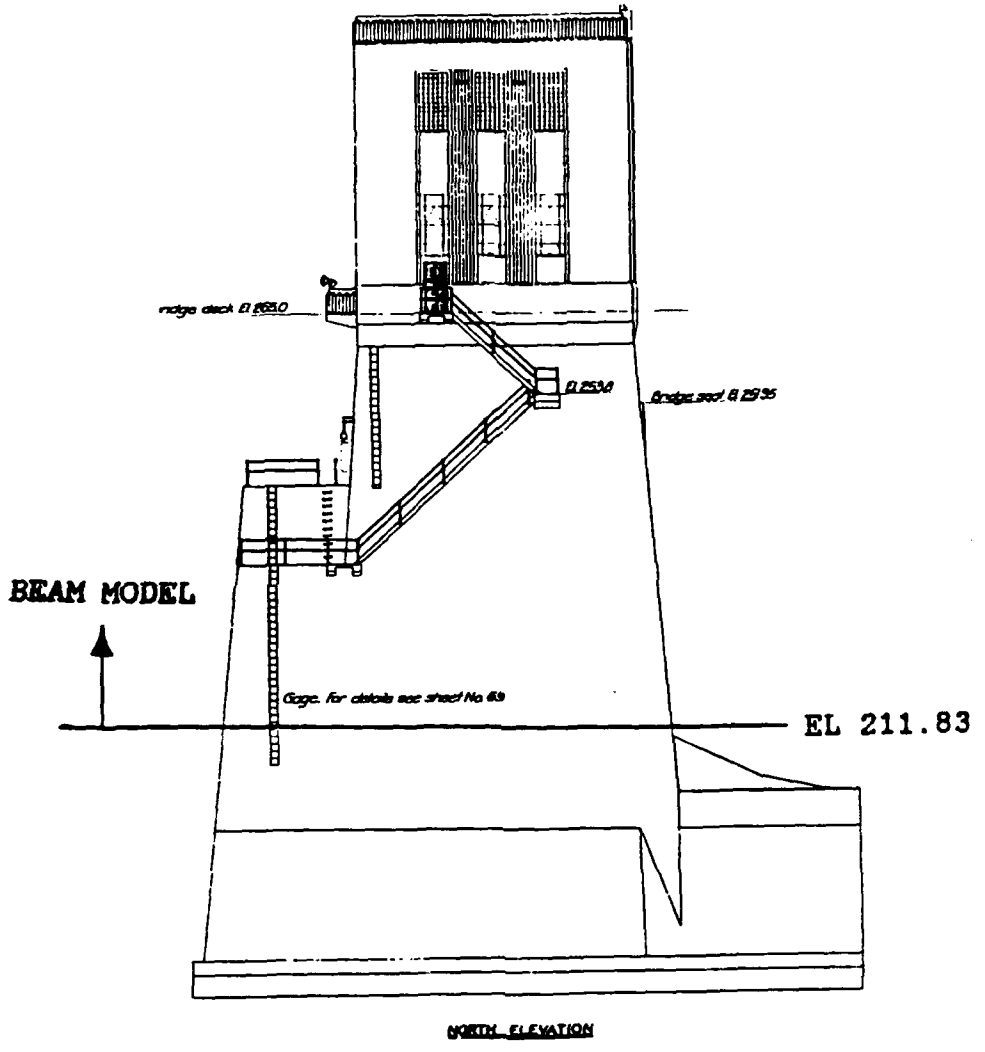

Figure 3. Portion of Arkabutla Tower modeled

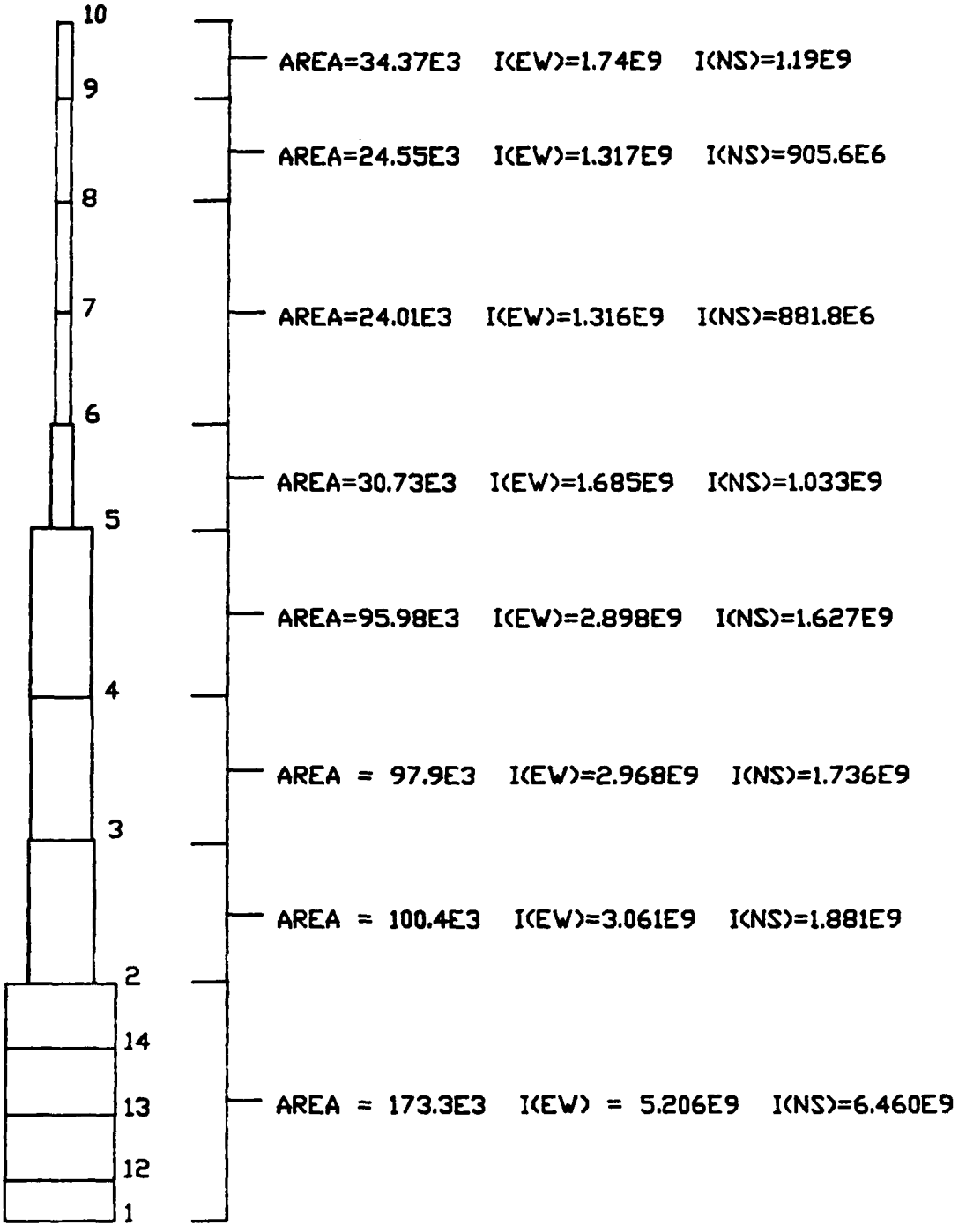

Figure 4. Beam model for the Arkabutla Tower (Area in in.^{2}, Moment of Inertia in in.^{4})

CENTROID:

X = 317.2
Y = 273.0
AREA = 173.3E3
I_X = 5.206E9
I_Y = 6.460E9
I_{XY} = 40.31E6

PRINCIPAL:

I_X = 5.206E9
I_Y = 6.460E9
I_{XY} = 0.00E0

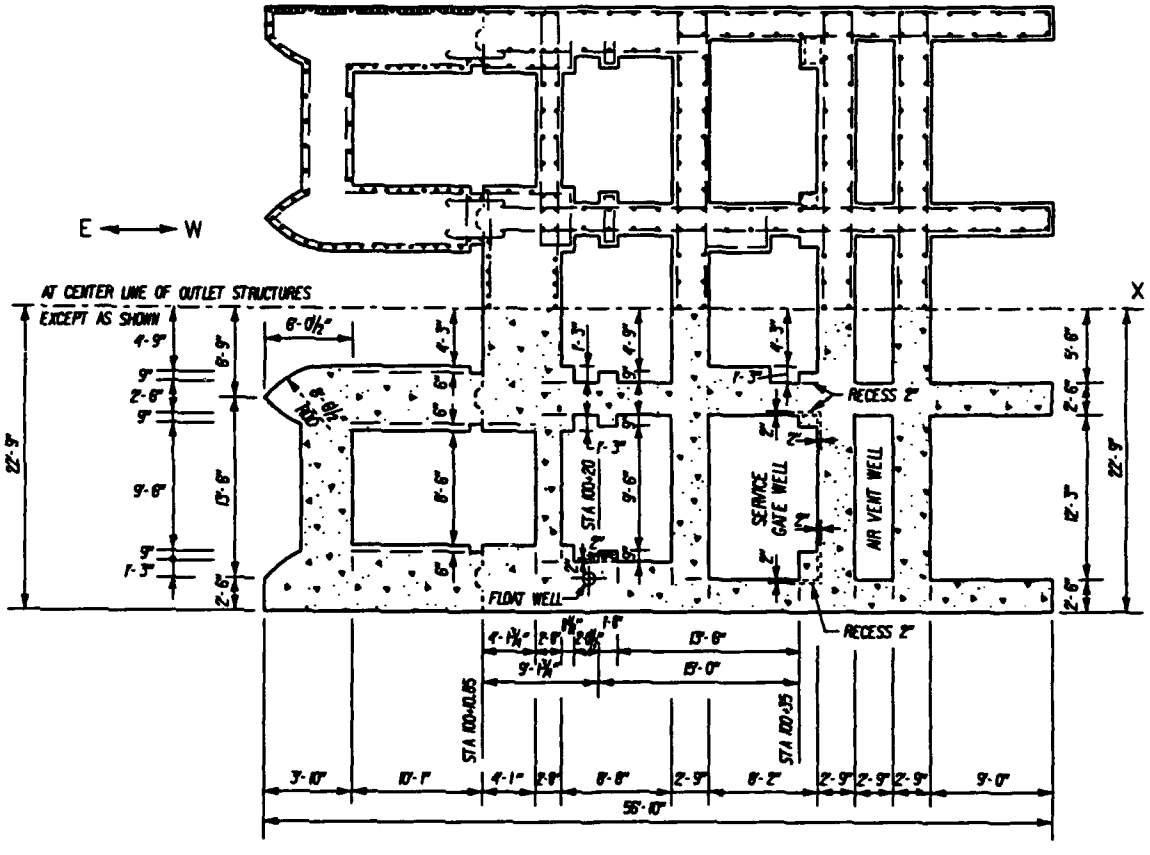

SECTION C-C

$I^{x}_{calc} = (49)(210)^3/12 + (24)(546)^3/12 + (33)(546)^3(3)/12 + 2(46)(216)^3/12 + 2(170)(54)^3/12 + 2(104)(45)^3/12 + 2(98)(30)^3/12 + 4(33)(30)^3/12 + 4(108)(30)^3/12 + 2(98)(39)^3/12 + 2(104)(30)^3/12 + 2(121)(48)^3/12 + 2(9522)(165)^2/$

$2(5808)(81)^2 + 2(9180)(246)^2 + 2(4680)(250.5)^2 + 2(3120)(81)^2 + 2(3822)(76.5)^2 + 2(2940)(258)^2 + 2(990)(258)^2 + 2(990)(81)^2 + 2(3240)(81)^2 + 2(3240)(258)^2 =$

$5.184 \times 10^9 \text{ in}^4 \approx 5.206 \times 10^9 \text{ in}^4$ O.K. Check for I_x

Figure 5. Cross section 1 (el 211.83 to el 230.0)

CENTROID:

X = 244.5
Y = 273.0
AREA = 100.4E3
I_X = 3.061E9
I_Y = 1.881E9
I_{XY} = 0

PRINCIPAL:

I_X = 3.061E9
I_Y = 1.881E9
I_{XY} = 0.00E0

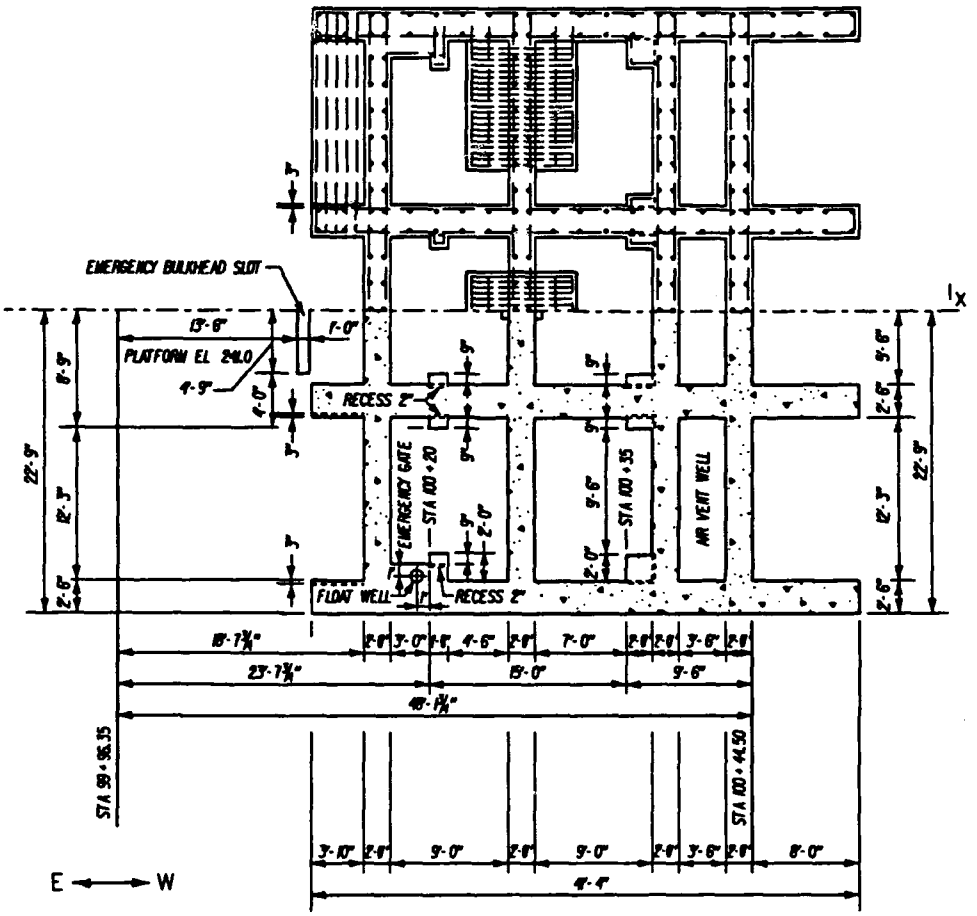

SECTION E-E

Figure 6. Cross section 2 (el 230.0 to 241.0)

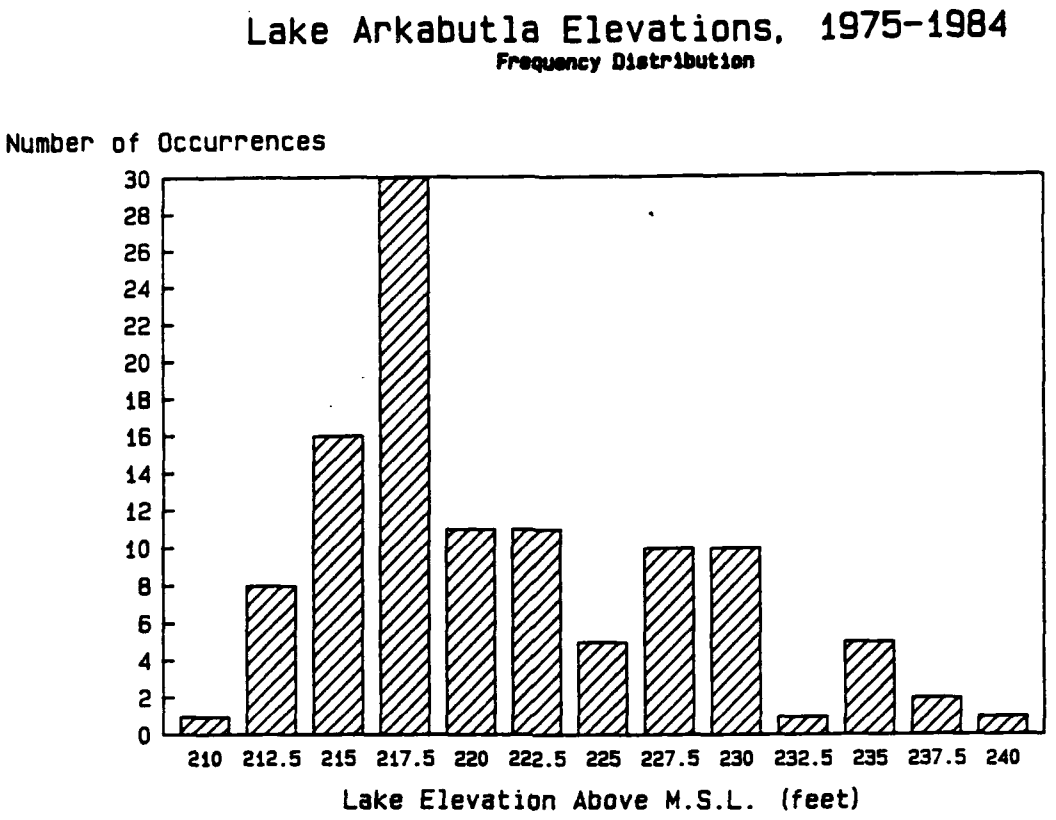

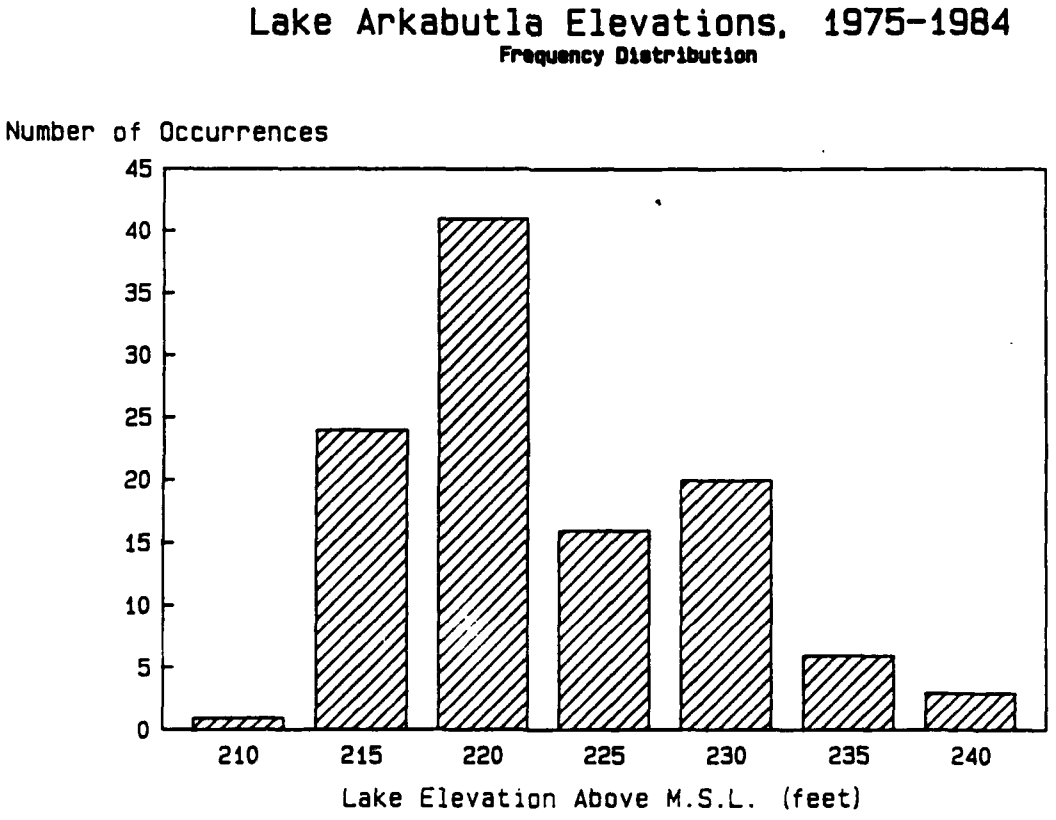

Figure 7. Histograms for pool elevations at Arkabutla Lake

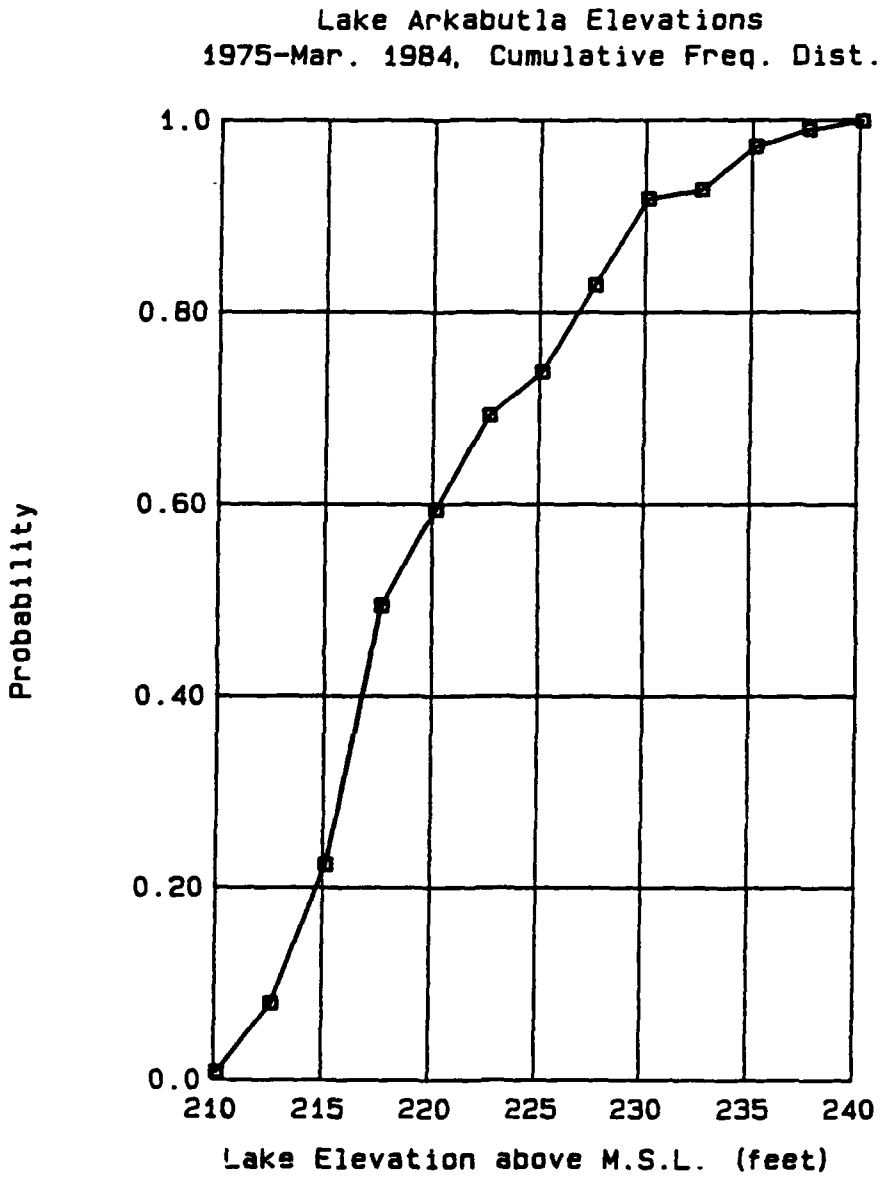

Figure 8. Probability plot for Arkabutla Lake elevations

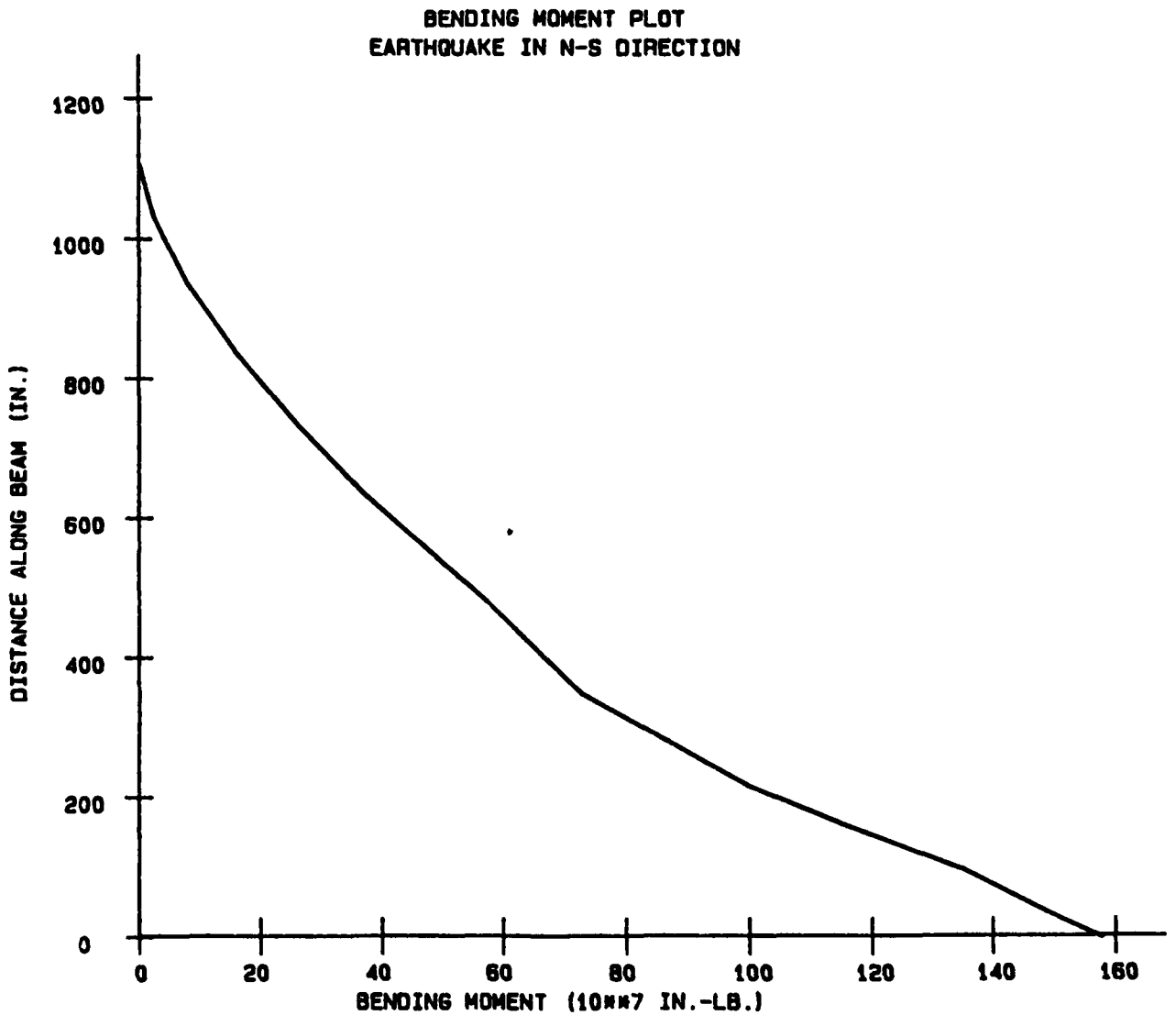

Figure 9. Bending moment plot for an earthquake in the N-S direction

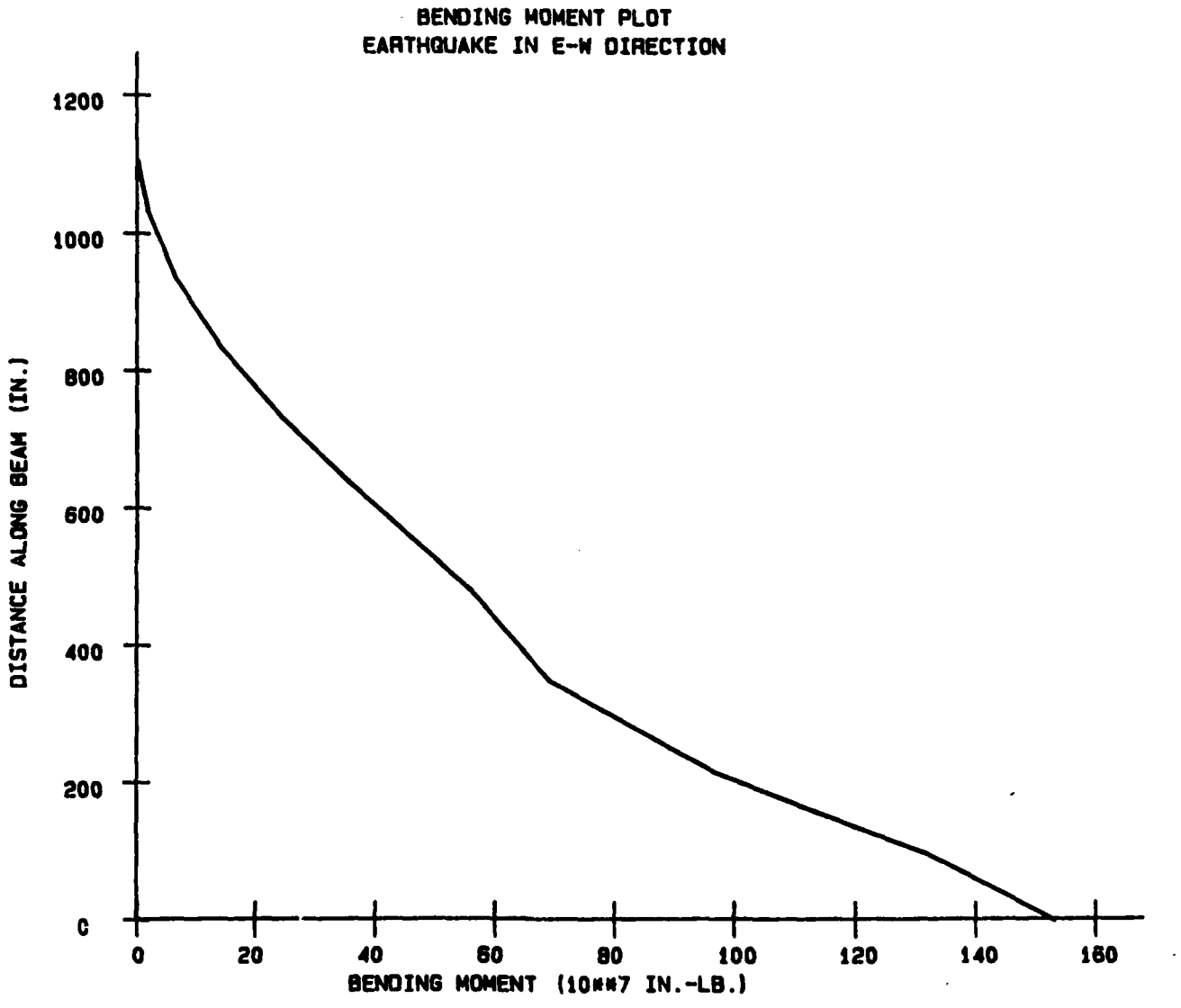

Figure 10. Bending moment plot for an earthquake in the E-W direction

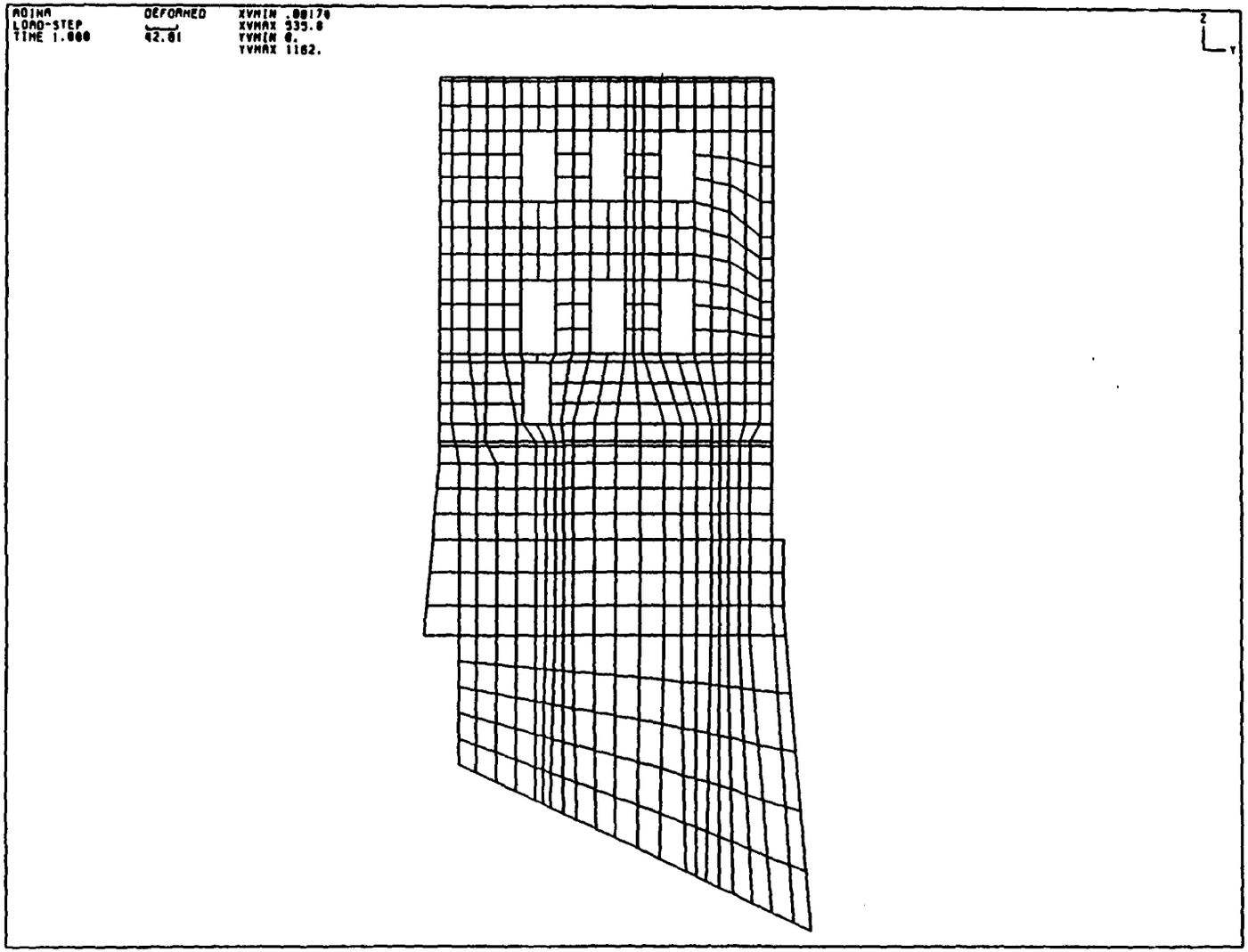

Figure 11. Grid for 2-D E-W finite element model

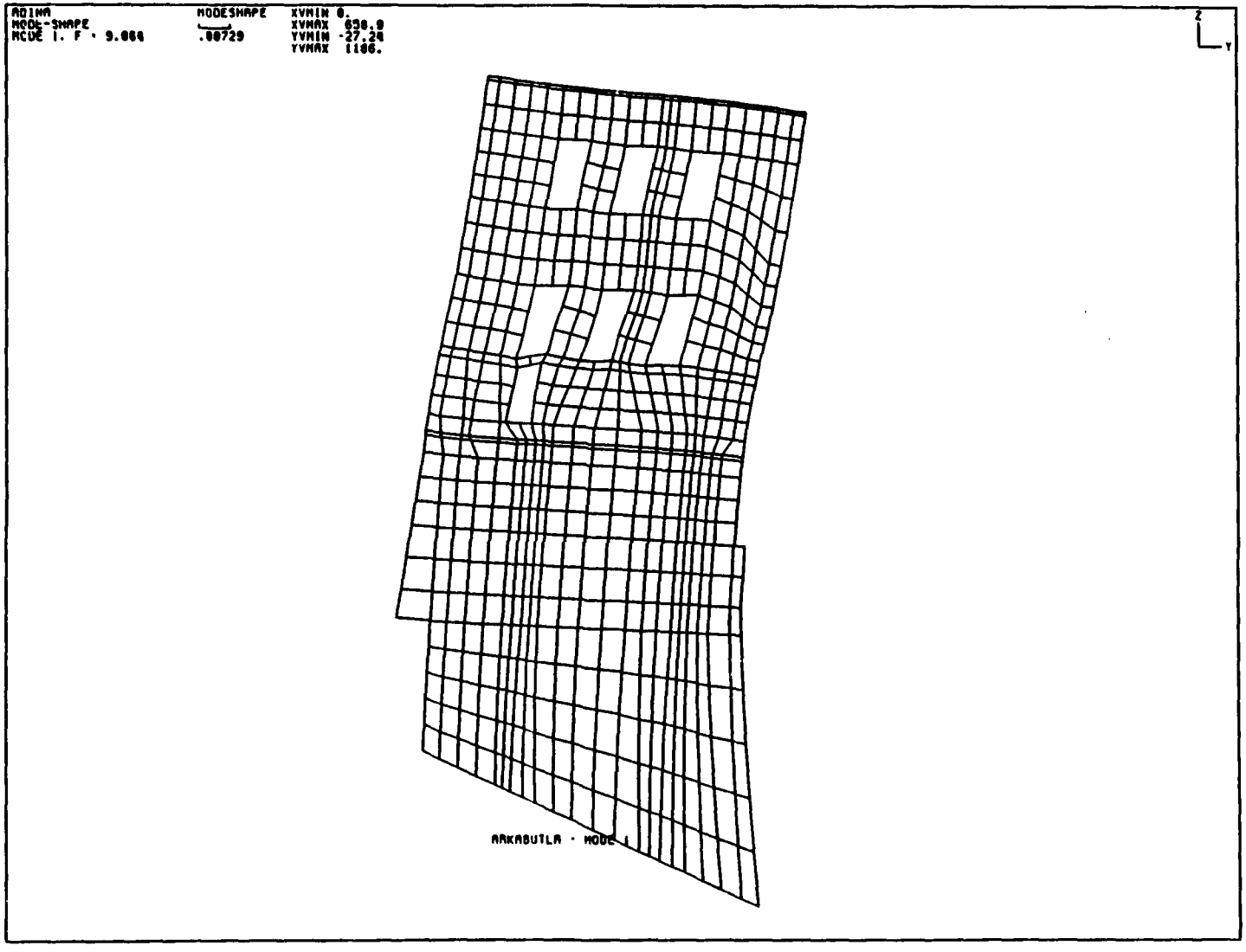

Figure 12. Mode 1 for 2-D model

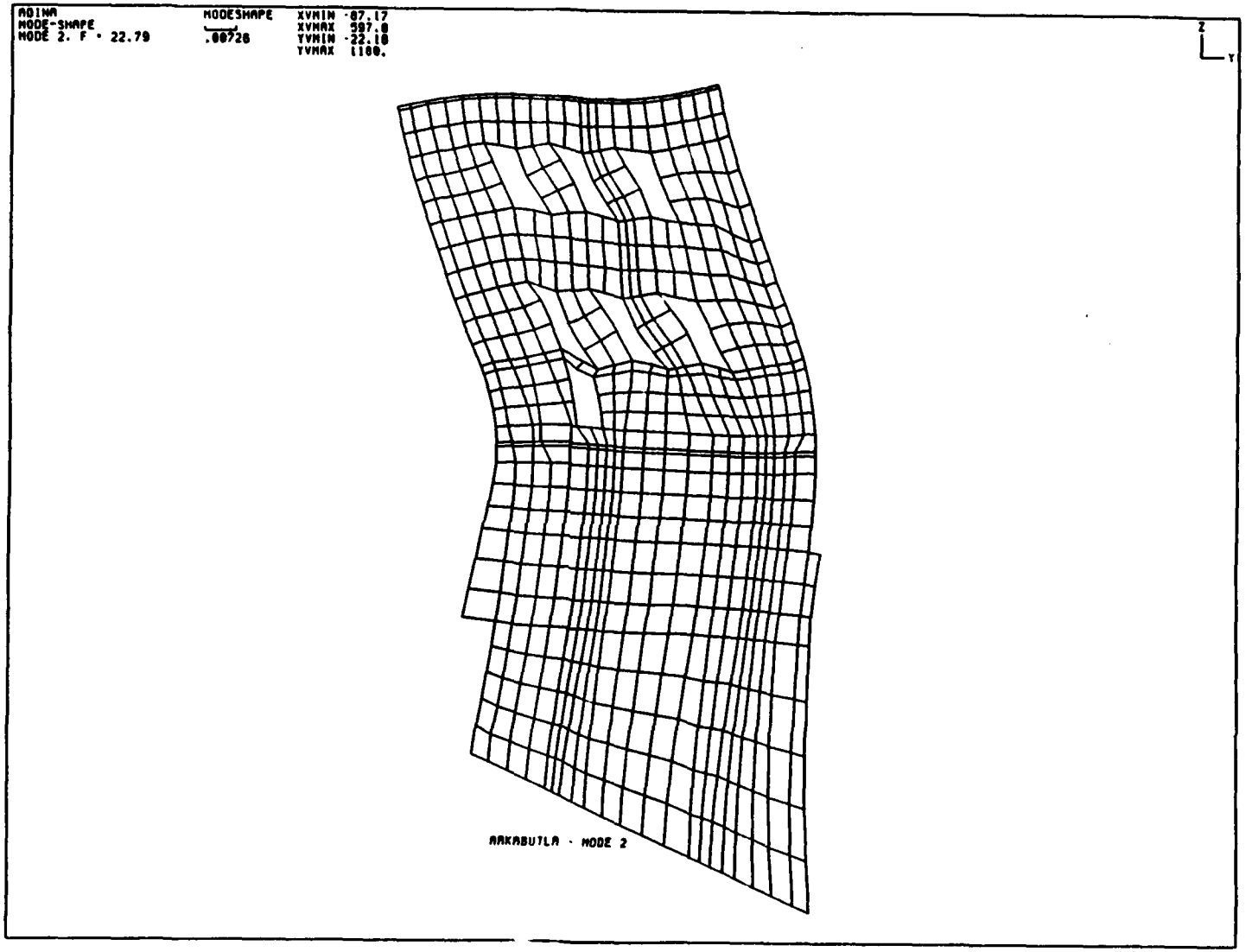

Figure 13. Mode 2 for 2-D model

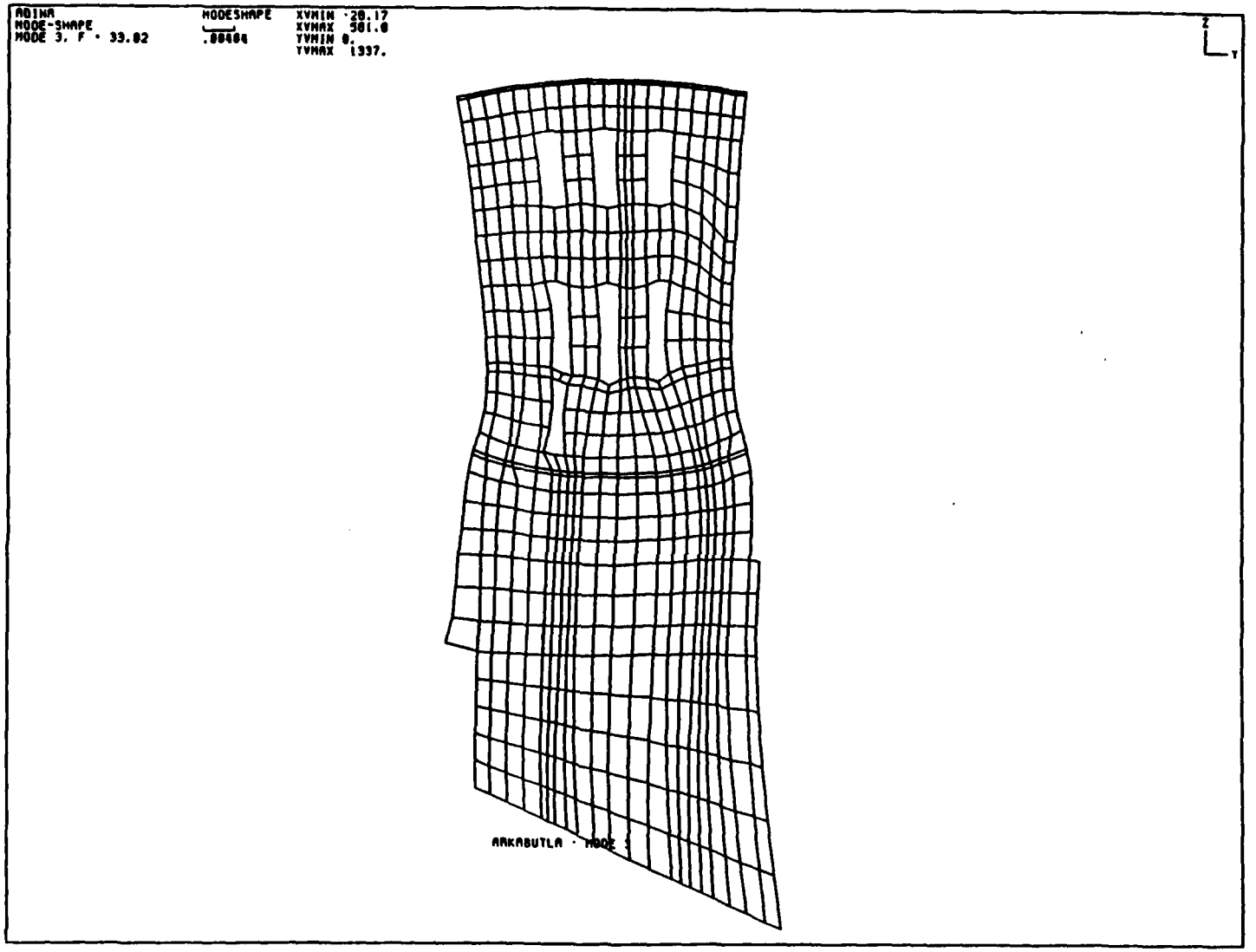

Figure 14. Mode 3 for 2-D model

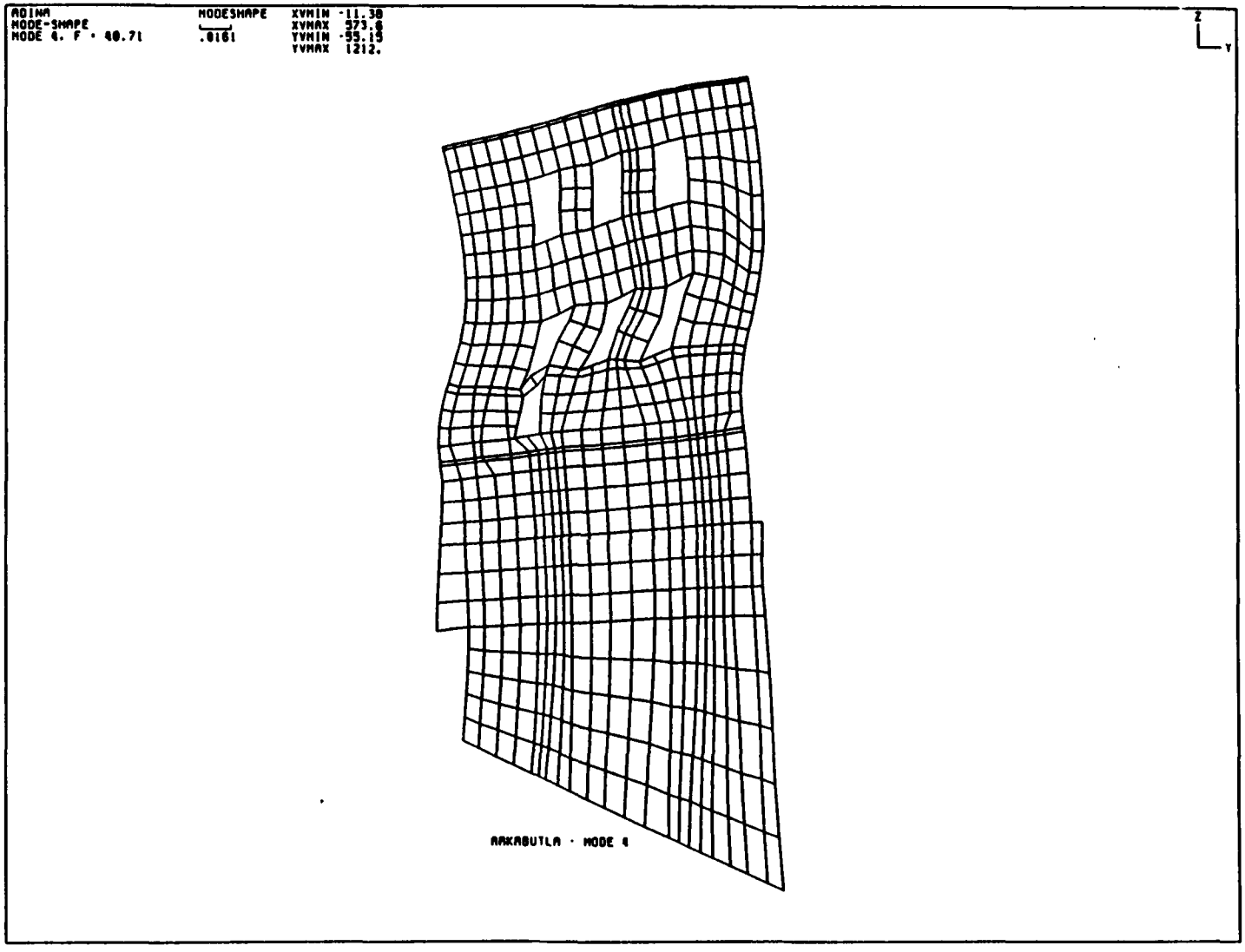

Figure 15. Mode 4 for 2-D model

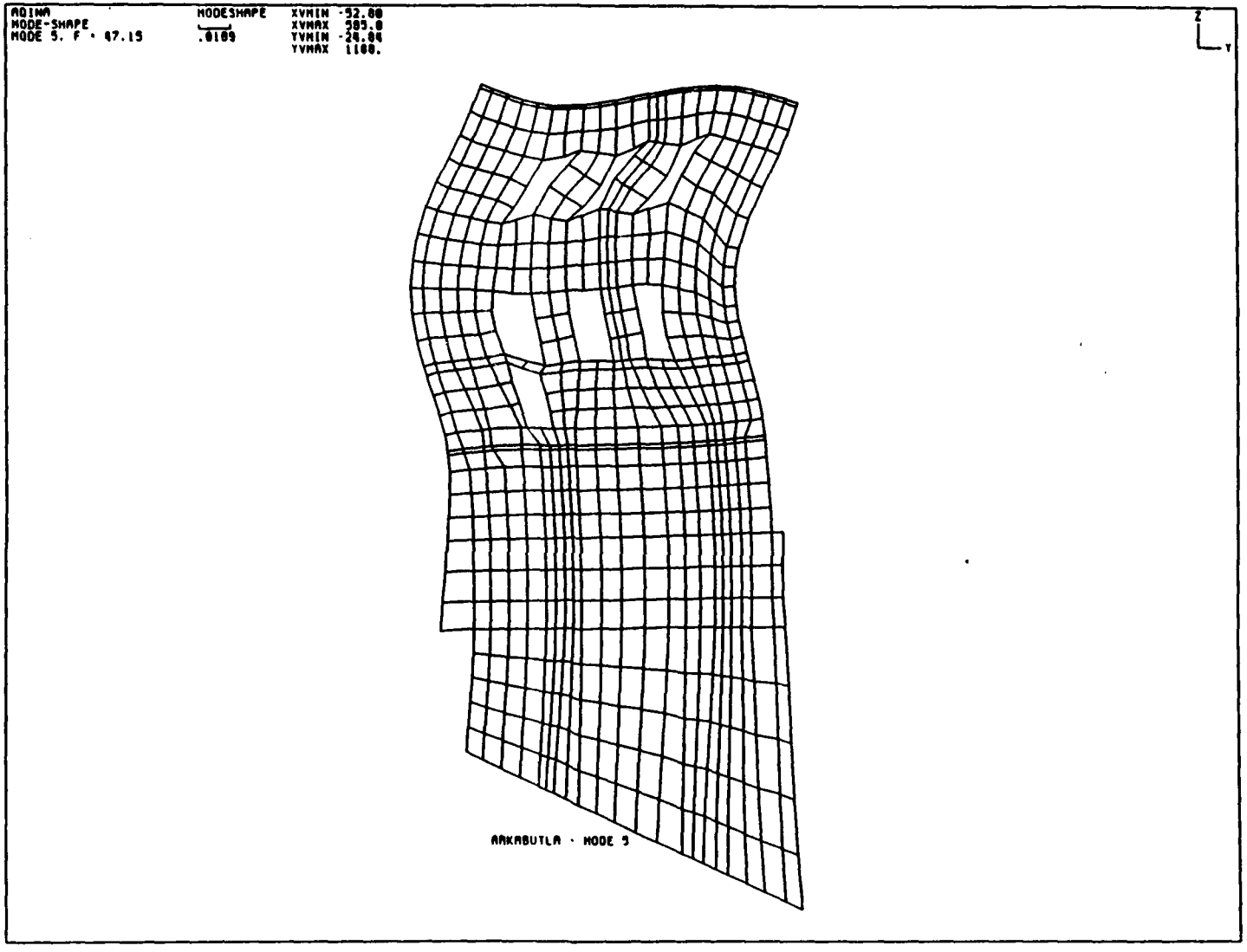

Figure 16. Mode 5 for 2-D model

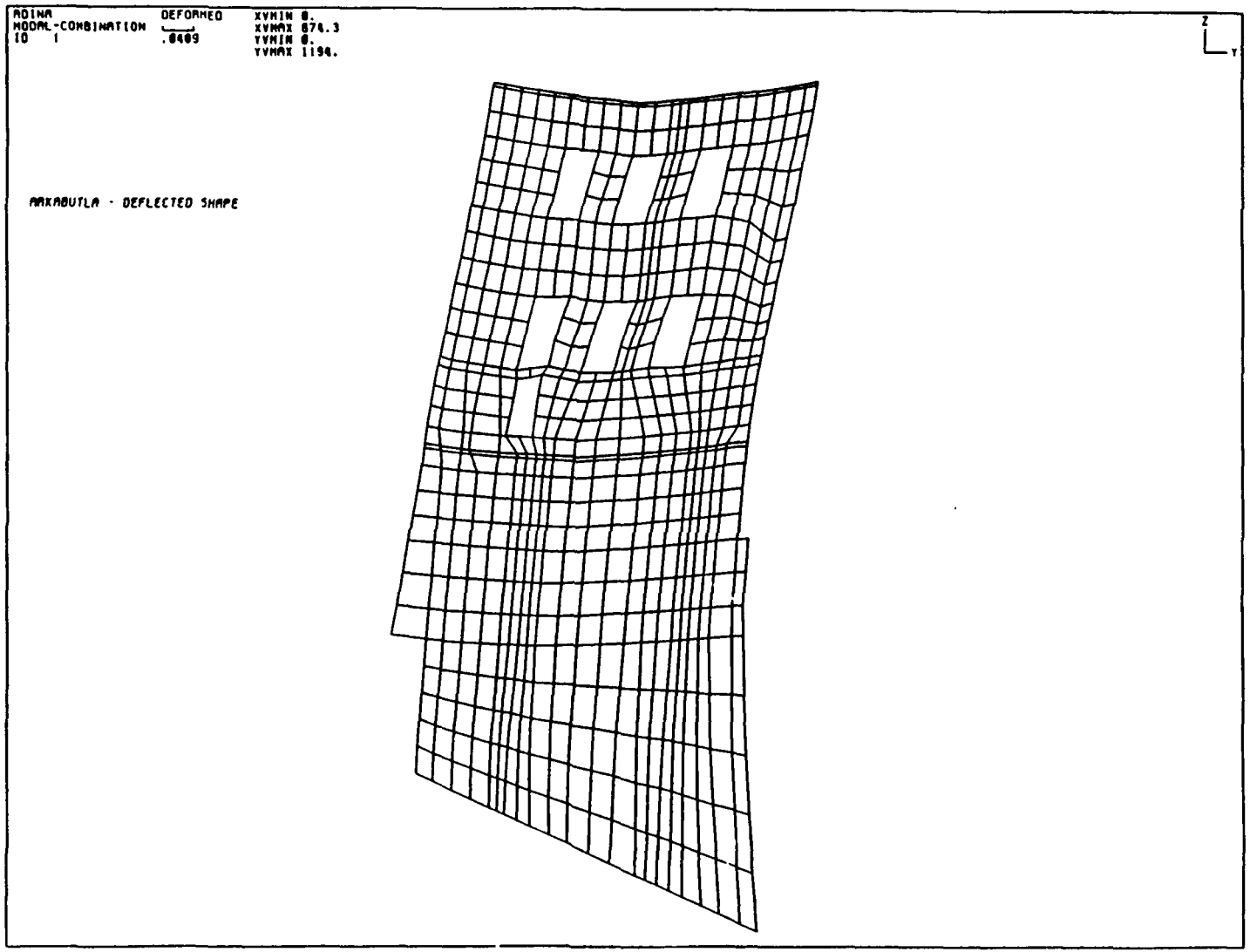

Figure 17. Deflected shape for the 2-D model - dynamic loading

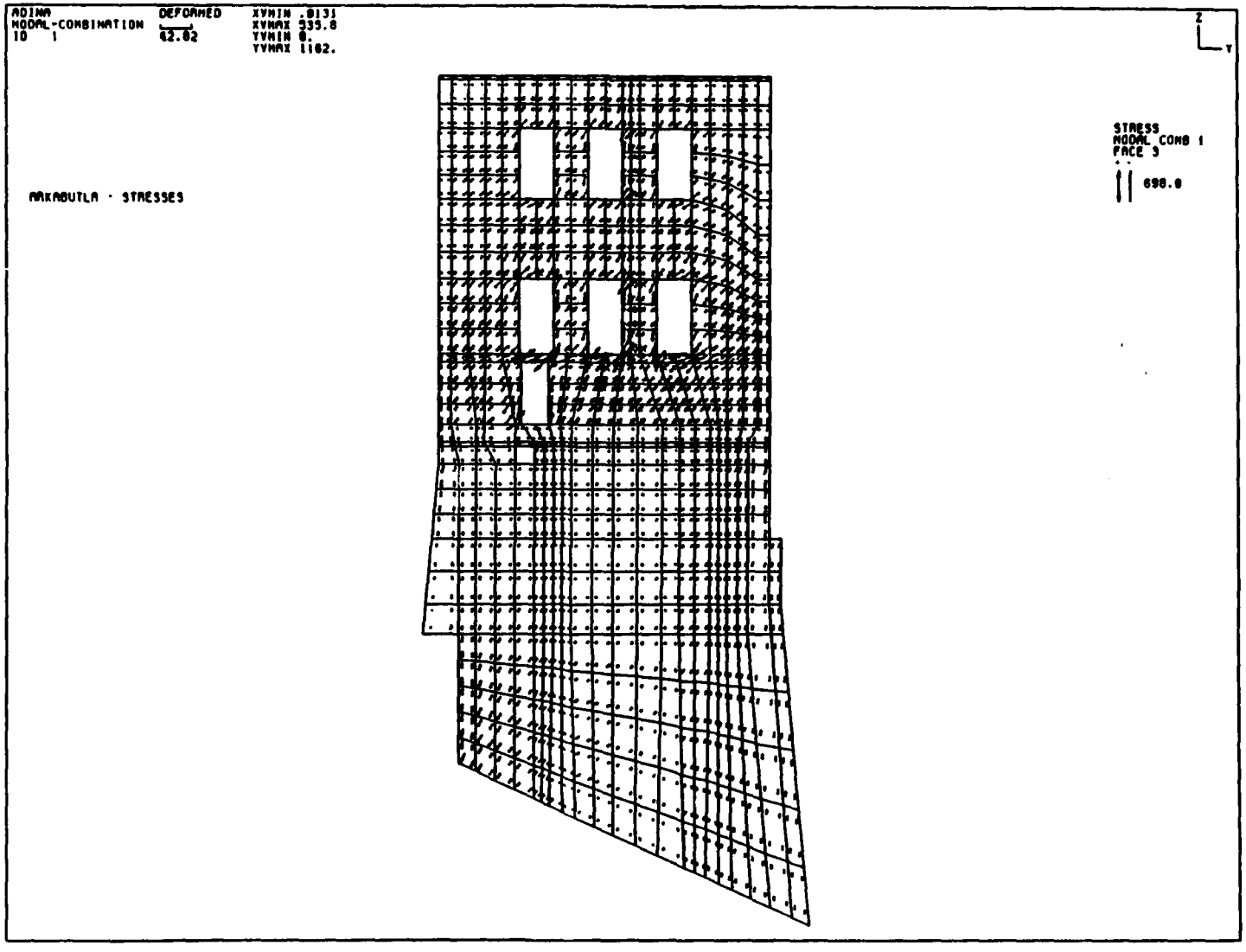

Figure 18. Principal stress vector plot for dynamic loading of the 2-D model

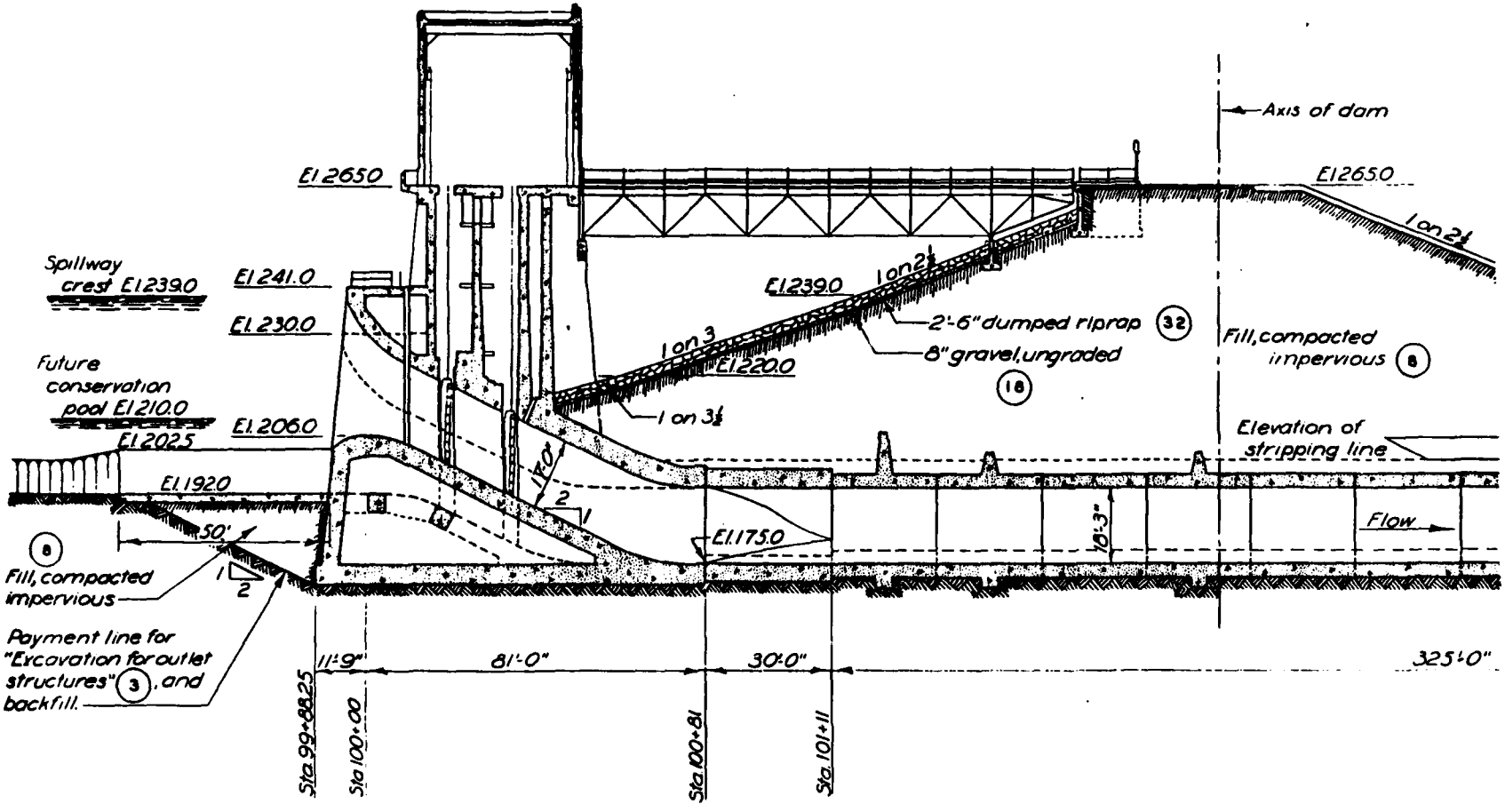

Figure 19. Cross-sectional view of the Arkabutla Tower

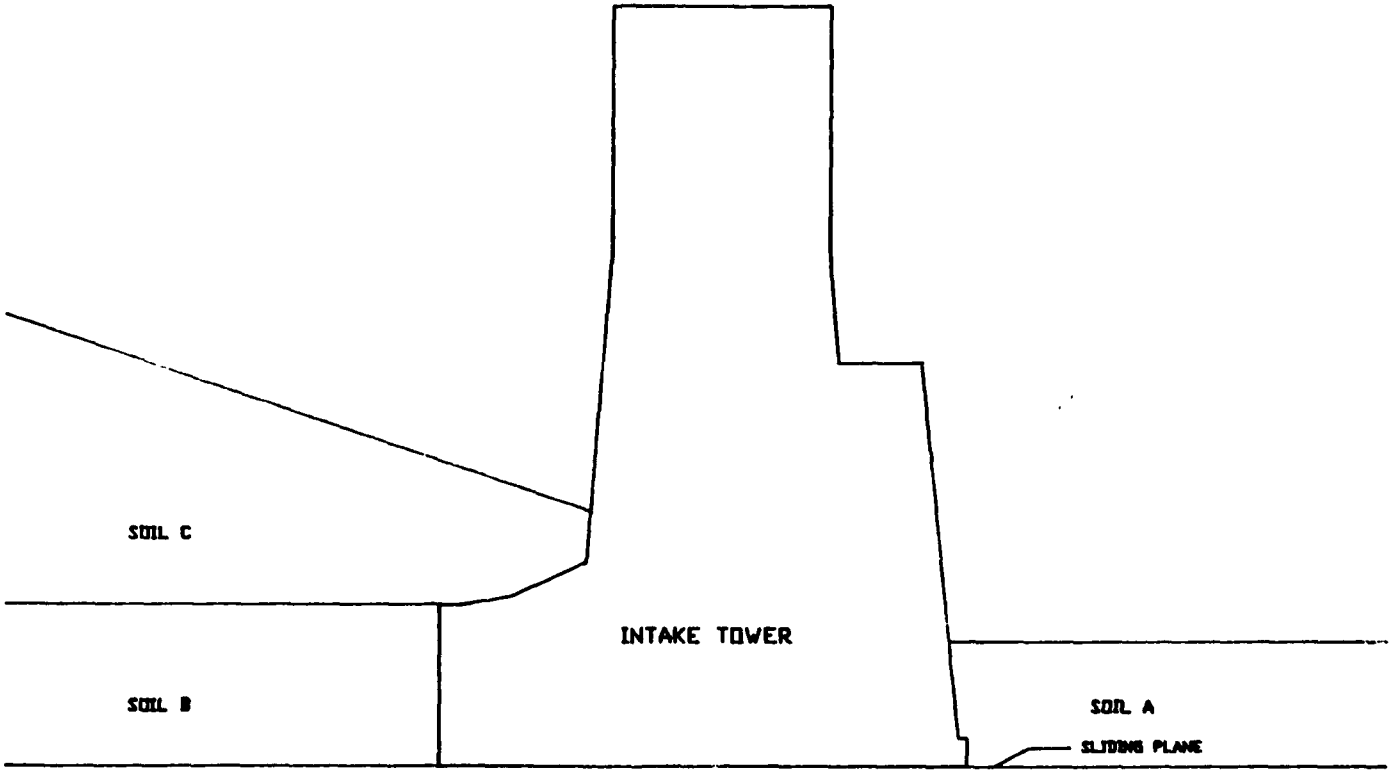

Figure 20. Model for sliding stability calculations

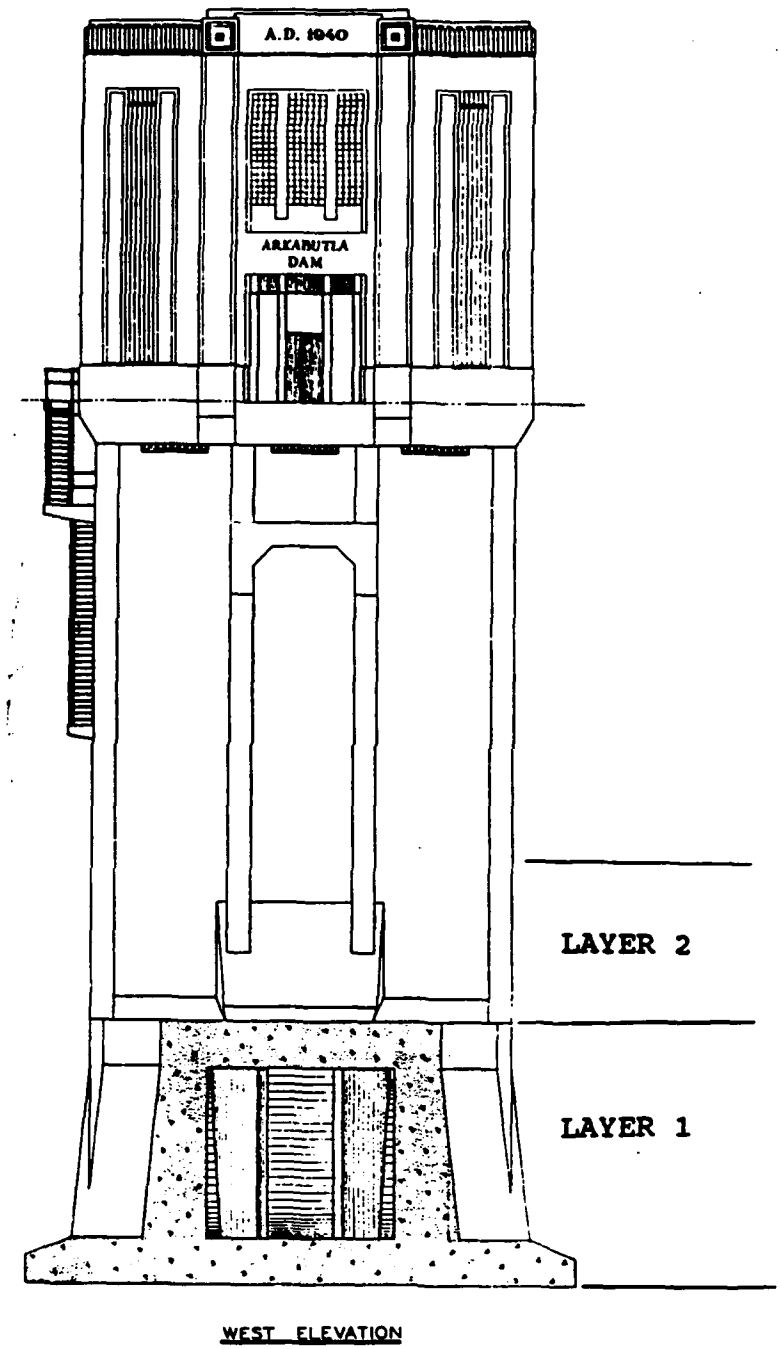

Figure 21. View showing the layers used in the active wedge

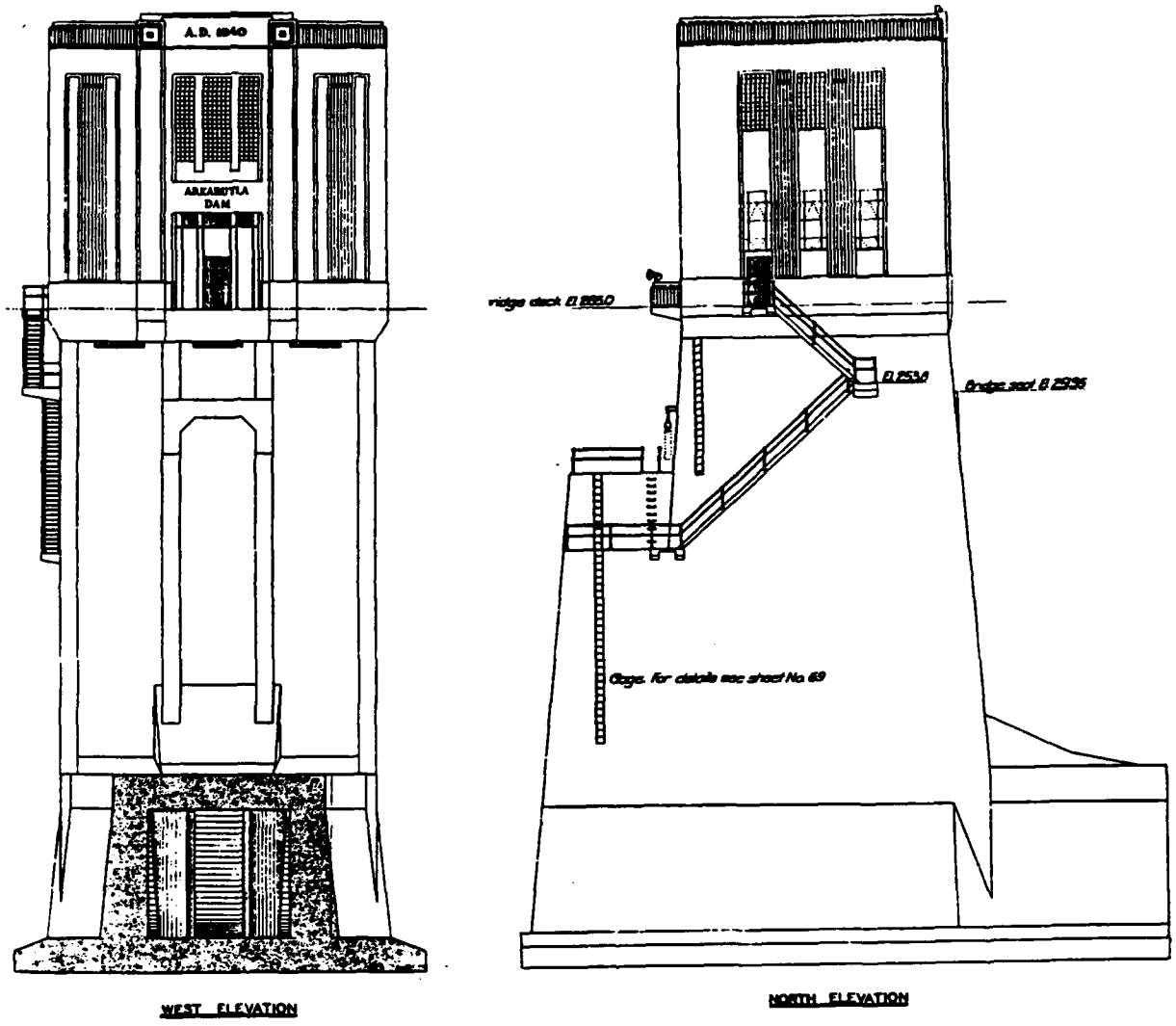

Figure 22. Arkabutla Intake Tower - two elevations

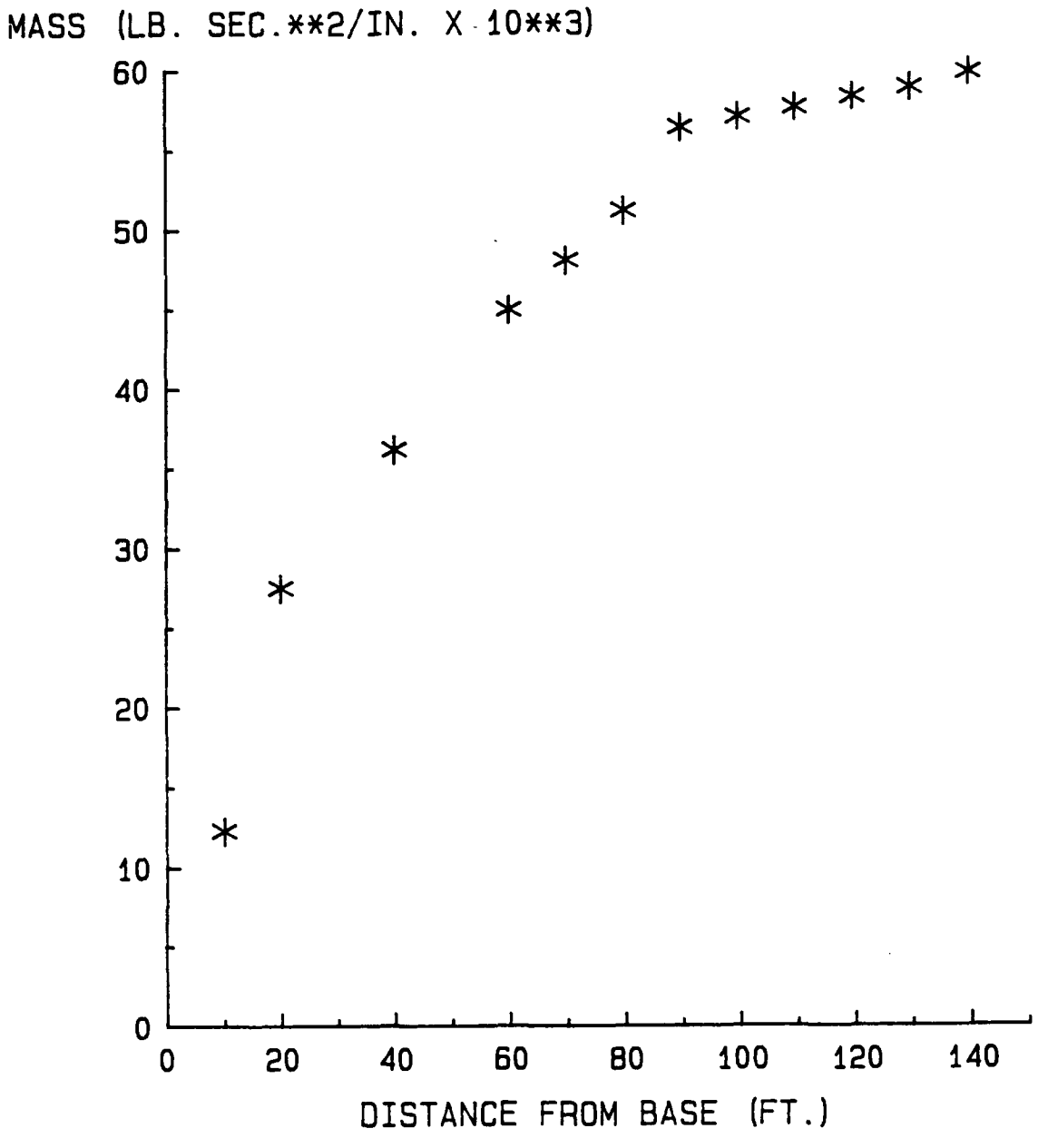

Figure 23. Cumulative mass distribution for the Arkabutla Intake Tower

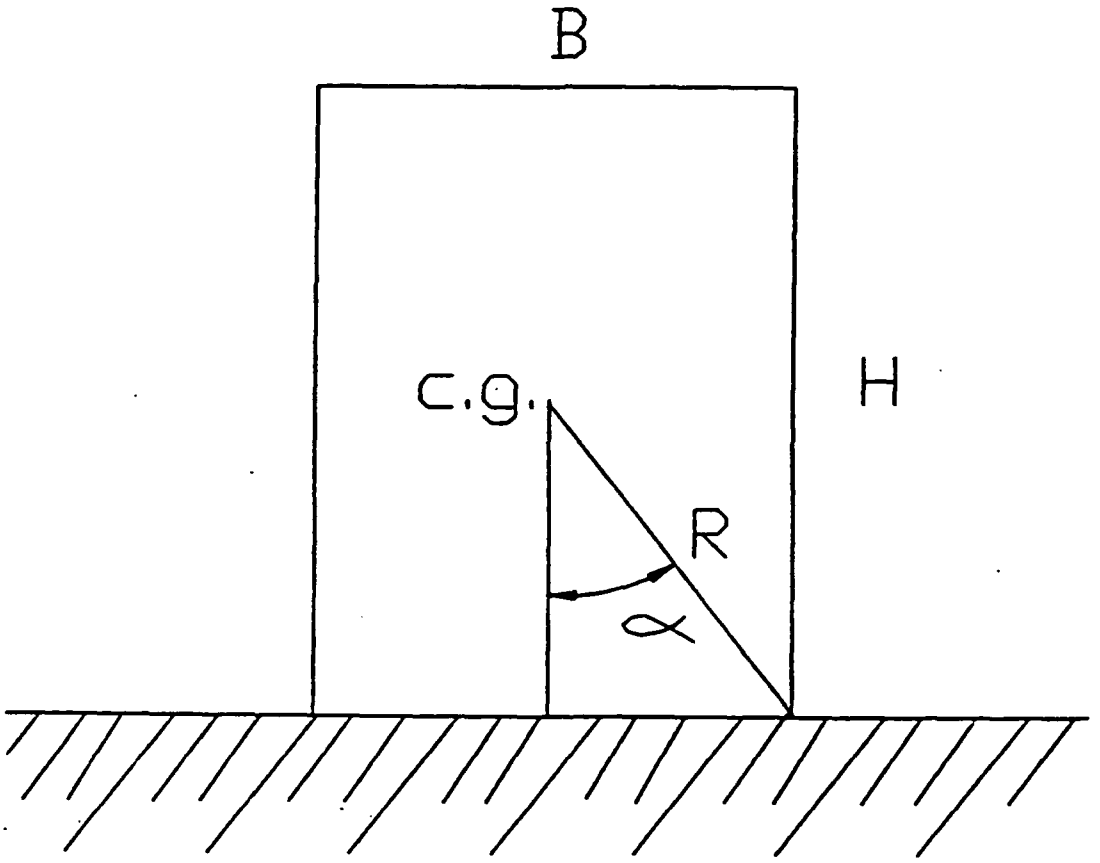

Figure 24. Housner's (1963) idealized block

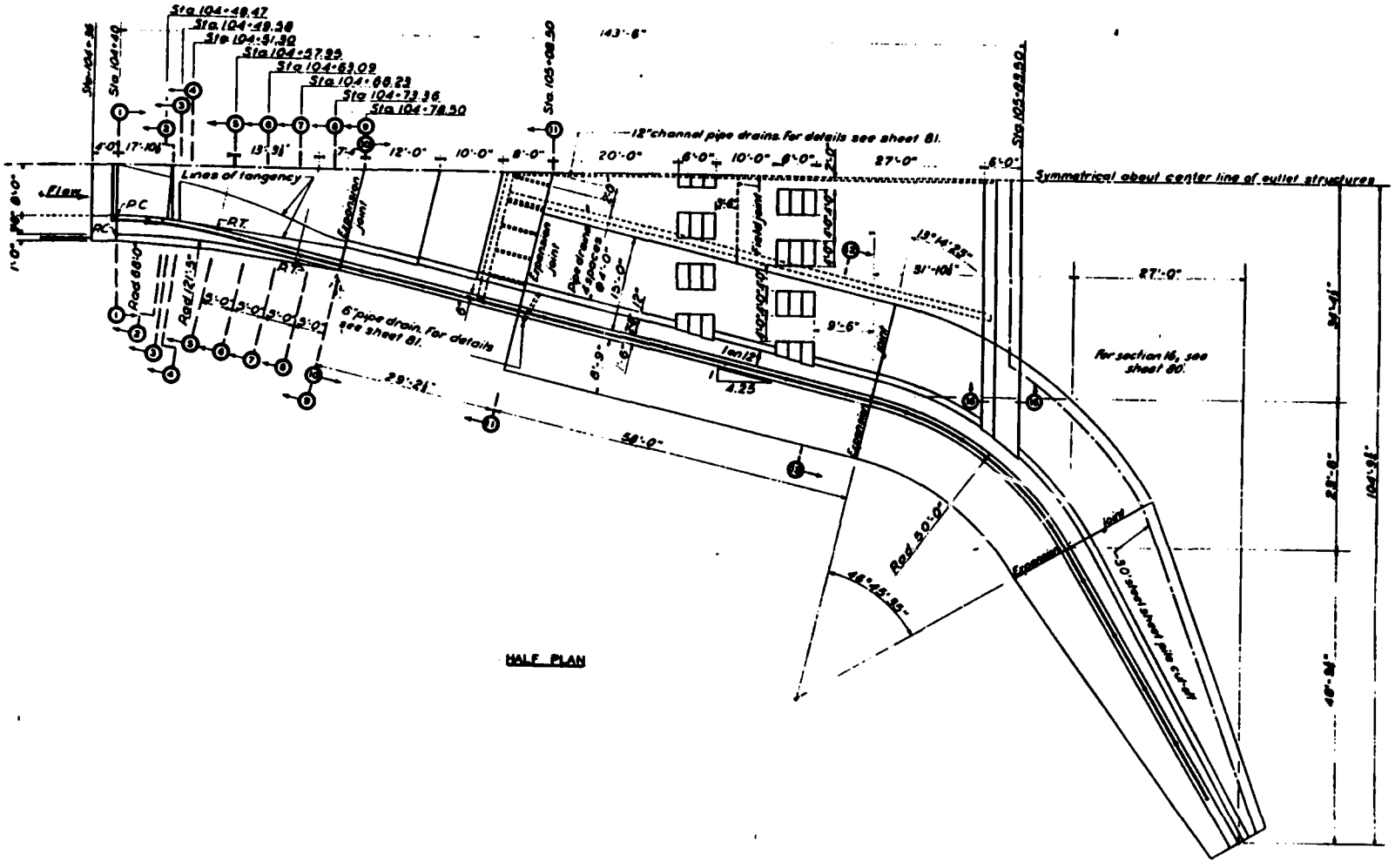

Figure 25. Plan view of Arkabutla outlet works

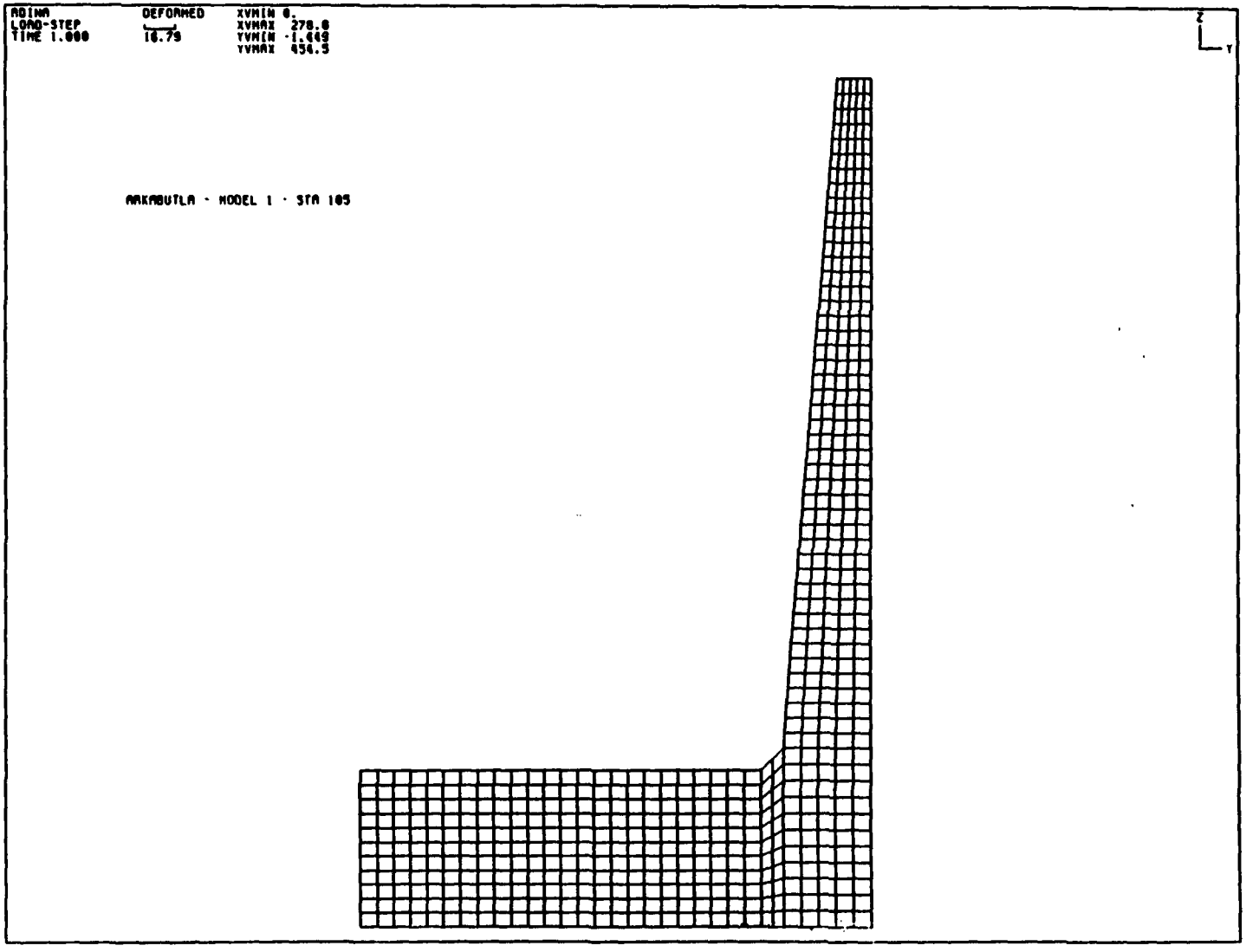

Figure 26. Grid for Station 105 + 8.50

I) Mononobe-Okabe Loads - Fixed Base

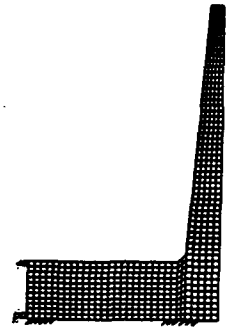

II) Soil-Spring, At Rest - Fixed Base

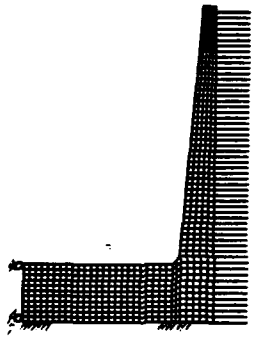

III) Mononobe-Okabe - Elastic Foundation

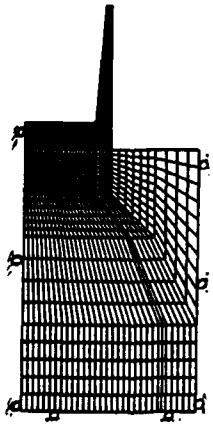

Figure 27. Models investigated

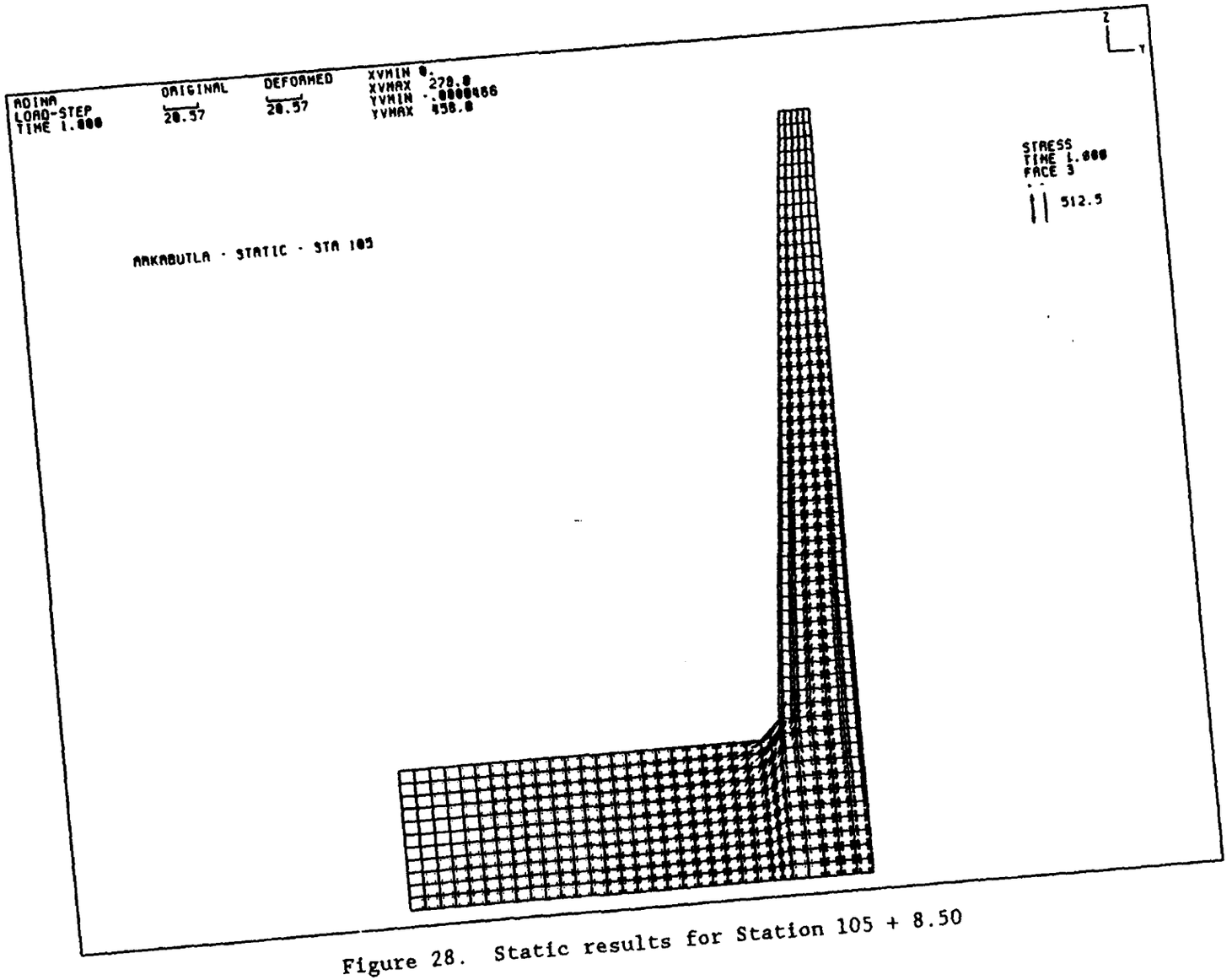

Figure 28. Static results for Station 105 + 8.50

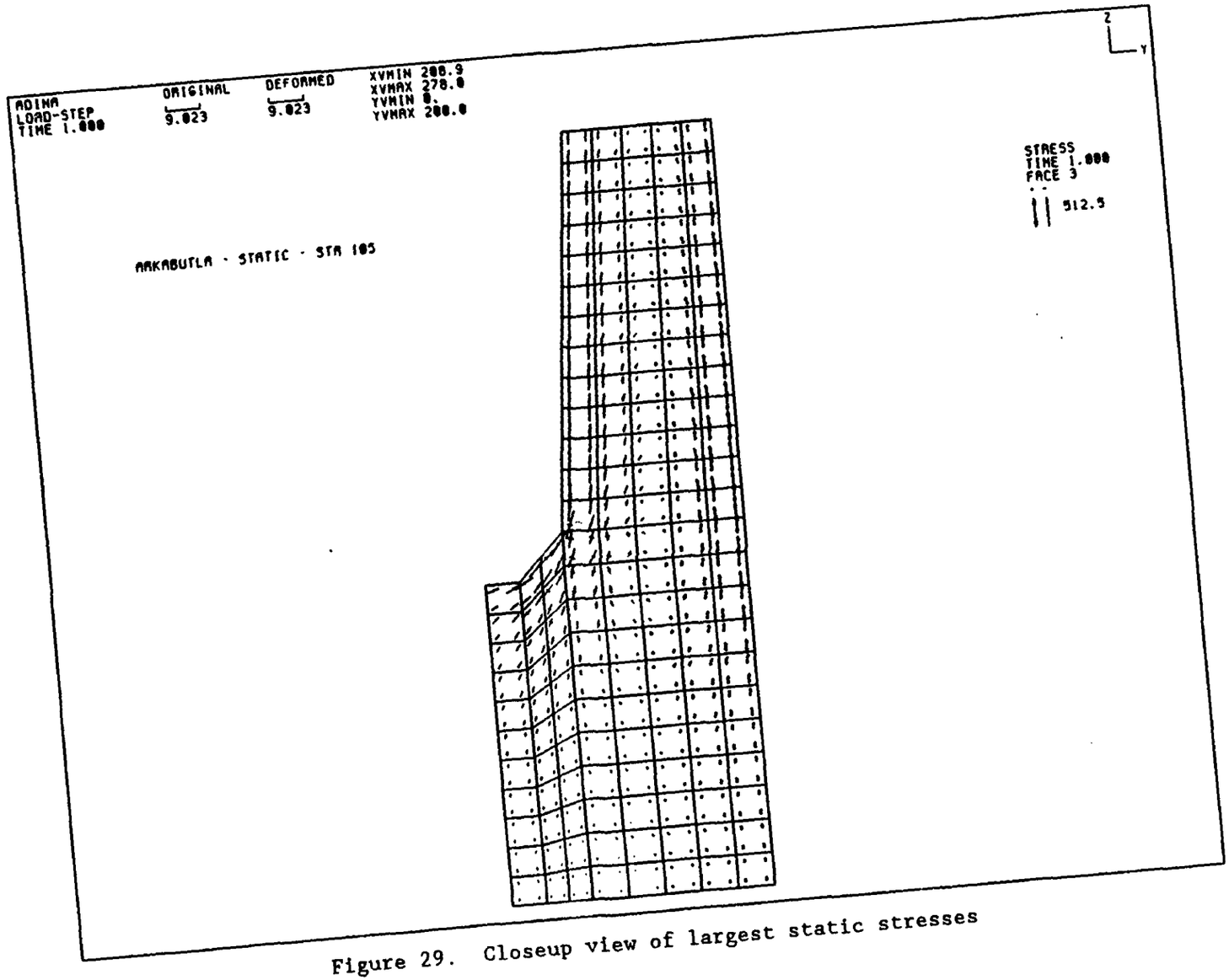

Figure 29. Closeup view of largest static stresses

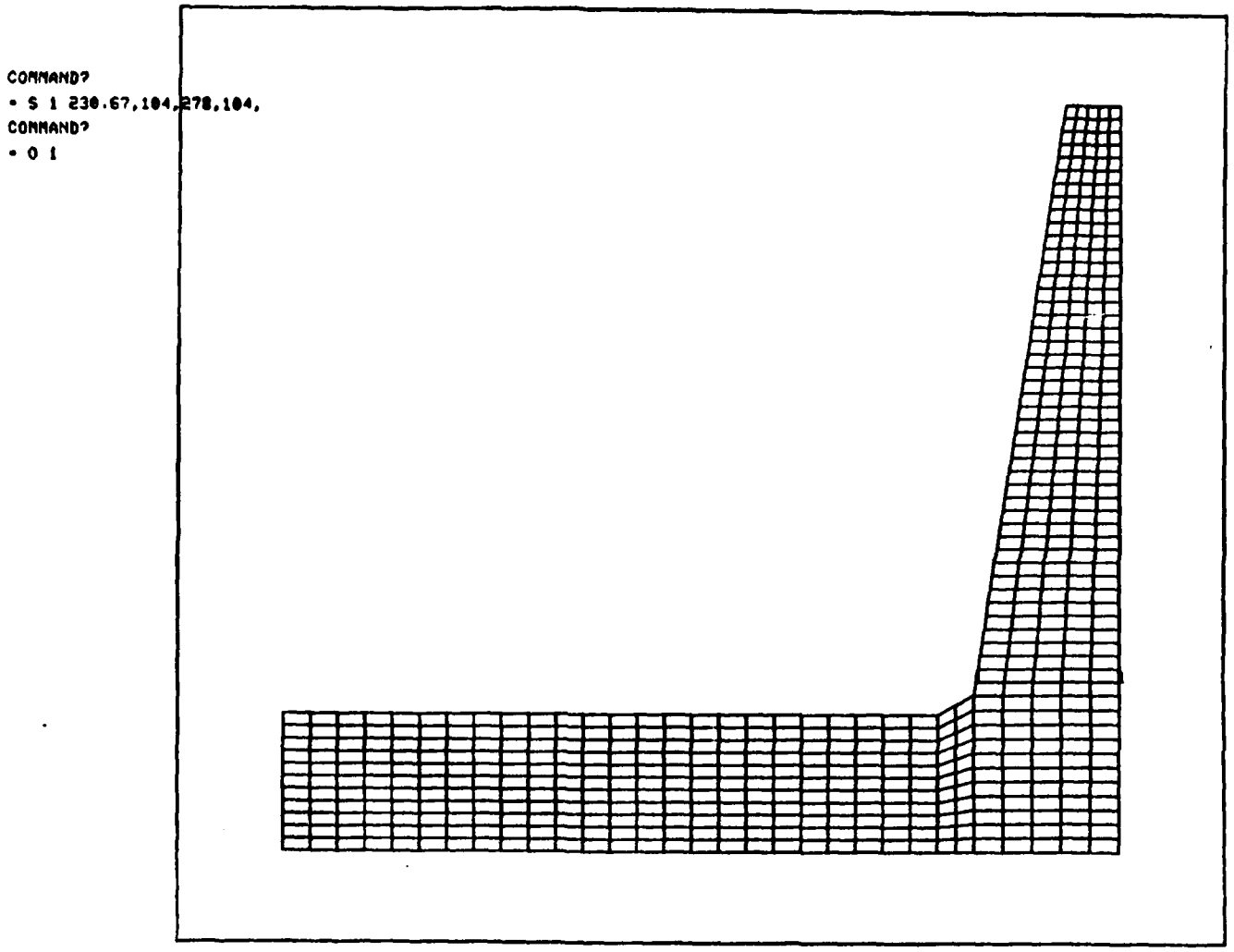

Figure 30. CSMT section location

001

001

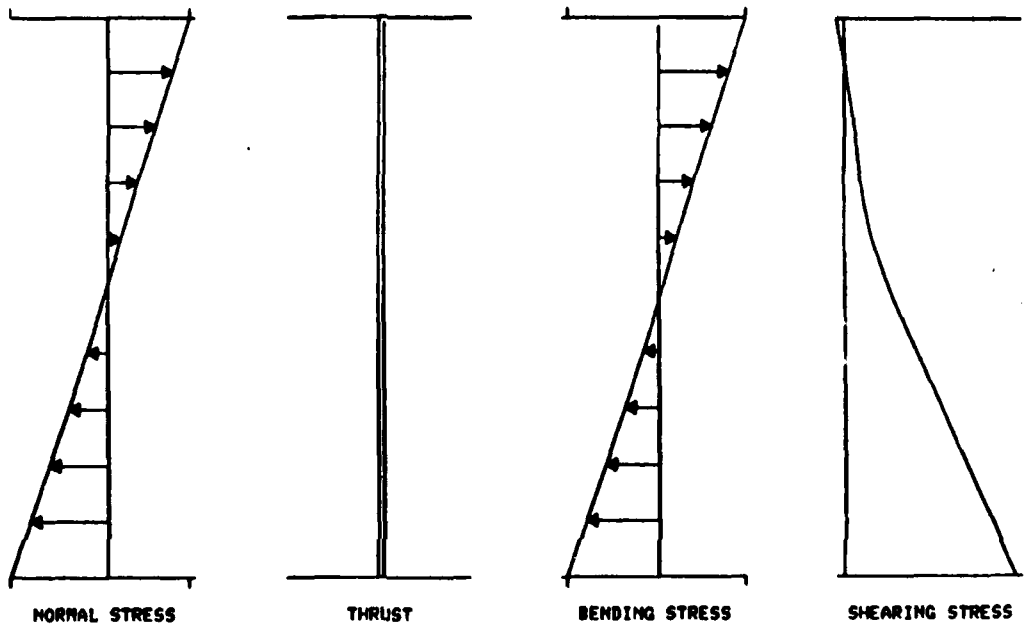

001

(X1, Y1) = (230.7,104.)
(X2, Y2) = (278.,104.)
NEUTRAL AXIS = (253.9,104.)
SHEAR = 1220.
MOMENT = -.1234E+6
THRUST = -962.9

SECTION NO. 1
ST

Figure 31. CSMT results

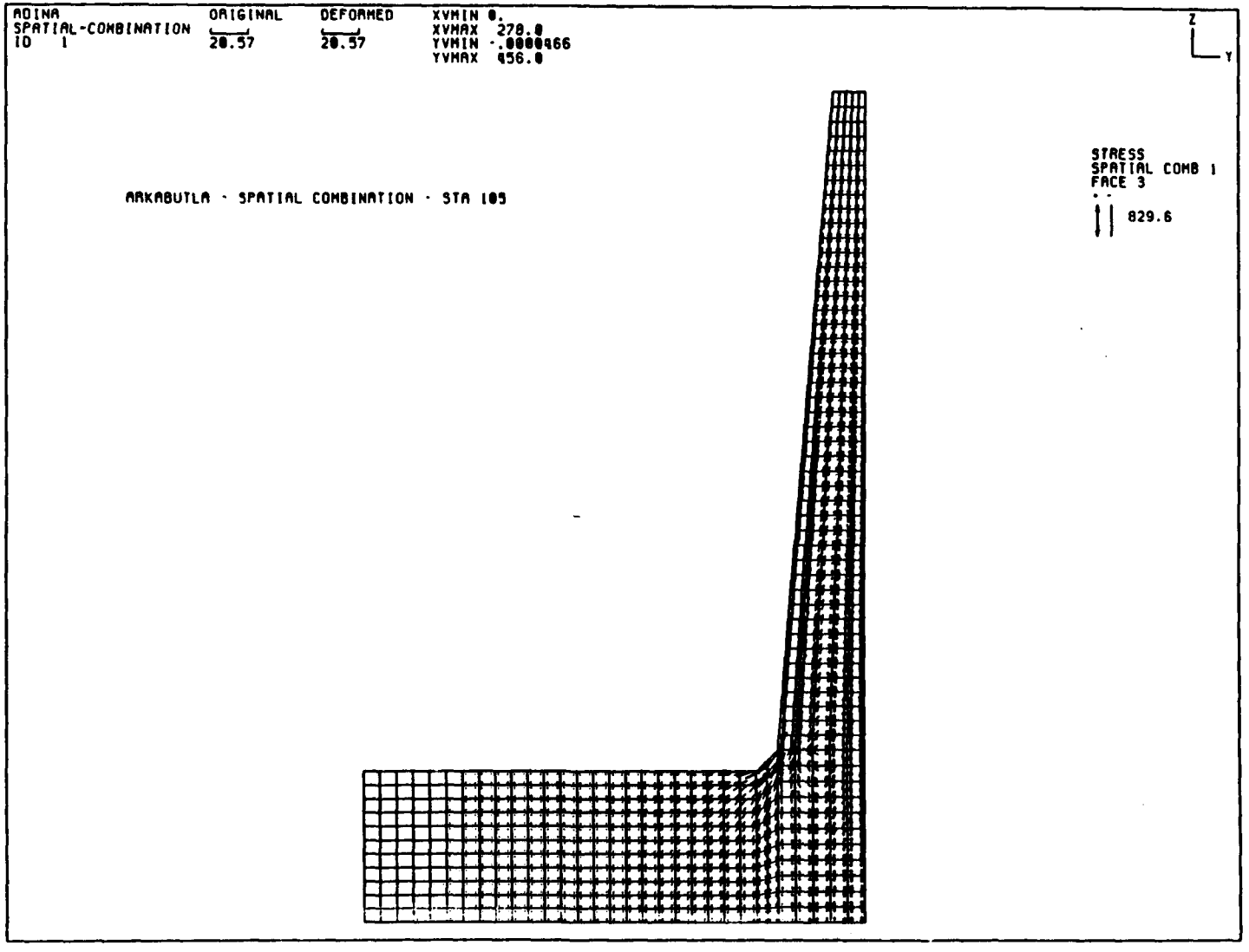

Figure 32. Dynamic results for Station 105 + 8.50

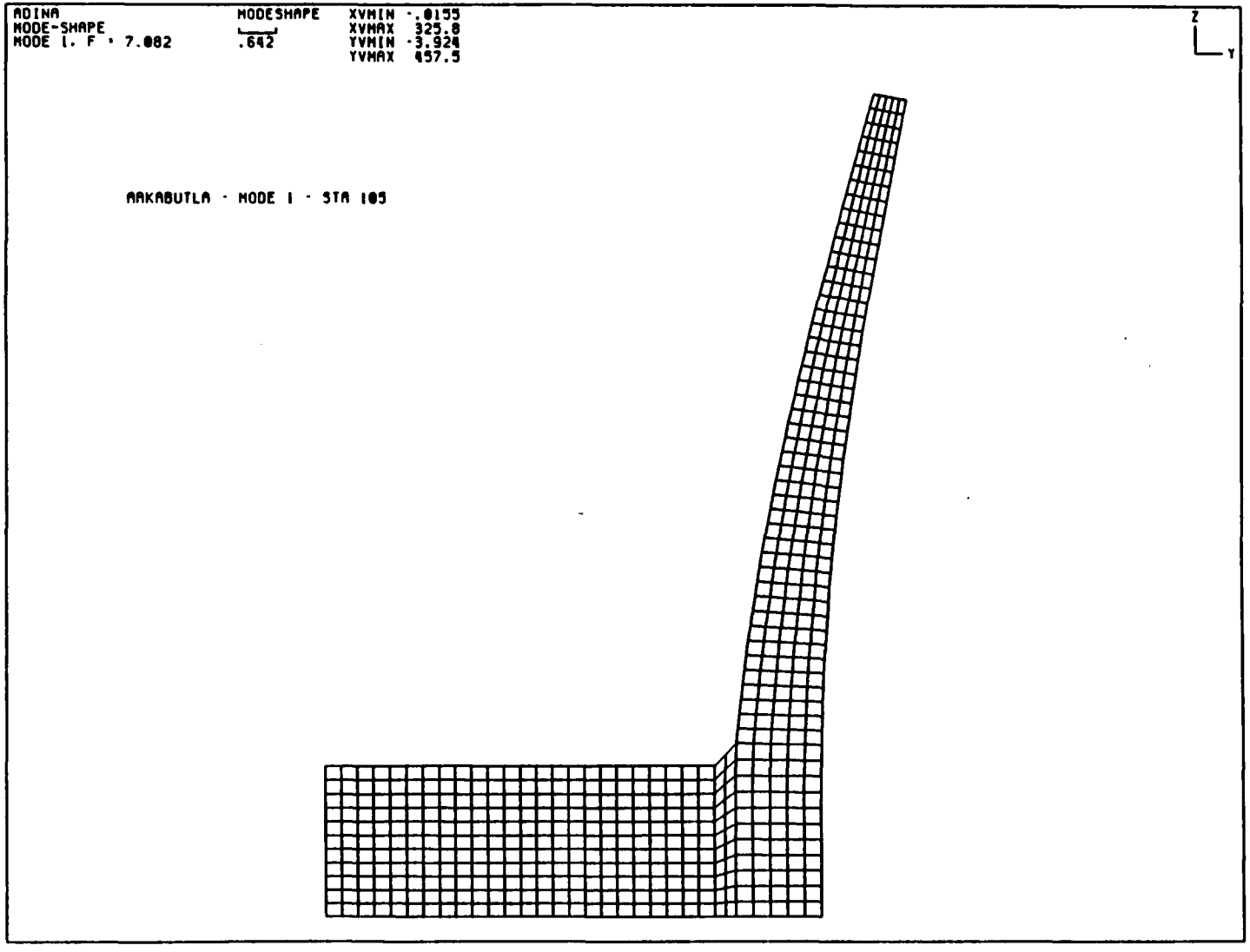

Figure 33. Mode 1

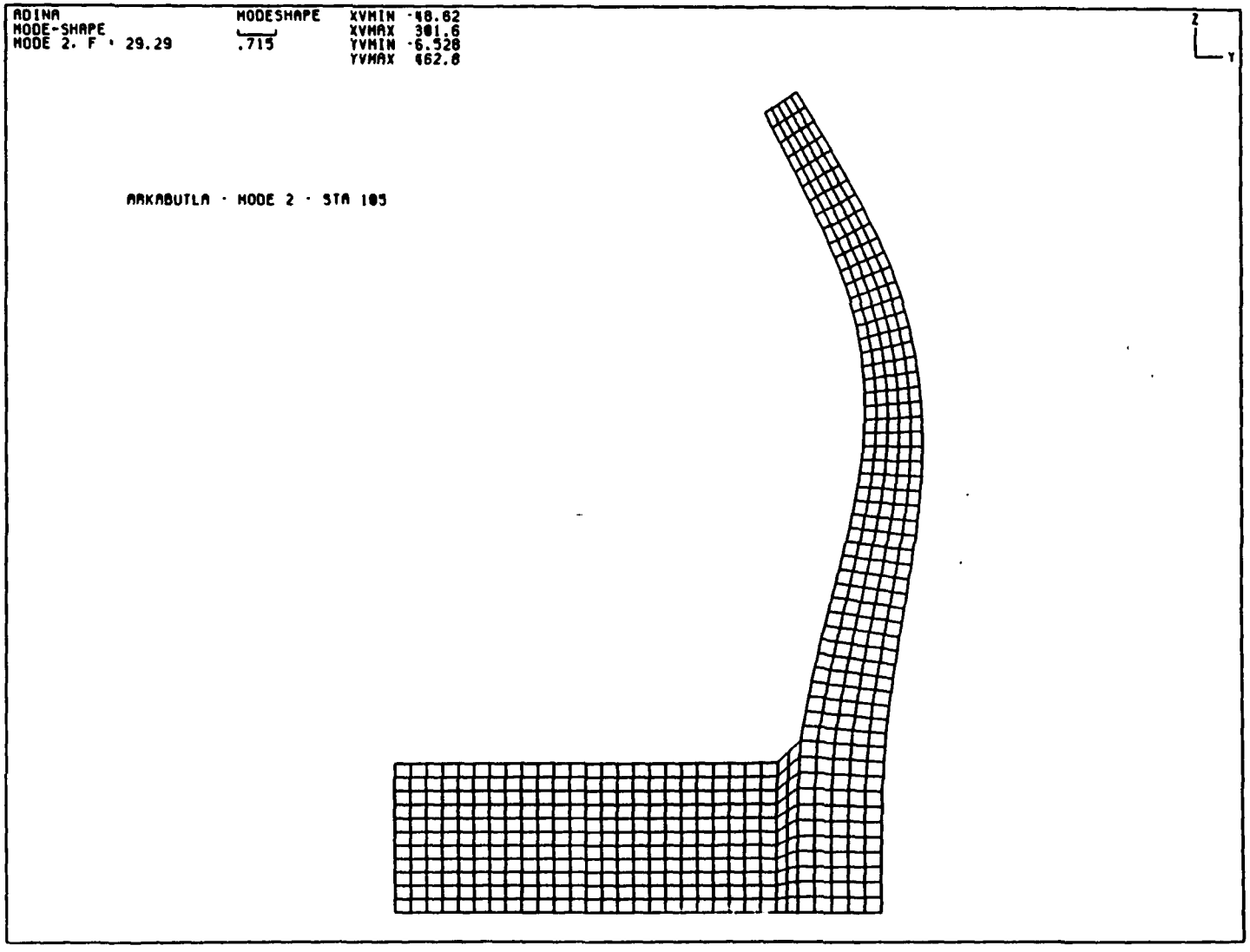

Figure 34. Mode 2

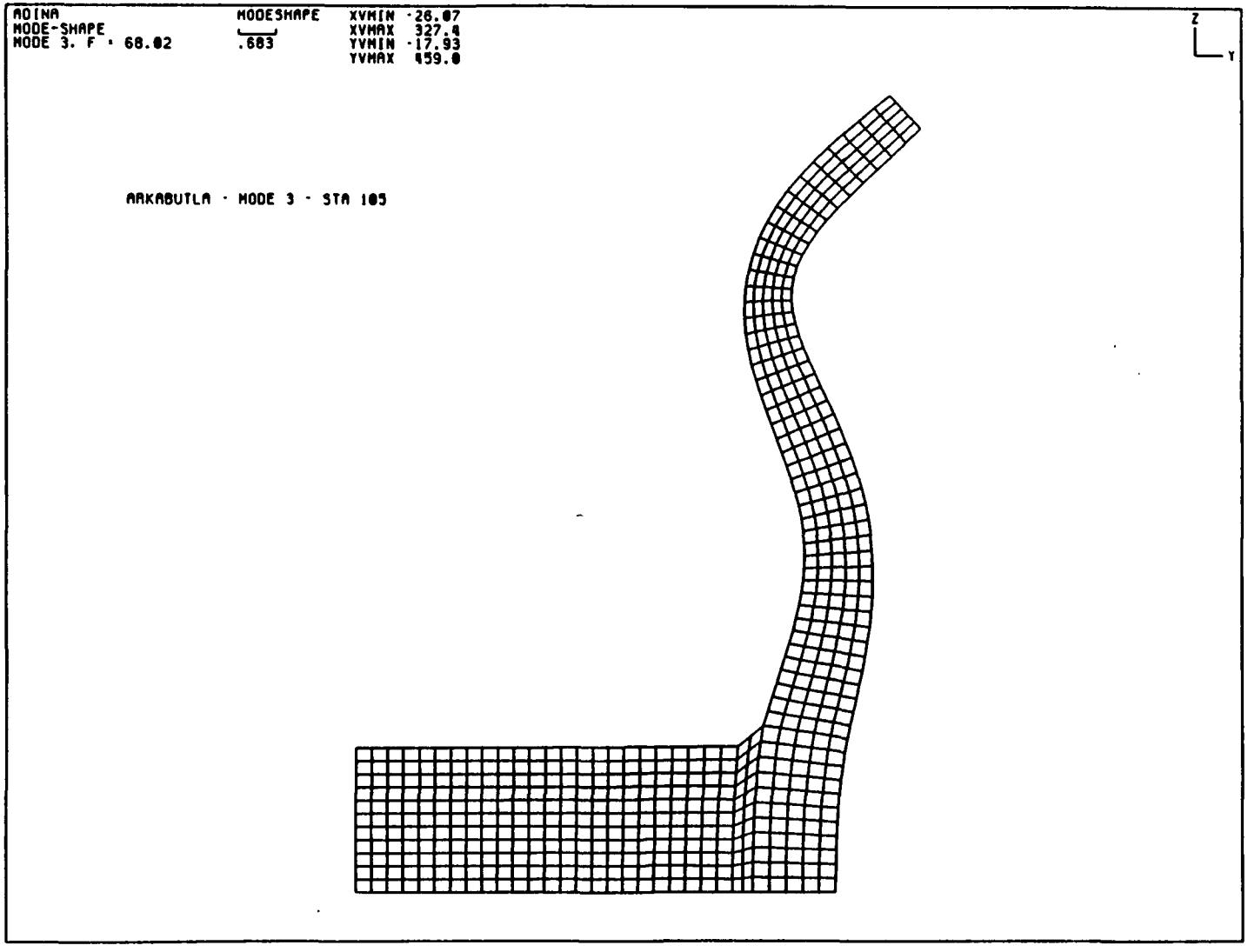

Figure 35. Mode 3

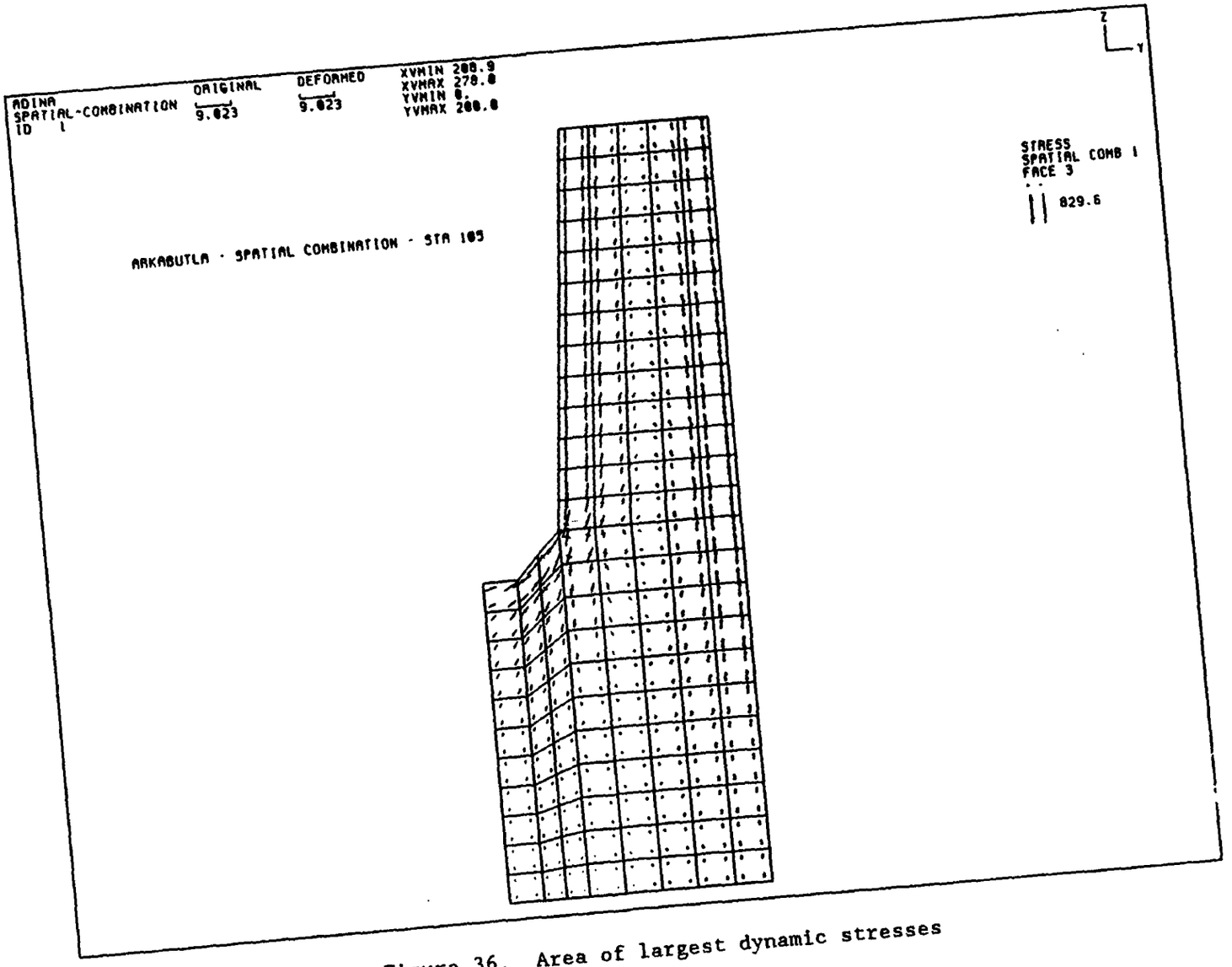

Figure 36. Area of largest dynamic stresses

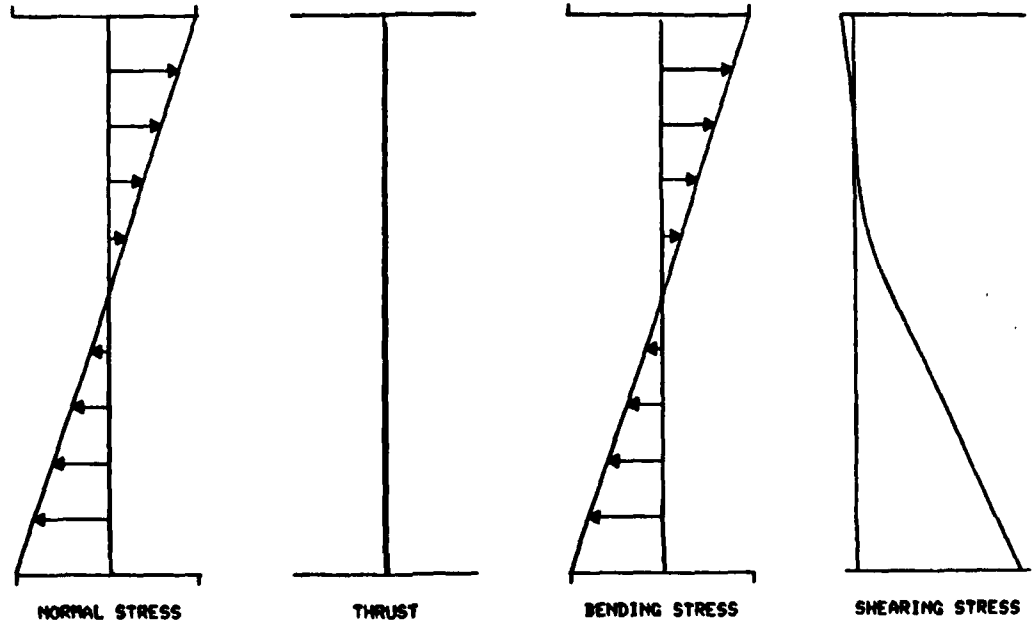

001

001

001

001

(X1, Y1) = (230.7,104.)
(X2, Y2) = (278.,104.)
NEUTRAL AXIS = (254.,104.)
SHEAR = 1682.
MOMENT = -.2106E+6
THRUST = -634.1

SECTION NO. 1

DY

Figure 37. CSMT results for the dynamic load case

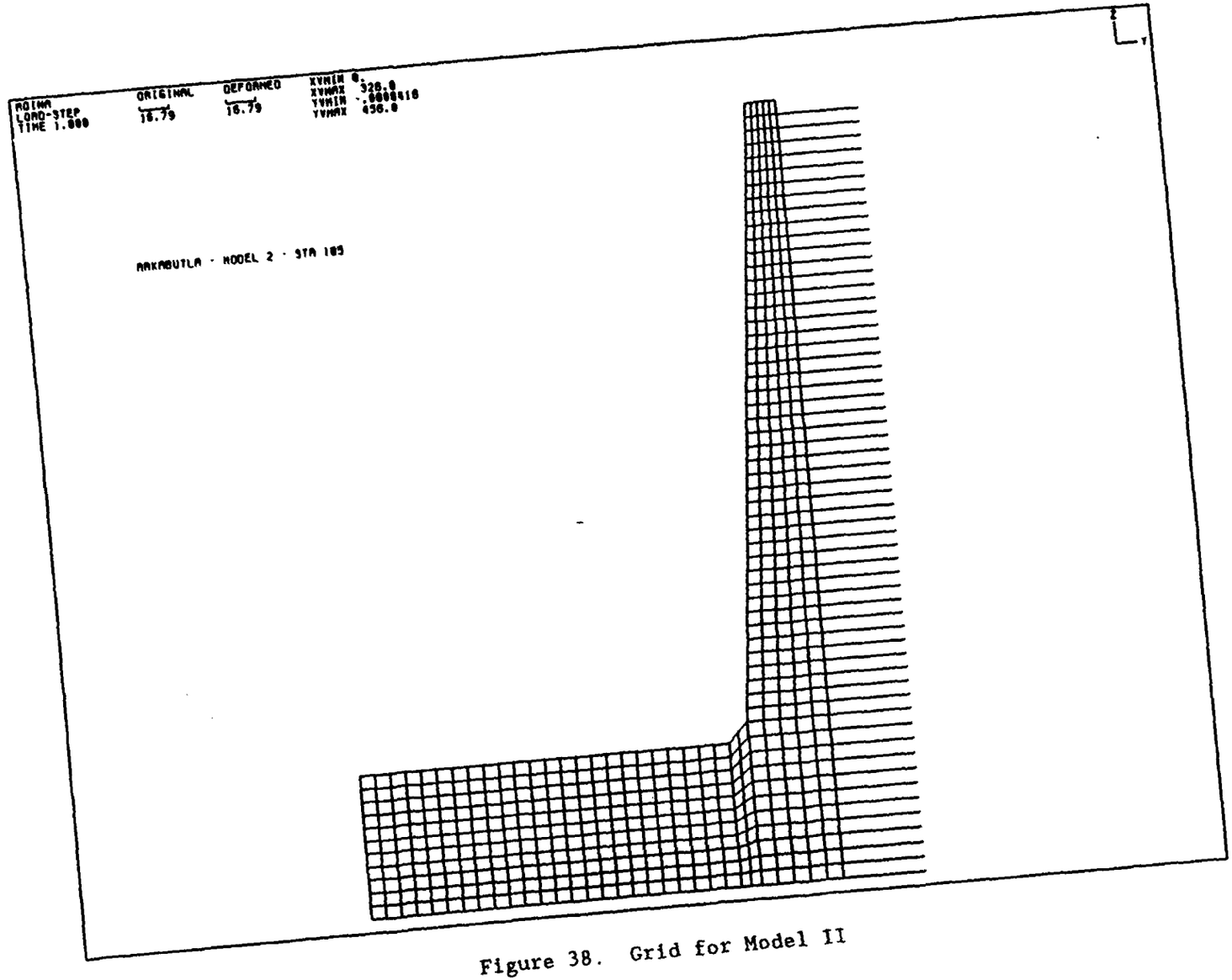

Figure 38. Grid for Model II

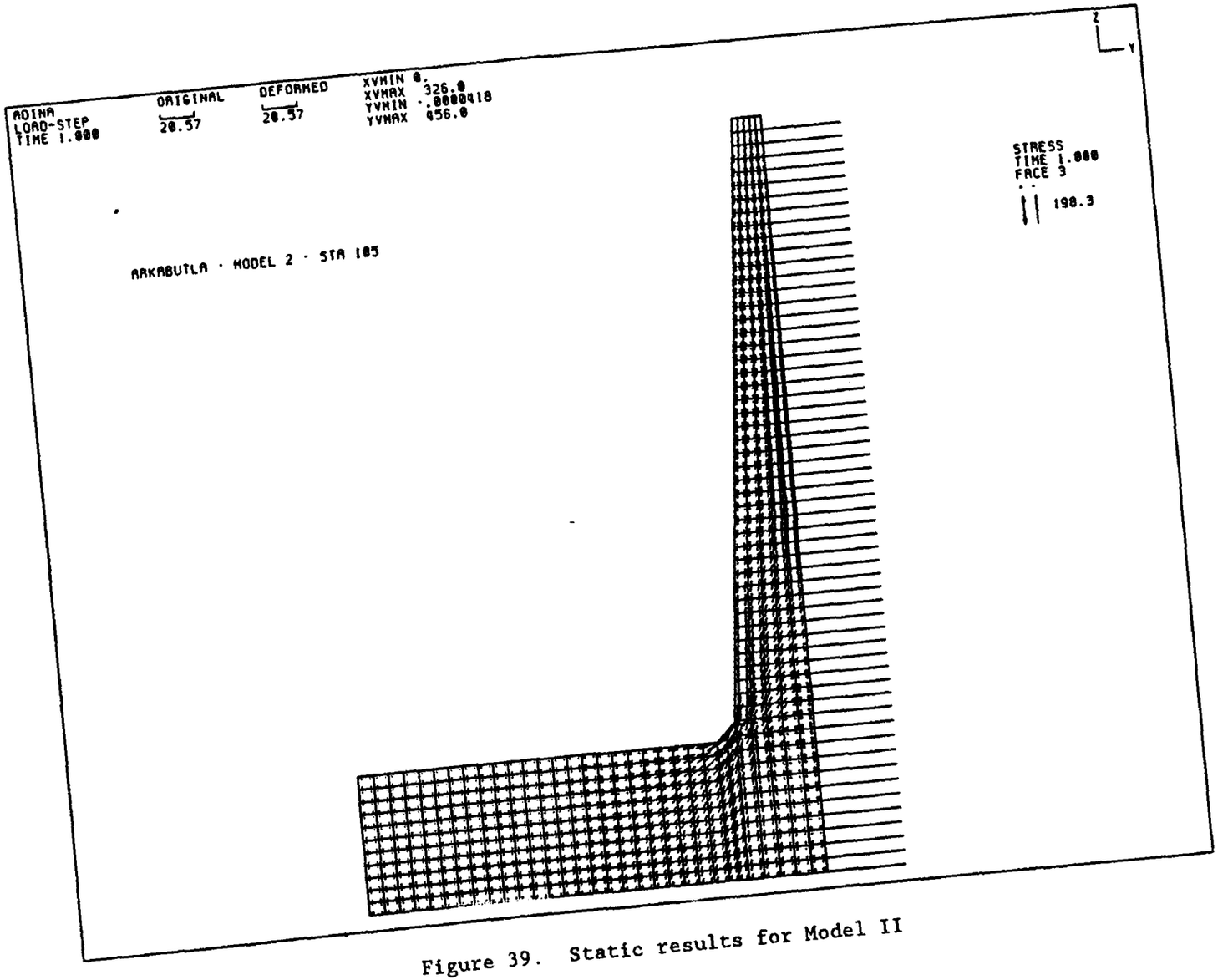

Figure 39. Static results for Model II

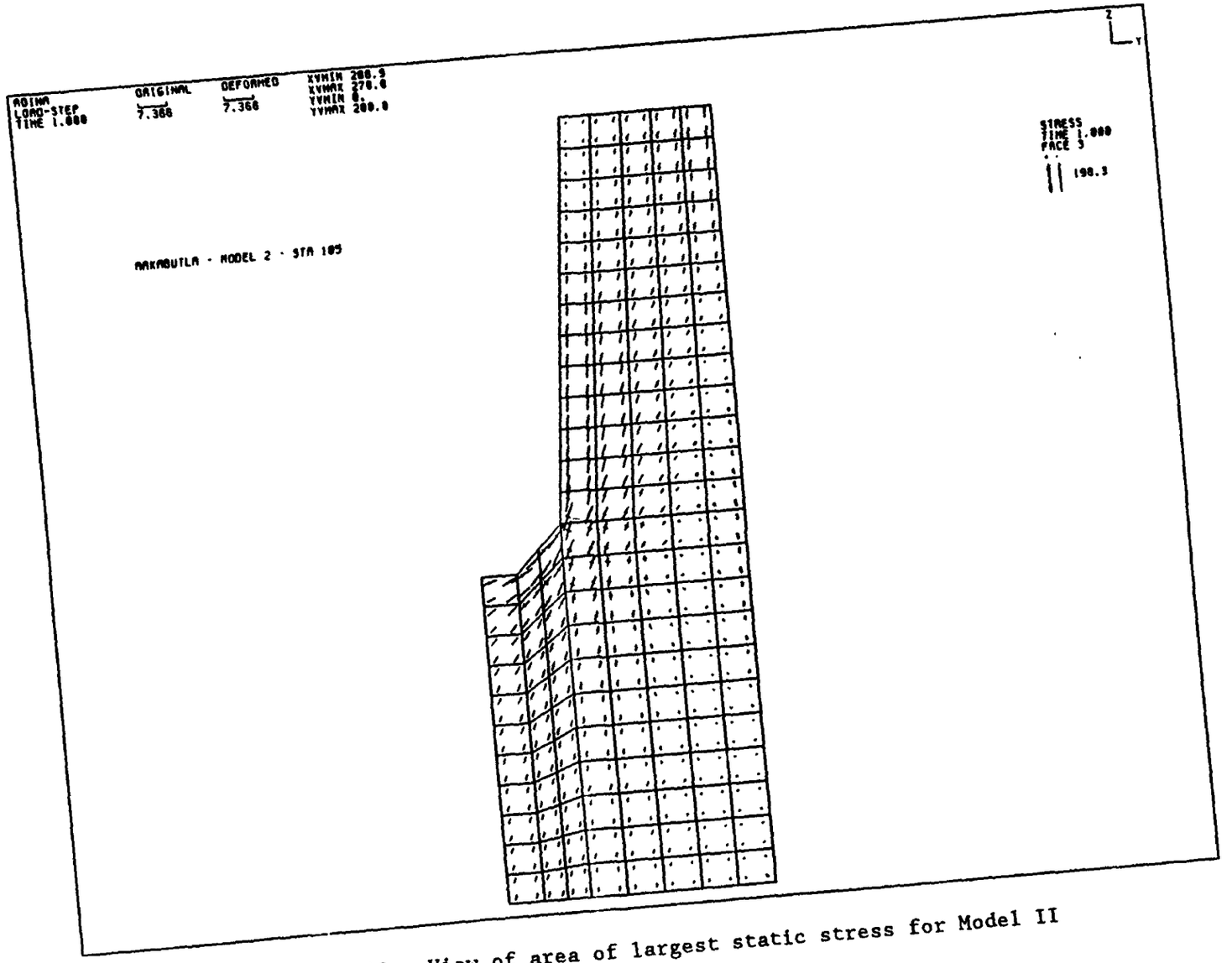

Figure 40. View of area of largest static stress for Model II

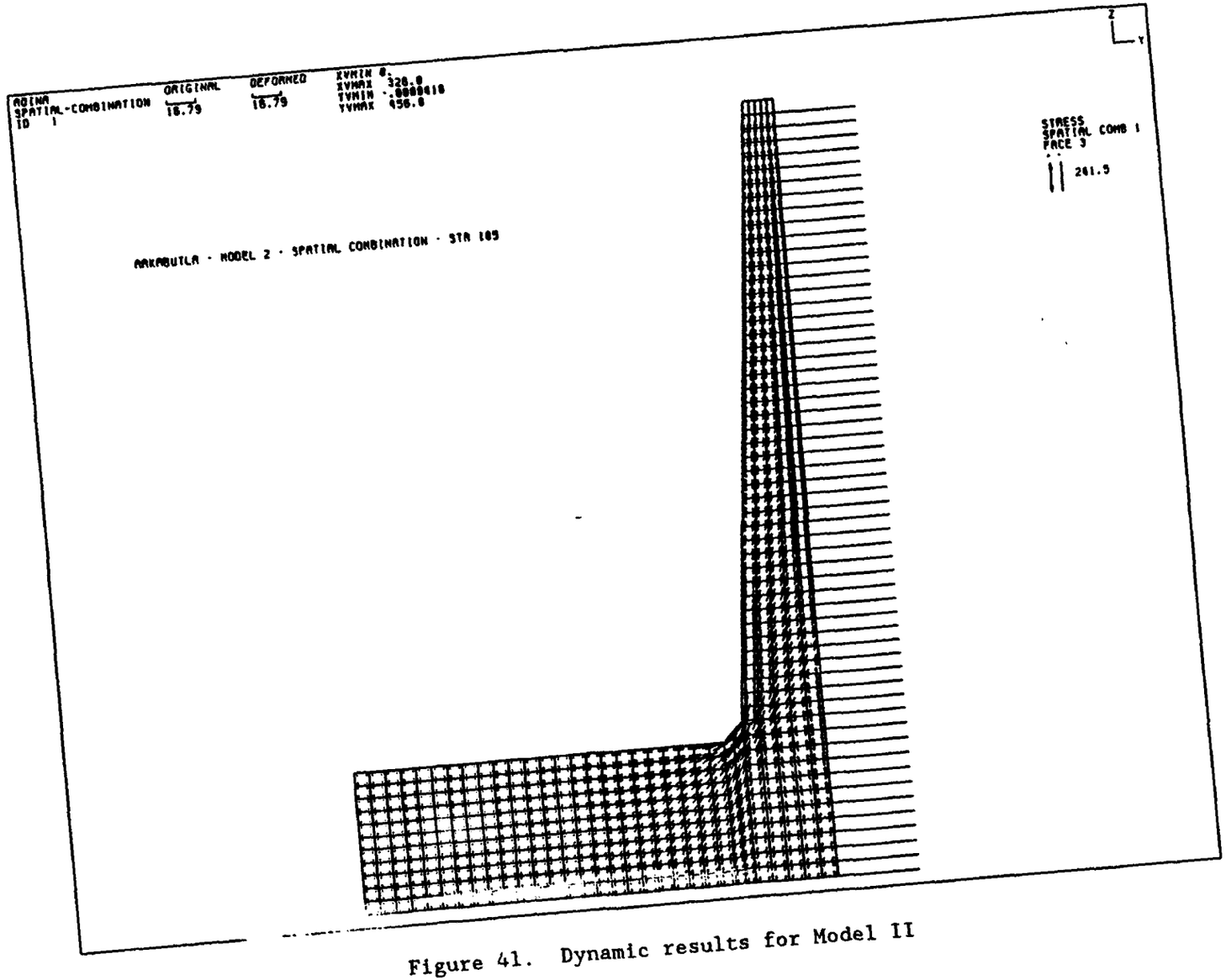

Figure 41. Dynamic results for Model II

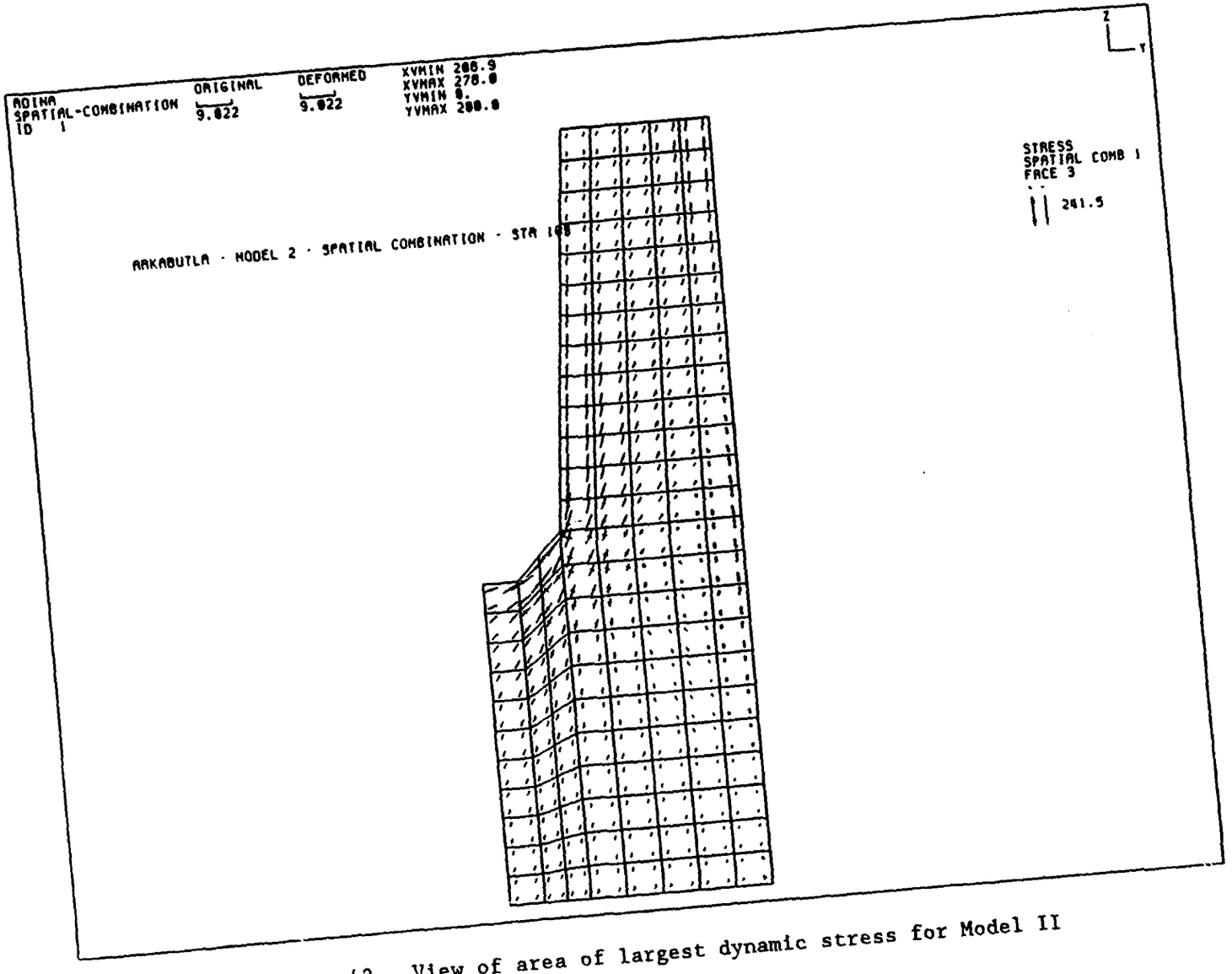

Figure 42. View of area of largest dynamic stress for Model II

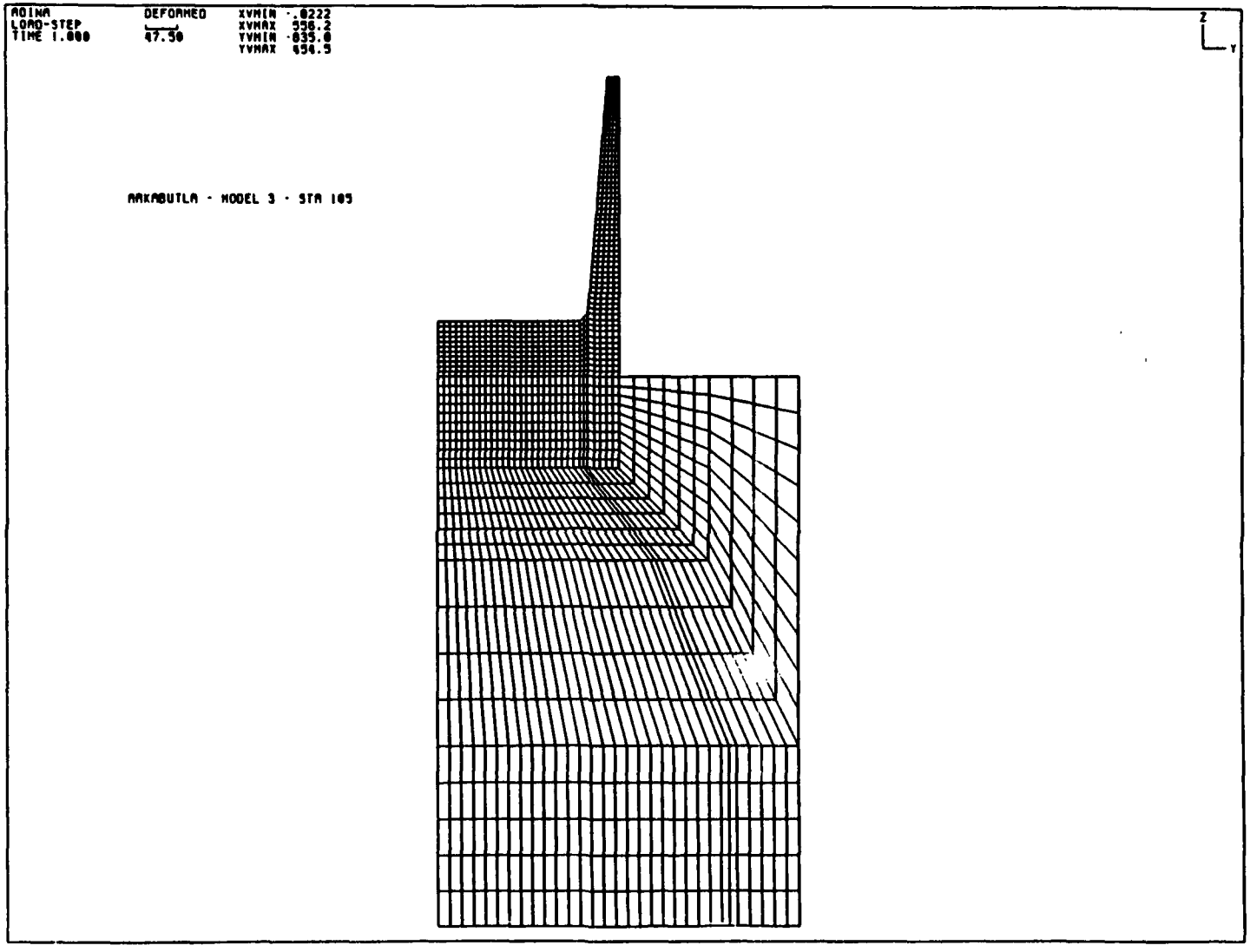

Figure 43. Grid for Model III

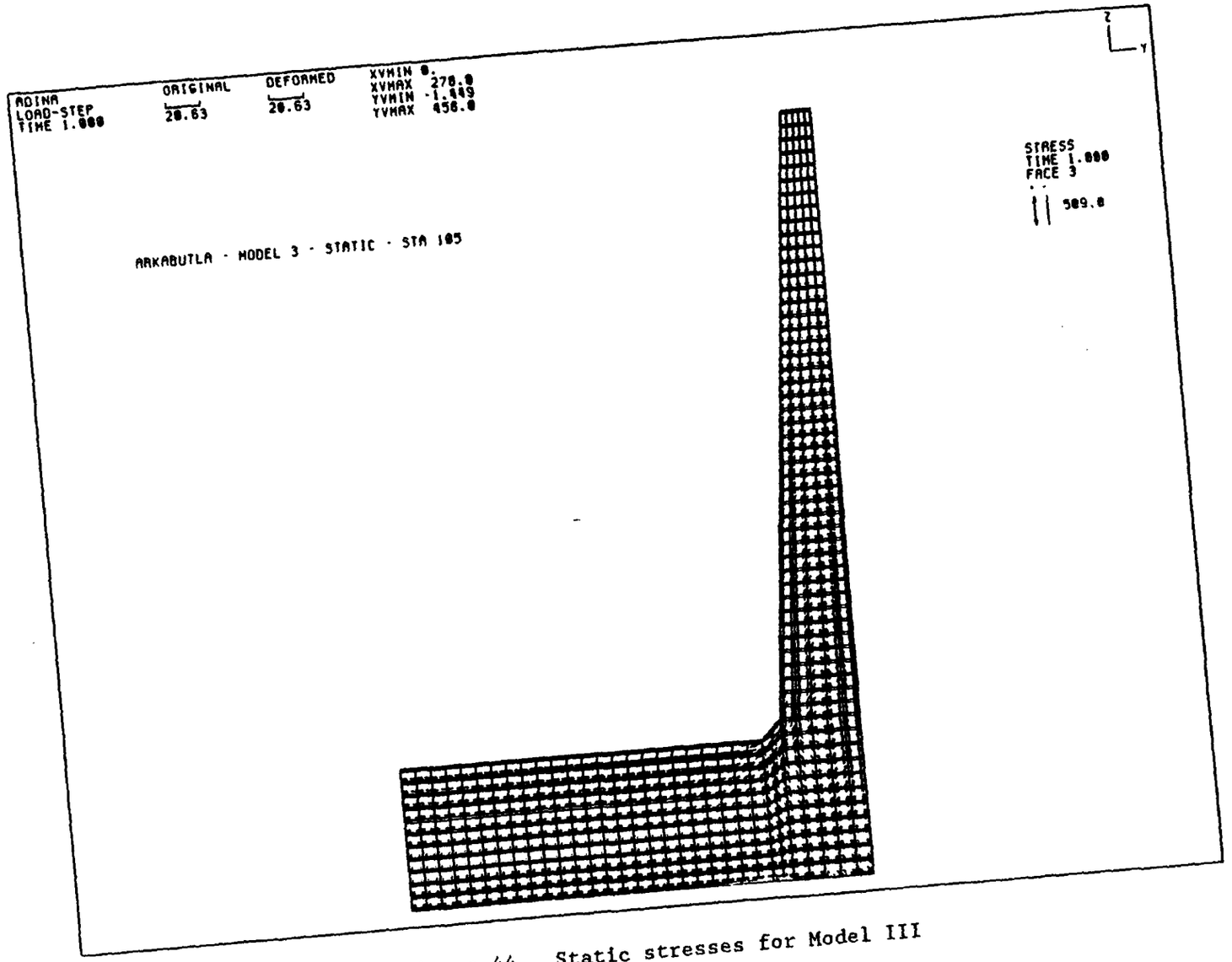

Figure 44. Static stresses for Model III

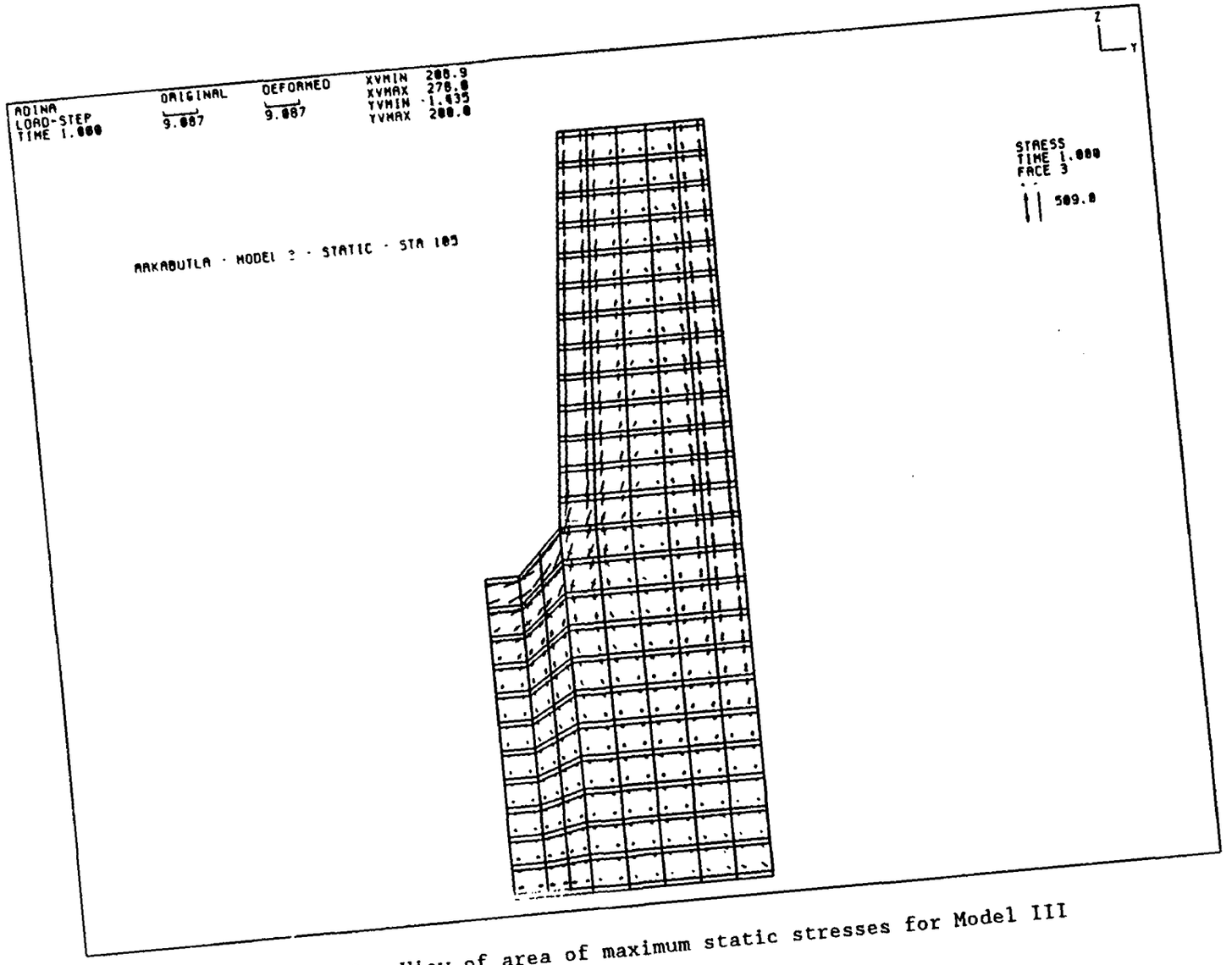

Figure 45. View of area of maximum static stresses for Model III

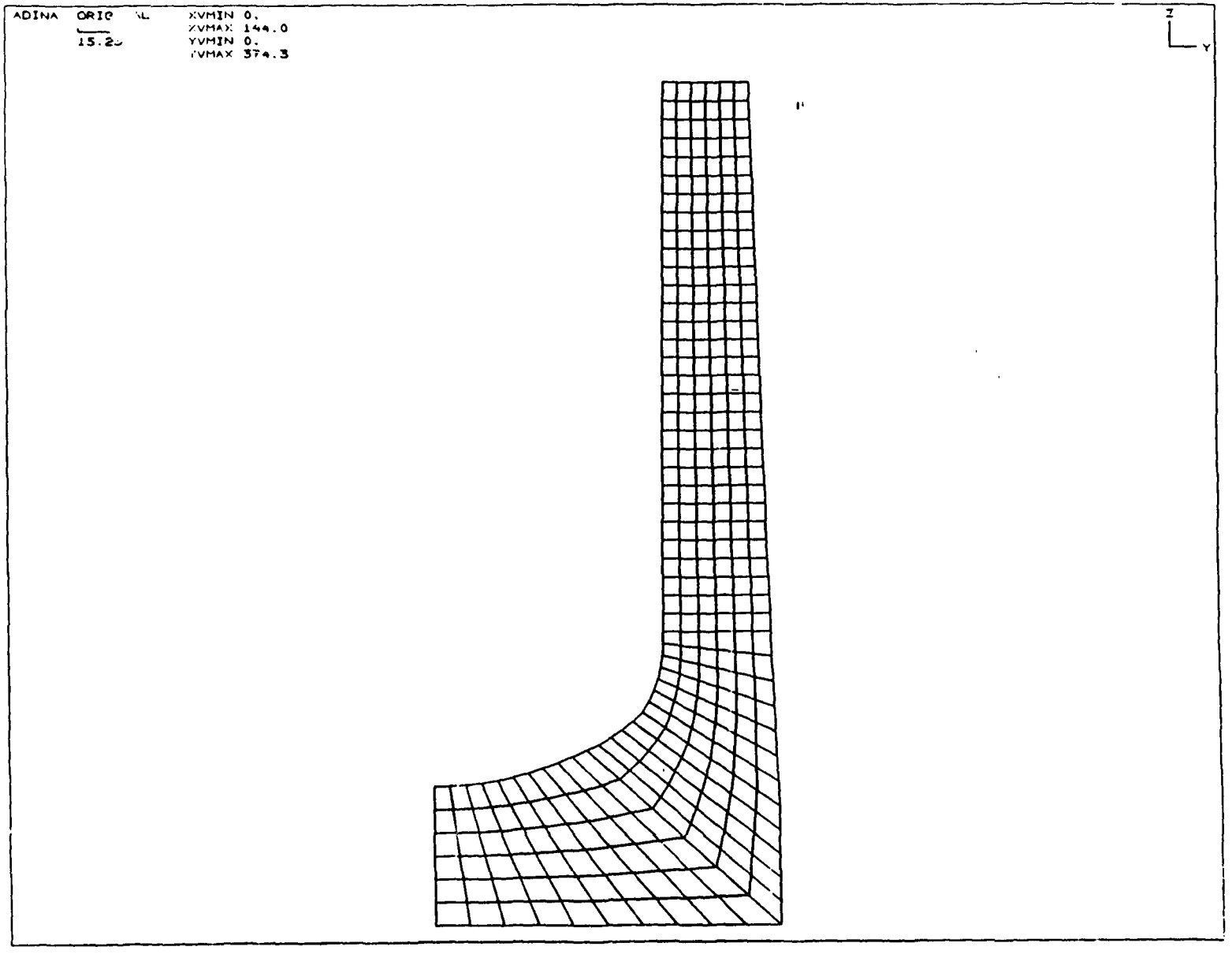

Figure 46. Grid for Station 104 + 80.0

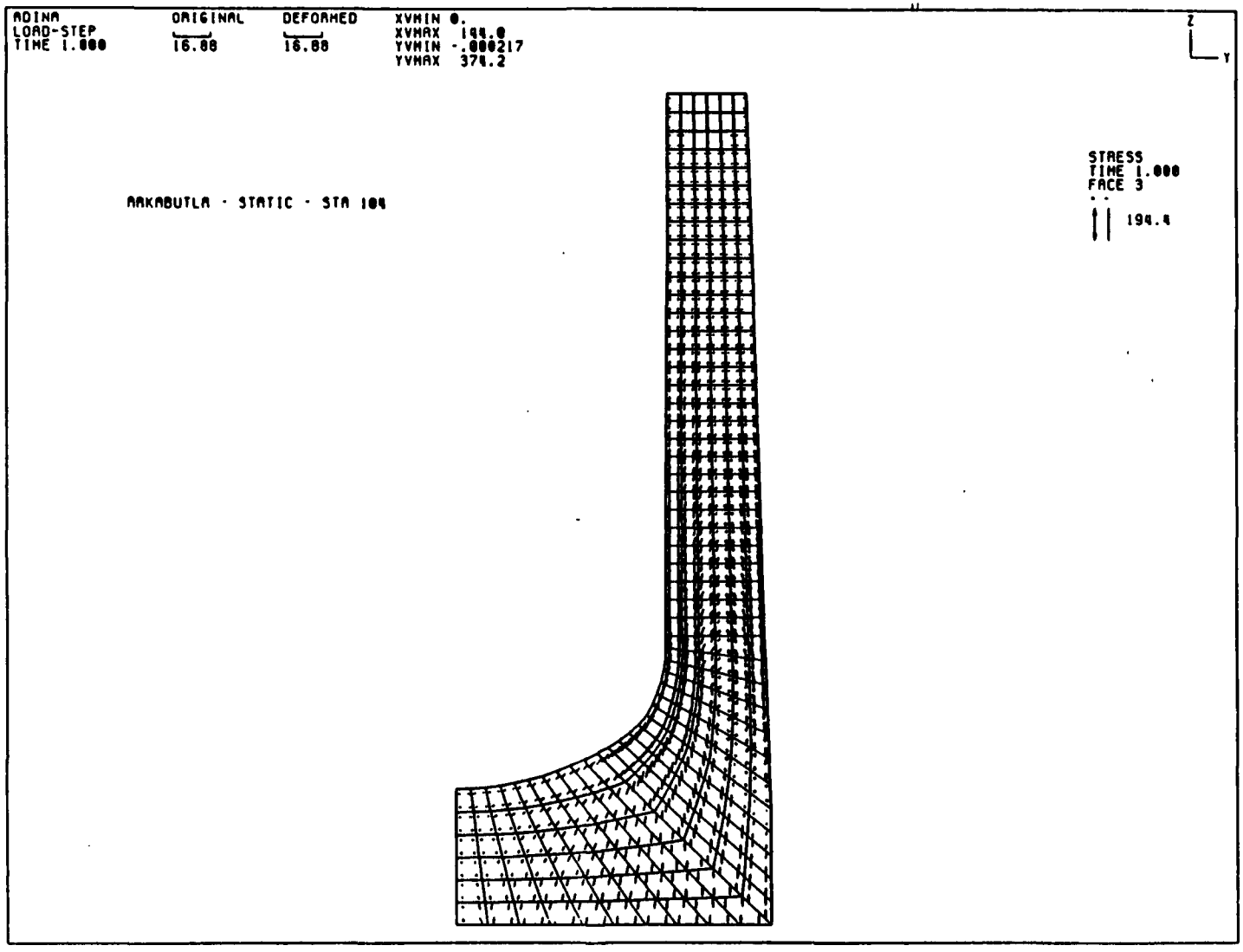

Figure 47. Static results for Station 104 + 80.0

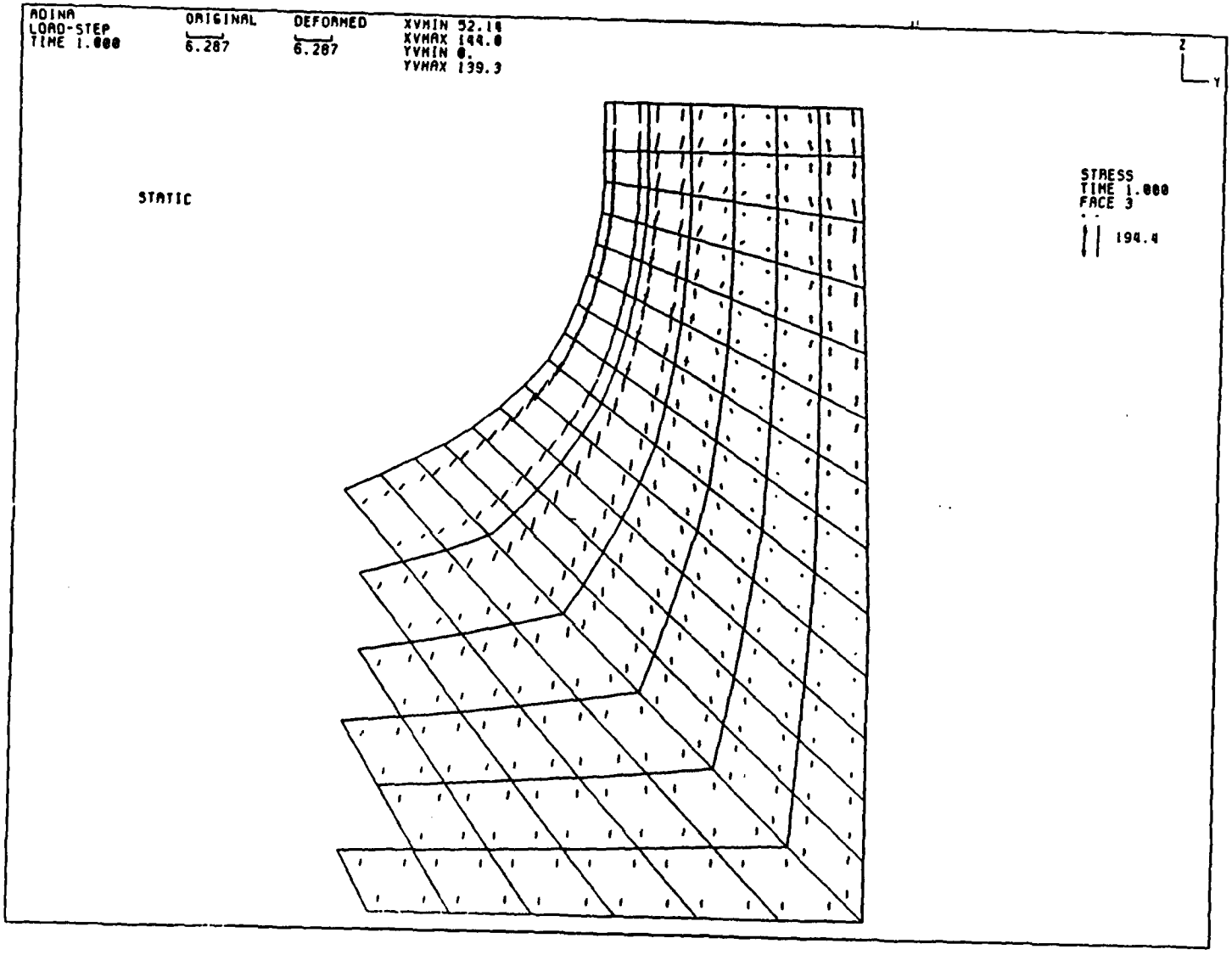

Figure 48. Area of largest static stresses for Station 104 + 80.0

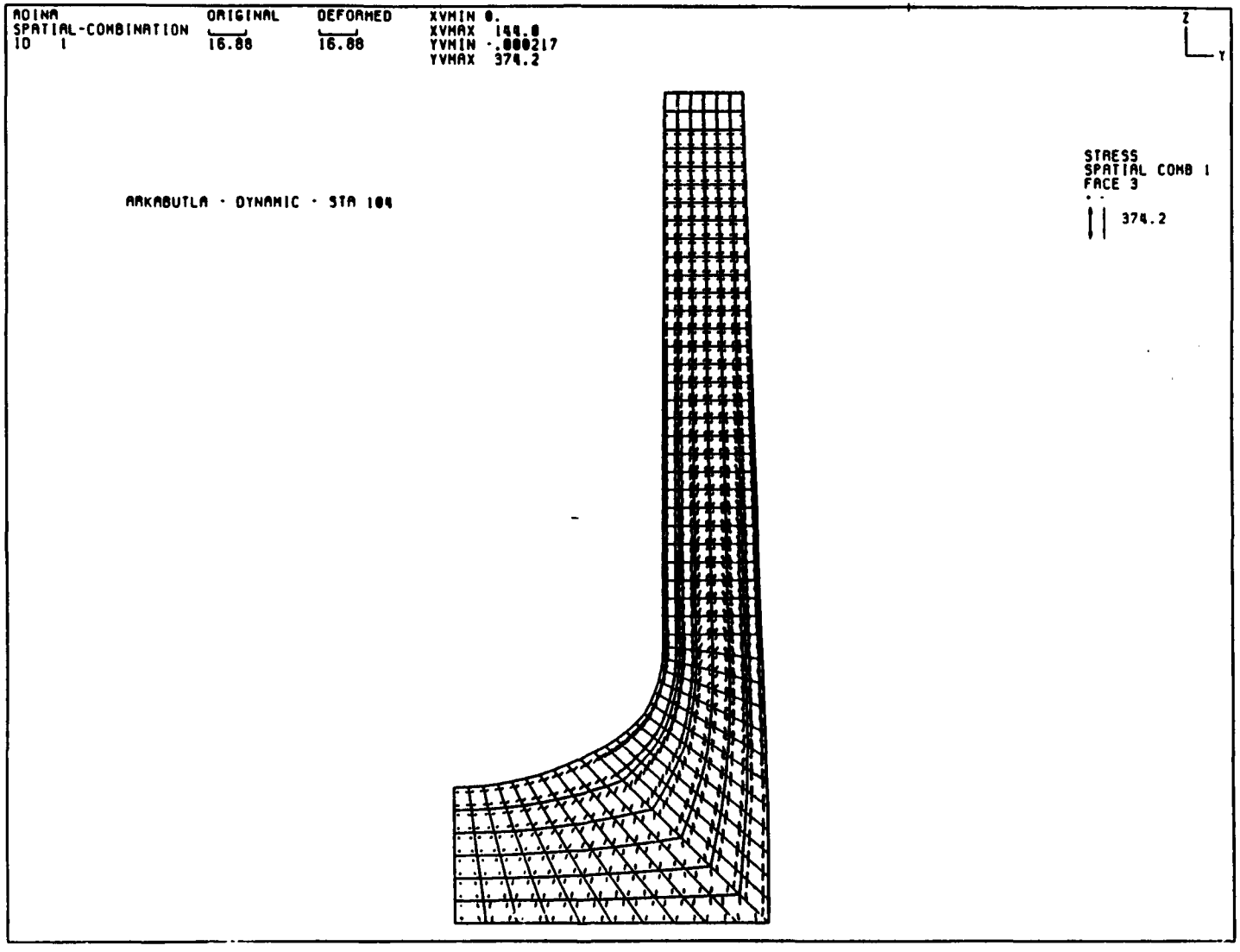

Figure 49. Dynamic stress results for Station 104 + 80.0

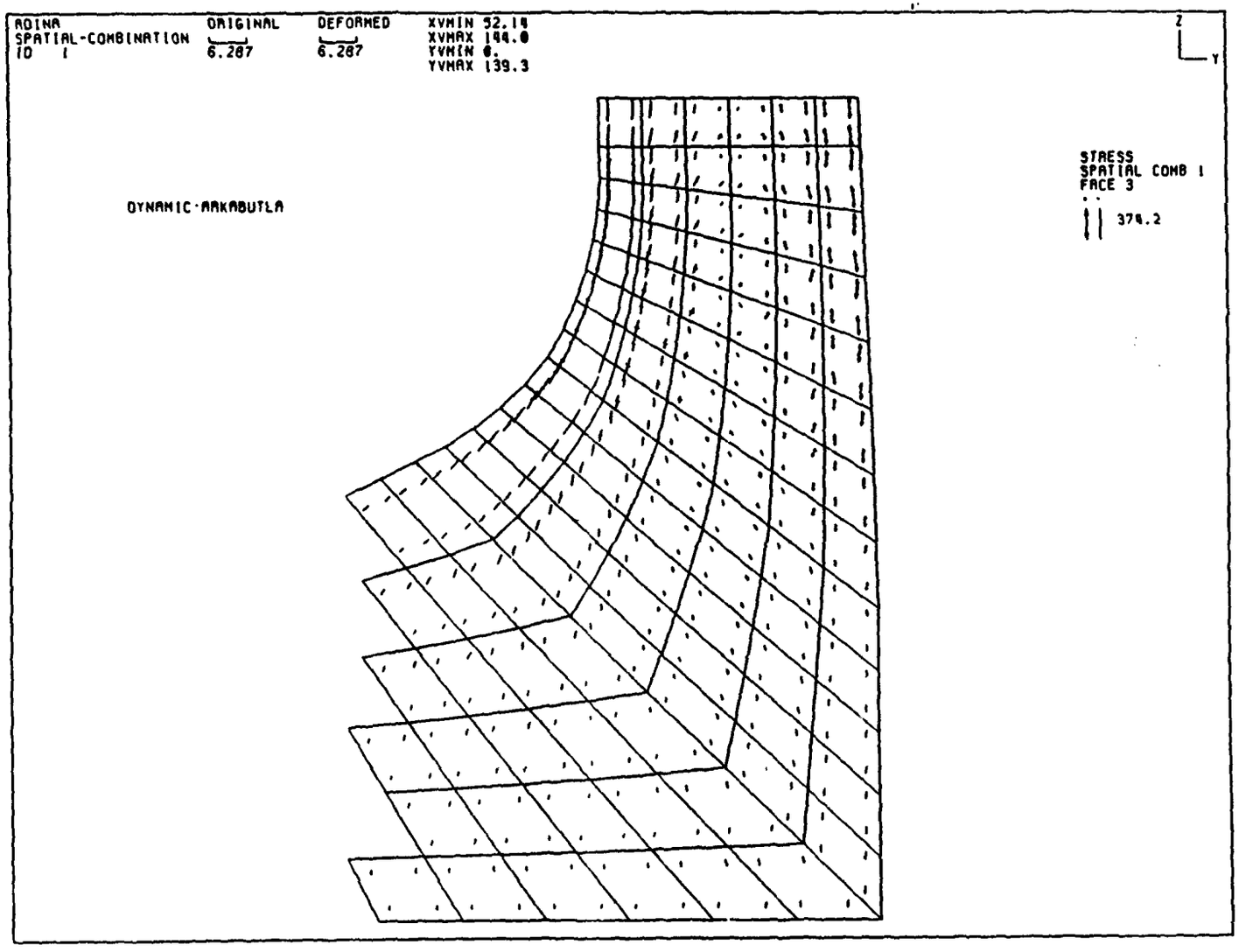

Figure 50. View of area of maximum dynamic stresses for Station 104 + 80.0

APPENDIX A: OVERTURNING STABILITY OF INTAKE TOWERS

by S. A. Kiger*

1. For structures on a firm foundation with uniform mass distribution, height H, and width B, rocking (and thus overturning) is not possible when the spectral acceleration associated with the first mode, Sa, is less than the fraction B/H of gravity g. This is usually referred to as WEST's formula (see Meek 1978 and Ishiyama 1980) and can be deduced by observing that the overturning moment of inertia is opposed by the moment of the structure weight. Thus, at incipient tipping

$$M \times Sa \times (H/2) = M \times g \times (B/2) \text{ or } Sa = g \times (B/H)$$

2. At lower values of Sa, no tipping will occur. When computing tower frequencies, hydrodynamic effects of the surrounding water (and water inside) should be considered.

3. For the San Bernardino intake tower (Figure A1), the first mode frequency (including hydrodynamic effects) is 2.05 Hz (Chopra and Liaw 1975) and the period is 0.49 sec. Site-dependent 5-percent damped acceleration response spectra (Seed, Ugas, and Lysmer 1974) indicate that at a distance of 20 miles from the San Fernando earthquake for stiff site and rock site conditions the first mode spectral accelerations are about 0.4 g and 0.15 g, respectively (See Figure A2). Note that these spectra are selected as an example, and may not be appropriate for the San Bernardino site. For the San Bernardino tower, the ratio of B/H is 0.31; therefore, rocking will not occur at a rock site but may occur at a stiff site. If possible rocking is predicted, further analysis is required.

4. Housner (1963) investigated overturning of rigid block-type structures with uniform mass of height H and base B as shown in Figure A3. If the earthquake energy input is computed from the velocity response spectrum, Sv, of the earthquake ground motion, the critical angle, α, is given by

---

* Formerly Research Structural Engineer, US Army Engineer Waterways Experiment Station, Vicksburg, Mississippi 39180-6199; currently Chairman, Civil Engineering Department, West Virginia State University, Morgantown, WV.

$$\alpha = Sv \sqrt{\frac{MR}{gIo}}$$

where M is the structure mass, R is the distance from the center of gravity to the corner about which tipping is taking place, Io is the mass moment of inertia about that corner, and α is the angle between the vertical and the line segment, R. For relatively tall towers, so that H is about equal to 2R, this equation may be written as

$$\alpha = Sv \sqrt{\frac{3}{4gr}}$$

5. This equation implies that for a given spectral velocity, Sv, a tower having the computed angle α will have approximately a 50-percent probability of being overturned (Housner 1963). If α is smaller, the probability of overturning is greater.

6. Note that this equation implies that larger towers are more stable than smaller towers with the same relative dimensions. Therefore, results of experiments with small blocks or observations of objects such as gravestones overturning during earthquakes cannot be used to predict overturning of large objects such as intake towers.

7. For the San Bernardino tower (Chopra and Liaw 1975), α is 17.2° and R is 100 ft. Thus, the required Sv to give a 50-percent probability of overturning is

$$Sv = (17.5)\ (\pi\ /180)\ \sqrt{(4)\ (32.2)\ (100)\ /\ (3)} = 20.0 \text{ ft/sec}$$

A value of Sv = 2.0 ft/sec represents strong ground motions in the United States; therefore, overturning of the San Bernardino tower is extremely unlikely. The damping effects of water surrounding the tower should further decrease the probability of overturning.

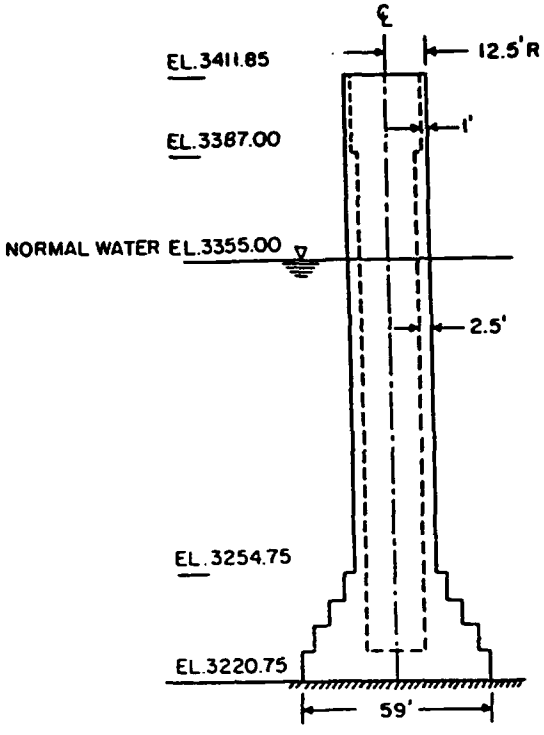

Figure A1. SAN BERNARDINO INTAKE-OUTLET TOWER
(From Ref. 3)

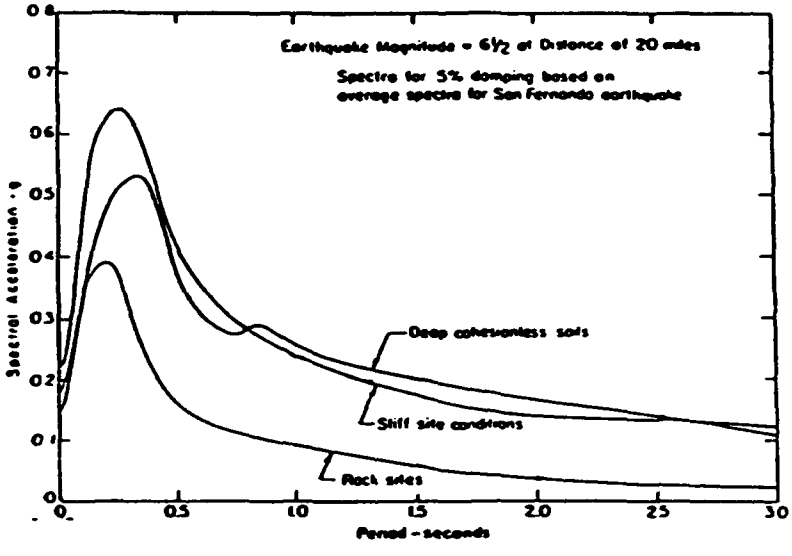

Figure A2. Anticipated acceleration response spectra at distance of 20 miles from epicentral region of San Fernando (1971) earthquake
(From Ref. 4)

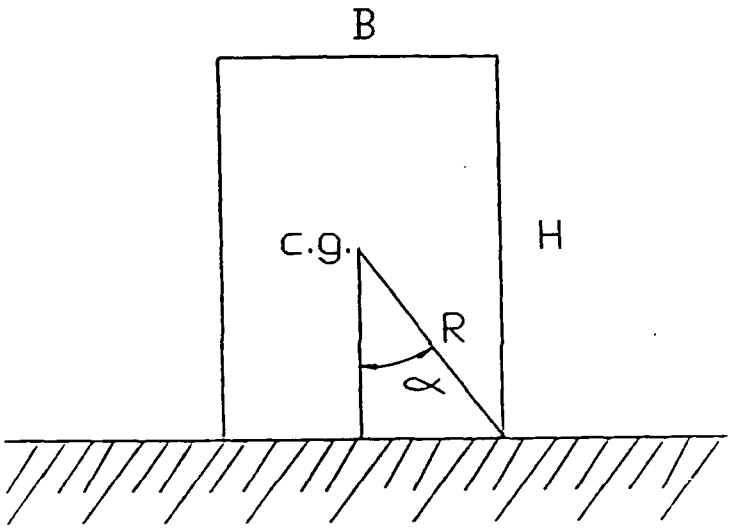

Figure A3. Rigid block structure

REFERENCES

1. Chopra, Anil K., and Liaw, C-Y. 1975 (Jul). Journal of the Structural Division, Proceedings of the American Society of Civil Engineers, Vol 101, No. ST7.

2. Housner, George W. 1963 (Feb). "The Behavior of Inverted Pendulum Structures During Earthquakes," Bulletin of the Seismological Society of America, Vol 53, No. 2, pp 403-417.

3. Ishiyama, Yuji. 1980 (Jun). "Review and Discussion on Overturning of Bodies by Earthquake Motions," BRI Research Paper No. 85, Building Research Institute, Ministry of Construction.

4. Meek, J. W. 1978 (Sep-Oct). "Dynamic Response of Tipping Core Building," Earthquake Engineering and Structural Dynamics, Vol 6, No. 5, pp 437-454.

5. Seed, H. Bolton, Ugas, Celso, and Lysmer, John. 1974 (Nov). "Site-Dependent Spectra for Earthquake-Resistant Design," Earthquake Engineering Research Center Report No. EERC 74-12.

Waterways Experiment Station Cataloging-in-Publication Data

Johnson, Wayne G.
Seismic analysis of Arkabutla intake-outlet structures / by Wayne G. Johnson, Vincent P. Chiarito, Randy L. Holmes ; prepared for Department of the Army, US Army Engineer District, Vicksburg.
92 p. : ill. ; 28 cm. — (Technical report ; SL-92-27)
Includes bibliographical references.
1. Earthquakes and hydraulic structures. 2. Structural dynamics. 3. Intakes (Hydraulic engineering) 4. Earthquake hazard analysis. I. Chiarito, Vincent P. II. Holmes, Randy L. III. United States. Army. Corps of Engineers. Vicksburg District. IV. US Army Engineer Waterways Experiment Station. V. Title. VI. Series: Technical report (US Army Engineer Waterways Experiment Station) ; SL-92-27.
TA7 W34 no.SL-92-27